AD-A062 995 ARMY ELECTRONICS RESEARCH AND DEVELOPMENT COMMAND WS--ETC F/G 17/1
BEHAVIOR OF FOUR SOUND RANGING TECHNIQUES IN AN IDEALIZED PHYSI--ETC(U)
SEP 78 W B MILLER, B F ENGEBOS

UNCLASSIFIED ERADCOM/ASL-TR-0018 NL

1 OF 1

AD
AD 62995

END
DATE FILMED
3-79
DDC

ASL-TR-0018

AD

Reports Control Symbol
OSD - 1366

BEHAVIOR OF FOUR SOUND RANGING TECHNIQUES IN AN IDEALIZED PHYSICAL ENVIRONMENT

SEPTEMBER 1978

By

W.B.MILLER

B.F. ENGEBOS

Approved for public release; distribution unlimited

US Army Electronics Research and Development Command

Atmospheric Sciences Laboratory

White Sands Missile Range, NM 88002

NOTICES

Disclaimers

The findings in this report are not *to* be construed as an official Department of the Army position, unless so designated by other authorized documents.

The citation of trade names and names of manufacturers in this report is not to be construed as official Government indorsement or approval of commercial products or services referenced herein.

Disposition

Destroy this report when it is no longer needed. Do not return it to the originator.

SECURITY CLASSIFICATION OF THIS PAGE *(When Data Entered)*

REPORT DOCUMENTATION PAGE

READ INSTRUCTIONS BEFORE COMPLETING FORM

1. REPORT NUMBER: ASL-TR-0018
2. GOVT ACCESSION NO.
3. RECIPIENT'S CATALOG NUMBER

4. TITLE *(and Subtitle)*: (6) BEHAVIOR OF FOUR SOUND RANGING TECHNIQUES IN AN IDEALIZED PHYSICAL ENVIRONMENT
5. TYPE OF REPORT & PERIOD COVERED: R&D Technical Report
6. PERFORMING ORG. REPORT NUMBER

7. AUTHOR(s): (10) W. B. Miller, B. F. Engebos
8. CONTRACT OR GRANT NUMBER(s)

9. PERFORMING ORGANIZATION NAME AND ADDRESS: Atmospheric Sciences Laboratory, White Sands Missile Range, New Mexico 88002
10. PROGRAM ELEMENT, PROJECT, TASK AREA & WORK UNIT NUMBERS: (16) DA Task No. 1L161102B53A/11

11. CONTROLLING OFFICE NAME AND ADDRESS: US Army Electronics Research and Development Command, Adelphi, MD 20783
12. REPORT DATE: (11) September 1978 (17) 41
13. NUMBER OF PAGES: 67

14. MONITORING AGENCY NAME & ADDRESS *(if different from Controlling Office)*
15. SECURITY CLASS. *(of this report)*: UNCLASSIFIED
15a. DECLASSIFICATION/DOWNGRADING SCHEDULE

16. DISTRIBUTION STATEMENT *(of this Report)*

Approved for public release; distribution unlimited.

(12) 74 pi

17. DISTRIBUTION STATEMENT *(of the abstract entered in Block 20, if different from Report)*

(9) Research and development technical rept

18. SUPPLEMENTARY NOTES

(14) ERADCOM/ASL-TR-0018

19. KEY WORDS *(Continue on reverse side if necessary and identify by block number)*

Sound ranging
Algorithms
Acoustics
Met data

20. ABSTRACT *(Continue on reverse side if necessary and identify by block number)*

Four contemporary sound ranging techniques are examined in an environment chosen to insure optimal performance characteristics for each. A data base is employed which is free of external contamination so that effects of truncation of arrival times and variations among algorithms are the sole contributors to observed differences in behavior. Noteworthy is the interplay which emerges between truncation effects and system response to meteorological errors. In addition, a direct comparison of techniques is given in context.

DD FORM 1 JAN 73 1473 EDITION OF 1 NOV 65 IS OBSOLETE

SECURITY CLASSIFICATION OF THIS PAGE *(When Data Entered)*

410 663

CONTENTS

INTRODUCTION

Within the artillery community, a renewed interest has been evidenced in the use of sound ranging as a passive mechanism for the location of hostile artillery and related functions [1,2]. Apparently, however, the subject is not without controversy, and no unified in depth treatment is evident. This lack of unity perhaps explains the existence of a considerable volume of literature containing a wide range of observation, interpretation, and opinion. Of special interest is a work of Hercz which has considerable scope and objectivity [3]; and historically, the works of Conant [4] make worthwhile reading.

To more effectively study the various problems peculiar to sound ranging, an effort was made in 1976 to construct a mathematical framework in which the sound ranging problem would be given a rigorous definition [5]. An offshoot of this study was a methodology whereby a hierarchy of sound ranging algorithms could be constructed based on physical assumptions concerning operating environment and on functional requirements of the algorithms themselves. Six such algorithms have been constructed and validated. Several properties of two members of this group are documented [6].

Of the above-mentioned six algorithms, one based on the simplest reasonable physical assumptions and with minimal functional requirements most nearly corresponded to a number of contemporary sound ranging techniques. This algorithm has been designated as Acoustic Location Program 1 (ALP-1).

In the study [6], certain behavior characteristics of ALP-1 were noted when the procedure was subjected to truncation of arrival times. Of interest also was the interplay exhibited between trucation levels and response to meteorological errors. It was natural then to ask whether the effects observed arose from peculiarities of ALP-1 or were traits held with other sound ranging schemes sharing common physical assumptions. To clarify this problem, three contemporary sound ranging techniques were examined on a side-by-side basis with ALP-1. It was recognized that perhaps straight analysis of the various techniques would yield the desired answers, but the course of action taken was considered more visible and expedient.

The first procedure chosen is derivable from information available in FM 6-122 [7] and utilizes a geometric approach in solving the sound ranging problem. This procedure corresponds to the standard field procedure which usually assumes the use of a six-microphone linear array. Use of the procedure produces a set of ten estimates of sound source location from which a single estimate is chosen. The ten points constitute a "polygon of errors," and when a median or mean technique is employed to derive the single source location estimate, the technique is called USRAN 1. For the controlled environment of this experiment, a median or mean technique may be employed without a significant difference in behavior. Under field conditions, departures from normal behavior in

estimates of arrival times give the median technique a distinct advantage in accurate target location.

USRAN 1 is a flexible program which will utilize up to six acoustic microphones with a minimum of three required. Inherent in the structure of this procedure is a graphical display availability which can prove useful for "on the spot" editing of arrival times. The error characteristics of ALP-1 and USRAN 1 are different, and the nature of the difference suggests that the two are mutually complementary.

Also, USRAN 1 and ALP-1 both allow for differing baseline geometries and may easily deal with loss or gain of function among the six acoustic microphones. USRAN 1 is a self-starting procedure, while ALP-1 requires an initial source estimate. ALP-1 appears to exhibit an accuracy potential which would suggest use of this algorithm as a "vernier" for a scheme such as USRAN 1.

In the same vein, a least squares refinement of estimates is possible, and a representative member of this class programmed by Lee [8] was readily available to the authors. In this presentation, that scheme will be called the Lee least squares algorithm. Like ALP-1, this computational process requires an initial estimate of source location. The results show that if initial source point estimates are sufficiently close to the true source point, the least squares algorithm and ALP-1 very nearly coincide. A little reflection will show that this must be the case. However, ALP-1 is considerably less sensitive to errors in source point location, while the least squares algorithm can at times tolerate larger errors in arrival times given good initial source point locations. This follows from the nature of the algorithms.

A final computational procedure was chosen reminiscent of that employed in USRAN 1, but with array flexibility sacrificed to obtain increased accuracy; i.e., this technique required a fixed and unalterable number of functional acoustic microphones. A technique of this nature designated as USRAN 3 utilizes six microphones [9]. A lesser number to the limit of three may be employed to construct an algorithm of this type, but as the number approaches three, the techniques merge into USRAN 1.

For the four sound ranging procedures mentioned previously, a physical environment exists in which all must exhibit optimal performance. In this environment, a meaningful side-by-side comparison of techniques is possible.

This environment may be characterized as follows: a flat featureless plane of uniform temperature and over which a wind of constant velocity is blowing. In such an environment, if spherical propagation of sound waves is assumed together with well-defined leading edges for all wave fronts, arrival times of such a front at any point on the plane may be calculated with great accuracy. It is then possible to examine effects of truncations in timing and system responses to meteorological errors individually, or in concert. Once the basic behavior traits of the

various systems are understood in this environment, effects of more complex environments may more readily be interpreted.

It is realized that a well-defined leading edge for wave fronts, and in fact the entire physical model, is an abstraction and that any real physical situation will be expected to depart from this simple model. However, presently, such considerations could obscure points fundamental to an understanding of system error behavior. It might be noted that any concept of "effective" meteorological results is the approximation of a real physical environment by one of exactly the simple form given above. In this light it would appear that there is justification for system comparison under the stated assumptions. For the purposes at hand, attention will be focused on truncation effects, system response to meteorological errors, and interaction of the two. Ranges are considered up to 30 kilometers, and flanking angles from 0 to 75 degrees. Flanking angle here is defined to be the angle measured clockwise from the perpendicular bisector of the array to the target.

As a mathematical convenience, the plane in the scenario previously mentioned will be made to coincide with the plane $Z = 0$ of a rectangular Cartesian system and maximum use will be made of symmetry to reduce data volume. Nonetheless, the amount of data necessary to complete this analysis is considerable. All data are available for interested readers, but only data selected on significant results will be included here. Results presented in most graphs or figures will be typical, or will be related to other results not presented by a predictable line of cause and effect. As will be seen, the behavior traits indicated and the comparison presented provide an understanding of the basic properties of the algorithms considered and will be used as a stepping stone to the study of more realistic physical models.

SCENARIO AND DATA BASE GENERATION

The physical environment to be described will be fundamental in the study to follow. It may be visualized as a flat featureless plane of uniform temperature continually swept by a wind of constant velocity. For mathematical convenience, a rectangular Cartesian coordinate system (X, Y, Z) will be assumed, with the above plane corresponding to the plane $Z = 0$.

Suppose that at time t_o, a blast occurs at the point (X_o, Y_o, Z_o). The assumption will be that a spherical wave front will propagate outward in such a fashion that if (X, Y, Z) obeys the relationship:

$$W(x, y, z, t) = [(x - x_o) - u(t - t_o)]^2 + [(y - y_o) - v(t - t_o)]^2$$

$$+ [(z - z_o) - q(t - t_o)]^2 - c^2k(t - t_o)^2 = 0, \qquad (1)$$

then (x, y, z) will lie on the wave front at time t. Here, the vector $(u, v, q) \equiv \vec{v}$ represents the wind and k the temperature in degrees Kelvin,

both from the original physical environment. The letter c is a constant whose value in this report will be taken as 20.06 consistent with the MKS system of units and the assumed physical modeling assumptions.

From the assumptions inherent in (1), the equation must satisfy the relationship

$$t = t_o + \frac{\sqrt{(\vec{v}\cdot\vec{x})^2 + [c^2k - (\vec{v}\cdot\vec{v})]\ (\vec{x}\cdot\vec{x})} - (\vec{v}\cdot\vec{x})}{[c^2k - (\vec{v}\cdot\vec{v})]} \qquad (2)$$

where $[(x - x_o),\ (y - y_o),\ (z - z_o)] \equiv \vec{x}$

Note that the mode of construction of each of the computational procedures to be examined assures that optimal performance may be expected when expression t is used in context to provide requisite arrival times for the estimation of $(x_o,\ y_o,\ z_o)$.

It is intrinsic to (1) that in time an expanding wave front must possess a well-defined leading edge. This effectively bypasses one critical issue in the sound ranging problem, that of break point identification. This problem exists distinct from algorithm performance except as it affects the choice of a vector of arrival times. The reaction of a given algorithm to such errors is insensitive to the causes involved except when those causes possess a reasonable determinative structure. For such a case, advantage may be taken of such structure and a suitable algorithm fabricated. Among the procedures considered at this time, none possess this form of structure, but algorithms which may prove to be of merit exist on the horizon, and these algorithms utilize the idea of degradation of timing accuracy with range and other characteristics.

The problem of arrival time accuracy is complex and has points of ambiguity, at least at the current state of the art. Several factors influence the behavior of the problem, and a comprehensive random model is quite involved, although useful information may be gleaned from randomization of expression (2). For these reasons, at present, algorithm behavior is examined apart from considerations of the nature of arrival time errors. If such were included at this point, behavior traits might be introduced which would obscure points of interest which would otherwise be clear. The problem of arrival time accuracy and its error structure is currently being addressed.

For a preliminary examination of the chosen algorithms, a configuration of 66 systematically located sound sources was found to afford an adequate picture of behavior characteristics of interest. Source points were located at 5 to 30 kilometers at 5-kilometer intervals and along flanking angles of 0 through 75 degrees at 15-degree increments (figure 1).

Symmetry could be used in the placement of acoustic microphones to derive information equivalent to that supplied by the above configuration, but with only 36 source points. This method considerably

diminishes the volume of data to be treated and affords an adequate picture of the characteristics of interest in this study. A denser grid of source points could be used to spotlight frequency effects of truncation of arrival times but would not especially increase information in current context. In addition, all computational procedures exhibit continuity except for specified juxtapositions of source points and microphone locations; and after a point, behavior with respect to truncations, or general variation at a sufficiently small variance, must be smooth.

In the generation of timing data, a set of microphone positions (x_1, y_1), $\cdots, (x_6, y_6)$ was defined by

$$x_j = 7000 - 2000j$$
$$y_j = -1000$$
$$j = 1, 2, \ldots, 6$$

where (x_j, y_j) is given in meters.

For a source point as described previously, definition of the wind vector (u, v, q) and the temperature k, will produce a vector of six arrival times. For present purposes, a wind vector of (0, 0, 0) and a temperature of 295°K were employed. Other values of wind and temperature were employed without altering basic results, and so were omitted.

Arrival times for all source points were calculated at the full accuracy of the HP 9830-A. Four increasingly degraded cases of timing accuracy were considered: full accuracy for initial verification which is not included, then 0.1-, 1-, and 10-millisecond truncation levels. The 100-millisecond truncation level was also examined but produced such erratic behavior in all algorithms that it was not included.

When the version of USRAN 1 is considered, the Lee least squares technique and the algorithm ALP-1 all may account for a loss of as many as three microphones without loss of function. Behavior of truncation effects together with microphone loss and errors in meteorological parameters is being addressed separately and introduces a number of interesting insights. This study should be available in the near future.

After figure 1, which indicates the relative positions of microphones and source points employed in this study, all figures will have a similar construction. Each will consist of four subfigures. The top two plots always indicate comparative miss-distances for the indicated versions of USRAN 1, USRAN 3, and the algorithm ALP-1, and for truncation levels of 0.1 and 1.0 milliseconds as specified. The bottom left plot always presents a similar format, but for a timing level of 10 milliseconds.

The bottom right plot is a special case, and presents maximum and minimum miss-distances at the 1.0-millisecond level for the Lee least

squares technique. The deviations were derived from the fact that four initial estimates for sound source location were routinely made. These estimates were at 12:00, 3:00, 6:00, and 9:00 o'clock and at a distance 20 percent of range of the midpoint of the microphone array to the target from actual target. In the Lee technique, an appreciable amount of variation was found among responses to these estimates. In ALP-1, almost no variation was observed; hence no special plot was required.

Note that the vertical scales used in a given figure change. This change is dictated by the behavior of the algorithms and is necessary if meaningful resolution is to be maintained.

EXACT METEOROLOGICAL INFORMATION

In this and the succeeding sections, the effects of timing information degraded by truncation are examined. In all situations presented, each algorithm is provided with the exact meteorological data as the data exist in the previously described physical environment.

In the examination of figures 2 through 7, which represent increasing flanking angles of 0 through 75 degrees, the most striking feature shared by all algorithms is the abrupt increase in erratic behavior when the 10-millisecond truncation level is reached. Also, observation shows that the degree of erratic behavior experienced by all procedures tends to increase with distance. Limited analysis in addition to that presented tends to indicate that truncation effects in this context would produce a stochastic process with an increasing trend as distance increases, and with a similarly increasing variance. One might also note that the Lee least squares algorithm presents considerable deviations between maximum and minimum values as source point estimates vary. Minimal miss-distances in this case lie near those of ALP-1, while maximum excursions appear quite large. This difference would indicate that the Lee least squares probably would have little "stand alone" capability and would require a good initial estimate to function.

Figures 2 and 3 show that at the 10-millisecond truncation level, USRAN 1, USRAN 3, and ALP-1 may exhibit quite different performance characteristics, but when figures 2 through 7 are examined together, algorithm behavior due to truncation effects shows a general behavior agreement.

Error increase with increasing flanking angle is evident through changes in scale; also lack of consistency in behavior at the various levels can be noted. All algorithms degrade in performance as flanking angle increases. It might be deduced that millisecond timing would be a worthwhile goal, with considerable returns in stability and accuracy over a wider area.

EFFECTS OF ARRIVAL TIME TRUNCATION IN THE PRESENCE OF UNIT ERRORS IN TEMPERATURE

This section concerns the effects on miss-distance of the earlier defined levels of truncation, but in the presence of unit variations (degrees Kelvin) in temperature. The plots show that effects of truncation at the 0.1-millisecond level indicate a definite and very nearly linear trend of increase of miss-distance with range. Though not included, ALP-1 has been shown to produce a more and more linear trace as timing accuracy increases.

Figures 8 through 19 are arranged in such a manner that side-by-side comparisons may be made between positive and negative unit effects in temperature at all flanking angles. In the case of 0.1-millisecond timing, no great difference is exhibited in unit effects between algorithms, but ALP-1 exhibits a reflexive mode when positive and negative errors are encountered. The figures show that as timing errors decrease, so does the amplitude of the variations in effect of ALP-1; and at sufficient timing errors, these effects disappear altogether. The miss-distance at maximum accuracy is almost exactly the average of miss-distances of ALP-1 for positive and negative temperature fluctuations.

A 0-degree flanking angle and a 1.0-millisecond truncation of arrival times still retain an indication of linearity of miss-distance with horizontal range, but this tendency is not so pronounced as that observed for more accurate arrival times. For a truncation at 10 milliseconds, all evidence of linearity is lost except by use of statistical methodology. At higher flanking angles, similar results are encountered, but with increases in magnitude of miss-distances. In all cases, the truncation at 10 milliseconds produces a sudden increase in erratic behavior and loss of linearity of unit effects. Notice that at the 10-millisecond truncation of arrival times, the algorithms other than ALP-1 show a tendency to be reflective.

The Lee least squares algorithm exhibits a distinct separate behavior for varying initial estimates, with the most favorable values being near those of ALP-1 (top right plot of figure 13), with a good agreement of values occurring at 30 degrees. An increasing value of scale on the plots shows that all procedures exhibited greater errors as flanking angle increased.

Considerably more interpretive analysis is possible, but consistent with the purposes of this investigation, these must remain for consideration at some future time. At present, an examination of errors introduced by a combination of truncation of arrival times and unit errors in wind will be considered.

WIND ERRORS PERPENDICULAR TO ARRAY BASELINE

For the wind conditions utilized, little effect occurred due to unit errors in wind blowing perpendicular to the array baseline. This may be

observed by comparing figures 2 through 7 with those of 20 through 25. This holds true at a truncation level of 0.1 millisecond for all algorithms to a greater or lesser extent, with ALP-1 yielding near zero miss-distances from flanking angles of 0 to 60 degrees. At 75 degrees, ALP-1 remains near zero, but both USRAN 1 and USRAN 3 exhibit a strong increasing trend with distance.

Increases in miss-distance with increasing flank angle and target distance are evident, as in previous sections, with sudden increases in erratic behavior at the 10-millisecond truncation level readily observed. The Lee least squares algorithm closely parallels ALP-1 in behavior of its minimum miss values.

The question arises as to whether the apparent independence of results to perpendicular winds is in fact true or reflects a second-order effect. Toward this end, data were generated including a perpendicular wind of 50 knots. The ALP-1 algorithm was then utilized to find a source point at 10 kilometers range and 0 degrees flanking angle. Millisecond truncation produced a miss-distance of 3 meters, well within system roundoff error.

Additional information may be derived from the more advanced algorithms, and strong evidence of independence exists in this area. It might be observed that if an array is not linear, the observed behavior of perpendicular wind ceases to hold. A more formal presentation on the problem of independence may be presented at a later date. Presently, the differences in algorithmic behavior seen here are believed to be due to the technique USRAN 1 and USRAN 3 use for wind correction.

WIND ERRORS PARALLEL TO ARRAY BASELINE

Observation of figures 26 through 37 indicates that unit wind errors parallel to the array baseline exhibit a near perfect linear dependence of miss-distance on range when subject to truncation levels at 1.0 milliseconds or better at flanking angles from 0 to 30 degrees. At higher flanking angles, slight deviations from linearity are experienced.

A reasonable consistency is evidenced between algorithms, with ALP-1 exhibiting a reflective behavior at smaller truncation levels. As flanking angles increase, accuracy deteriorates and this deterioration holds also for increasing distance but to a lesser extent. As usual, a considerable increase in erratic behavior of miss-distances occurs at a truncation level of 10 milliseconds, and consistency of algorithms lessens considerably. Again as usual, the minimum miss values of the Lee least squares lie close to those of ALP-1.

As a whole, the various algorithms behave a bit more stably with regard to winds parallel to array baseline than those experienced with temperature.

A 5-METER/SECOND ERROR IN SOUTH AND WEST WINDS, AND A 5-DEGREE KELVIN ERROR IN TEMPERATURE

In this section meteorological errors of 5°C and 5 meters/second in both wind components are considered. These errors are used to demonstrate the linearity of unit effects due to errors in met parameters. An additional reason for utilization of errors of this magnitude is a demonstration of the relative independence of errors in meteorological variables when arrival time accuracy is adequate for corrective modes. These errors are not to be construed as representative of field type meteorological errors which would hopefully be smaller in magnitude.

Figure 38 indicates a linearity which appears to be strongest at a range in excess of 10 kilometers. Truncations of arrival time at the 0.1- and 1-millisecond level produce similar results. On the whole, linearity is preserved quite well at a 10-millisecond truncation, considering previous results. In this case, one would suspect a cancelling effect to be in operation, that is, a favorable interaction of meteorological conditions.

Figure 39 describes the behavior of the various algorithms for a 15-degree flanking angle. All techniques preserve linearity through 1.0-millisecond truncation of arrival times but deteriorate seriously at a 10-millisecond truncation.

Figure 40 begins to exhibit a divergence of unit effects between ALP-1 and USRAN 1 and USRAN 3. Observe that linearity of unit effects persists for all the algorithms through millisecond truncation of arrival times, but degrades at the 10-millisecond truncation, the typical behavior pattern. The behavior continues in much the same fashion through figure 43. The differences in techniques are not startling. However, at the higher flanking angles, note that these differences tend to be obscured to the casual glance by increasing vertical scale.

Overwhelming the variations in miss-distance for the different algorithms are effects due to the variations in timing truncation. This, the authors feel, is a most important consideration.

Whatever the reasons, a logical first step in developing enhanced sound ranging capabilities appears to be through some means of enhancing arrival time accuracy toward the nearest millisecond and preserving linearity of unit effects with distance. Then more powerful algorithms now available can be utilized. Without such timing enhancement, one logical system for obtaining maximum accuracy over an extended area appears to be a composite algorithm encompassing the best features of several algorithms. A number of such configurations are currently being studied to determine stability and field worthiness, with at least one showing promise.

As a final point, it should be stressed that the interplay between timing and required accuracy of meteorological data in no way implies

that meteorological information is not essential to accurate sound ranging. In fact, field accuracies in the foreseeable future would tend to indicate that a high degree of importance must be placed on accurate meteorology.

The behavior of the advanced algorithms ALP-2 and ALP-2T as demonstrated in tables 1 through 3 shows striking reductions. For the larger flanking angles (greater than 45 degrees), ALP-2T gives good results for all timing accuracies. This feature may possibly be exploited into a composite type algorithm to effectively extend the zone of coverage by sound ranging. Note also that by putting bounds on the timing, of the blast, in algorithms ALP-2 and ALP-2T the instability as observed in tables 2 and 3 can be prevented. This analysis will be forthcoming.

CONCLUDING REMARKS

In the performance of this comparison, one fact seems to predominate. For all ranges and flanking angles considered, accuracy deteriorates drastically when arrival times are truncated at the nearest 10 milliseconds. This phenomenon occurs for all techniques considered to a greater or lesser extent. In addition, linearity in distance of unit effects for wind and temperature, which are evident at 0.1- and often at 1.0-millisecond truncations of arrival times, are, in the majority, totally lost when accuracy is reduced to a 10-millisecond truncation. Therefore, it may be concluded that timing accuracy approaching a millisecond is needed.

Due to the problem of extreme stratification of sampling, a direct statistical comparison is difficult and adds nothing to the results of this study. In all cases, one might consider that no statistics are involved, but rather a tabulation of results from numerical algorithms.

Note that when wind or temperature deviations are introduced for an individual case, smaller or larger values of miss-distances do not guarantee how a given technique performs in general. For example, if zero miss-distance is observed at 20 kilometers without adjustment for meteorological conditions, then certainly the technique could not be called good, but lucky.

A general statistically unsupported statement is that USRAN 3 appears to offer improvement over USRAN 1, and ALP-1 compares favorably with USRAN 3. Also, if initial guesses are of sufficient accuracy, the Lee algorithm and ALP-1 exhibited similar behavior characteristics.

REFERENCES

1. Television Tape, 1977, "Field Artillery Sound Ranging Briefing," 2E/041-061-0628B, US Army Field Artillery School, Fort Sill, OK.

2. Coffman, Major Glen B., 1974, "Sound Ranging Revisited," Field Artillery Journal, pp. 19-21, Fort Sill, OK.

3. Hercz, A. R., 1971, "Investigation of Factors Affecting Sound Ranging," Literature Search and Analysis, ECOM 00013-20, Willow Run Laboratory, University of Michigan, Ann Arbor, MI.

4. Conant, J. B. (Chairman), 1946, "Detection of Land Mines and Sound Ranging," National Defense Research Committee, Office of Scientific Research and Development, AD 221-602, Washington, DC.

5. Miller, W. B., and B. F. Engebos, 1976, "A Mathematical Structure for Refinement of Sound Ranging Estimates," ECOM-5805, US Army Atmospheric Sciences Laboratory, WSMR, NM.

6. Miller, W. B., and B. F. Engebos, 1977, "A Preliminary Analysis of Two Sound Ranging Algorithms," ECOM-5826, US Army Atmospheric Sciences Laboratory, WSMR, NM.

7. FM 6-122, Artillery Sound Ranging and Flash Ranging, 1964, Department of the Army, Washington, DC.

8. Lee, R. P., 1975, "A Least Squares Algorithm," US Army Atmospheric Sciences Laboratory, WSMR, NM, unpublished manuscript.

9. Swingle, D. M., and R. Bellucci, 1973, "Improved Sound Ranging Location of Enemy Artillery," ECOM-5486, US Army Electronics Command, Fort Monmouth, New Jersey.

Source locations utilized in the evaluation of USRAN 1, USRAN 3, ALP-1, and the Lee least squares algorithm. Source positions are designated by asterisks, microphones by (M).

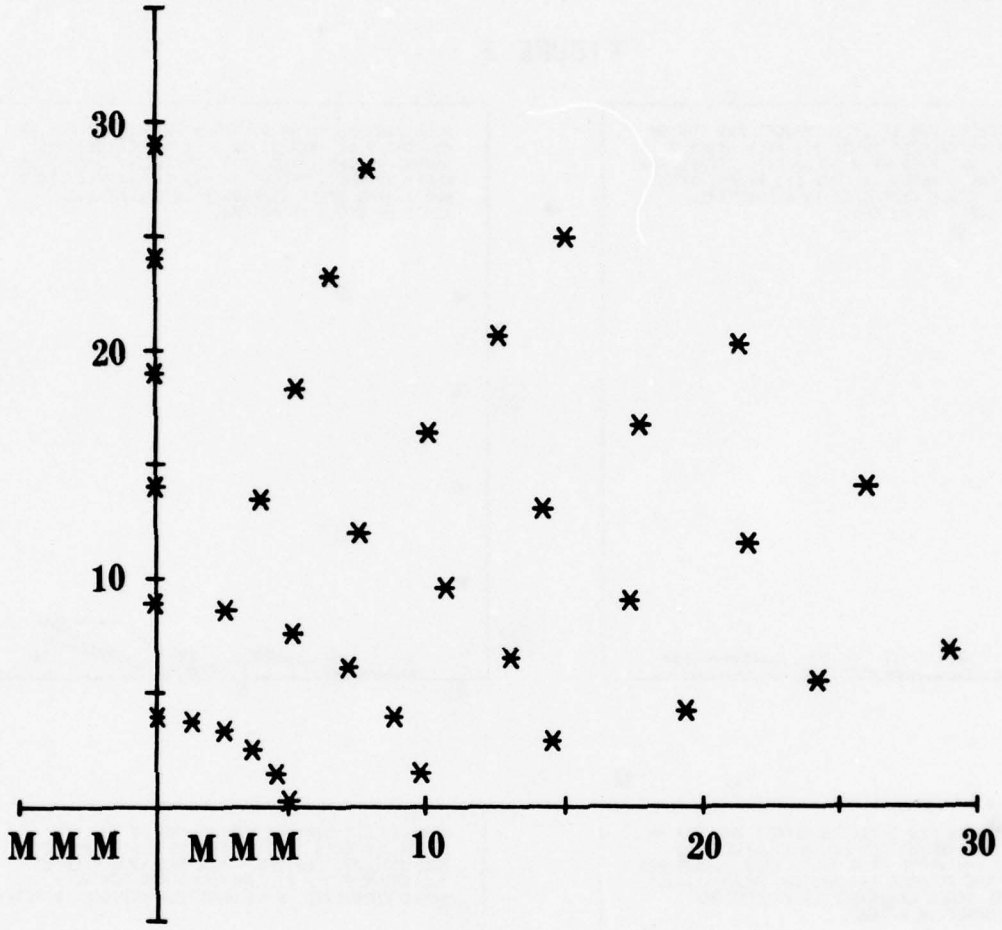

Horizontal and vertical scales 5.0 kilometers

Figure 1. Source and microphone locations.

MISS DISTANCE VERSUS RANGE (METERS) FOR SOURCE POINTS LOCATED AT A 0 DEGREE FLANKING ANGLE. SELECTED TRUNCATION POINTS ARE CONSIDERED AS INDICATED BELOW. NO METEOROLOGICAL ERRORS ARE ASSUMED.

FIGURE 2

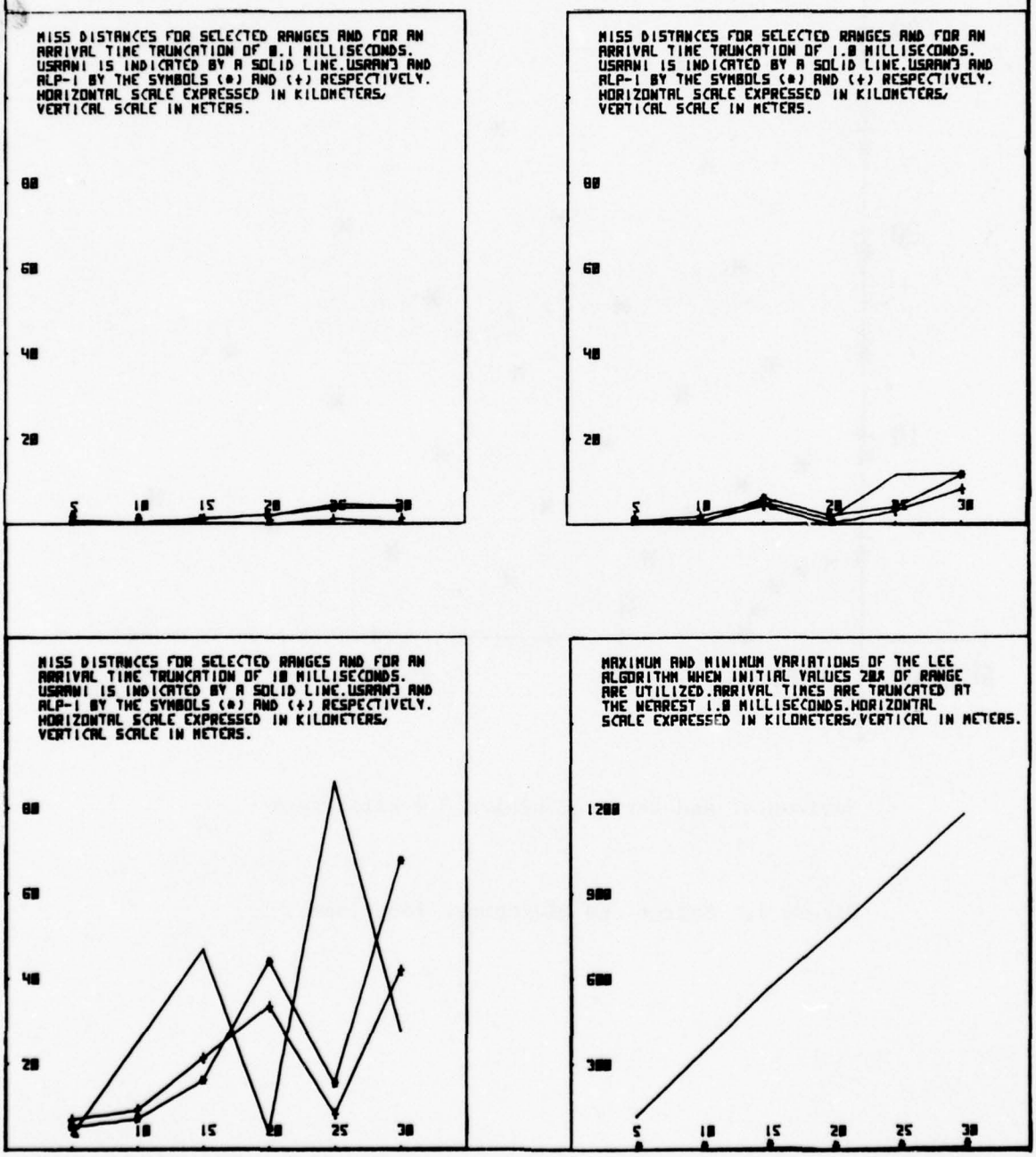

MISS DISTANCE VERSUS RANGE (METERS) FOR SOURCE POINTS LOCATED AT A 15 DEGREE FLANKING ANGLE. SELECTED TRUNCATION POINTS ARE CONSIDERED AS INDICATED BELOW. NO METEOROLOGICAL ERRORS ARE ASSUMED.

FIGURE 3

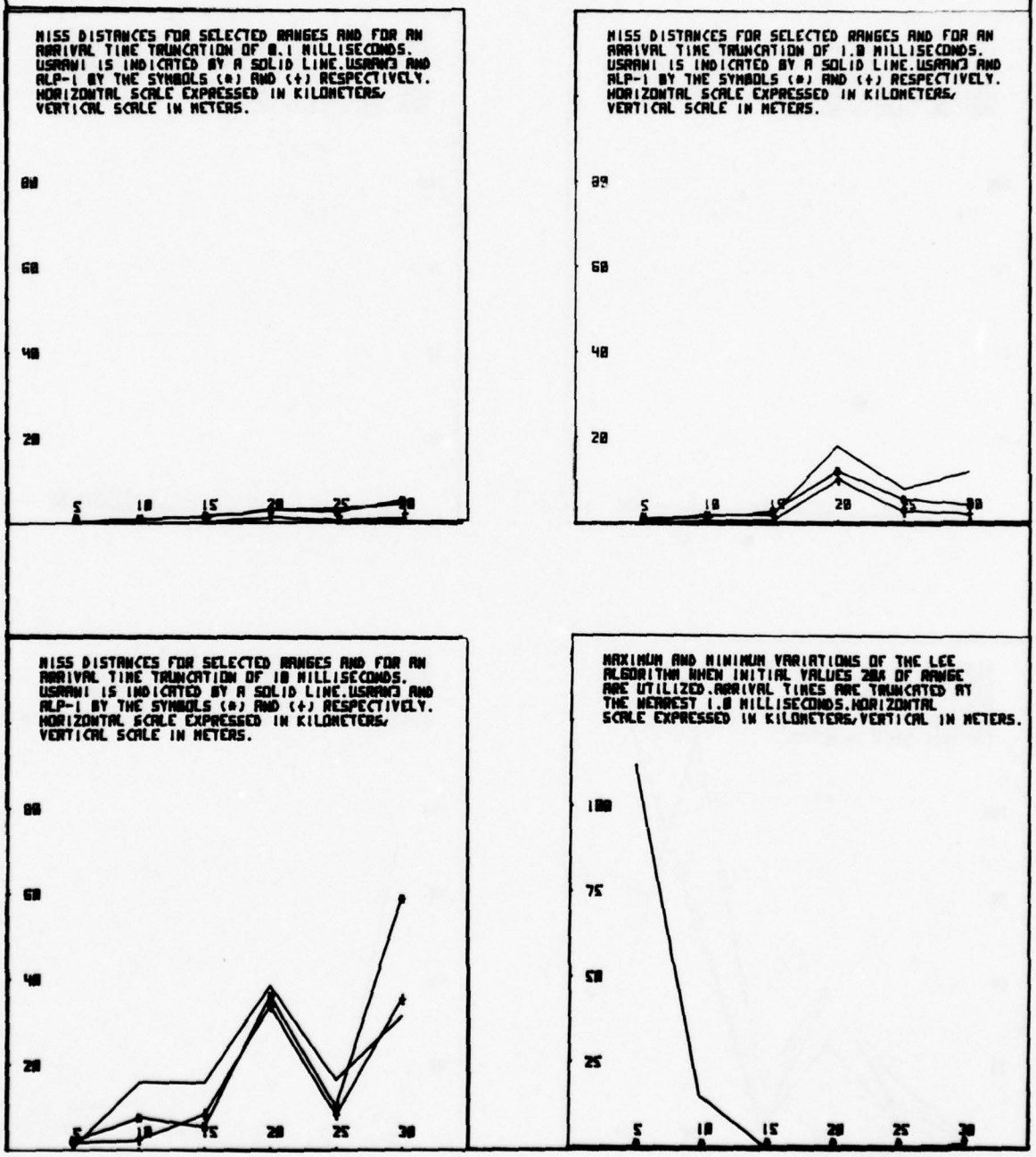

MISS DISTANCE VERSUS RANGE (METERS) FOR SOURCE POINTS LOCATED AT A 30 DEGREE FLANKING ANGLE.SELECTED TRUNCATION POINTS ARE CONSIDERED AS INDICATED BELOW.NO METEOROLOGICAL ERRORS ARE ASSUMED.

FIGURE 4

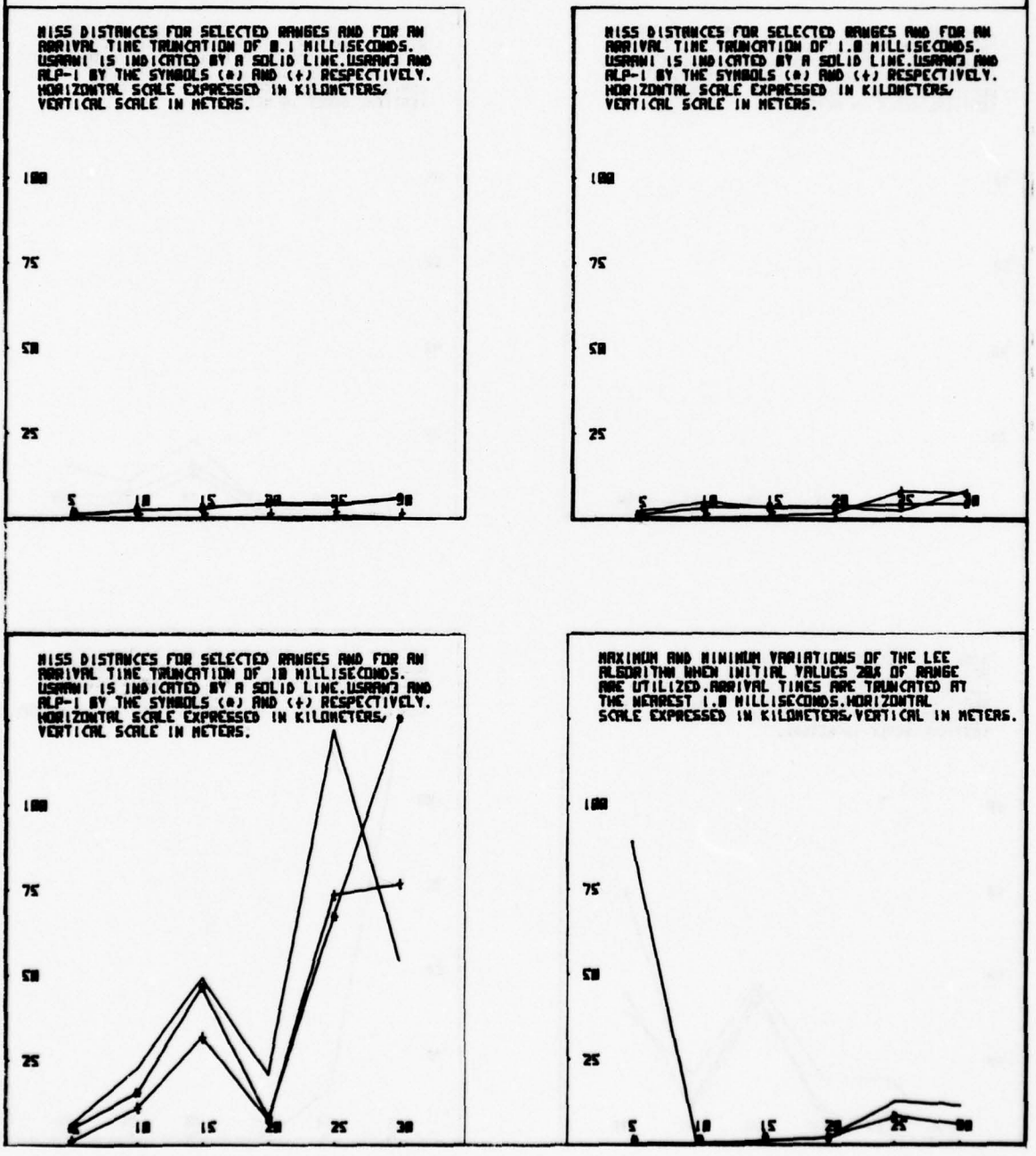

MISS DISTANCE VERSUS RANGE (METERS) FOR SOURCE POINTS LOCATED AT A 45 DEGREE FLANKING ANGLE. SELECTED TRUNCATION POINTS ARE CONSIDERED AS INDICATED BELOW. NO METEOROLOGICAL ERRORS ARE ASSUMED.

FIGURE 5

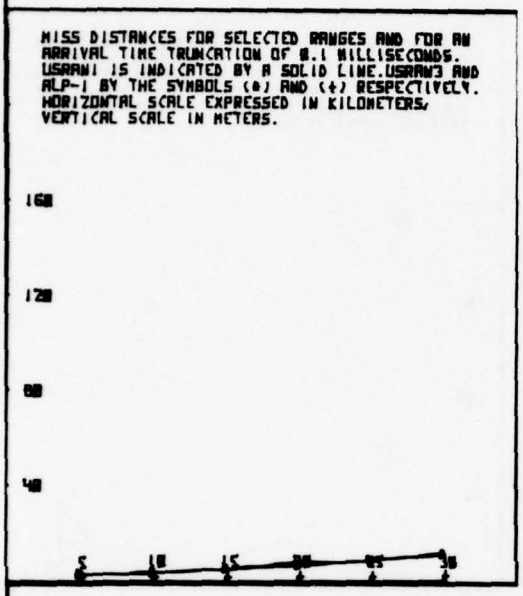

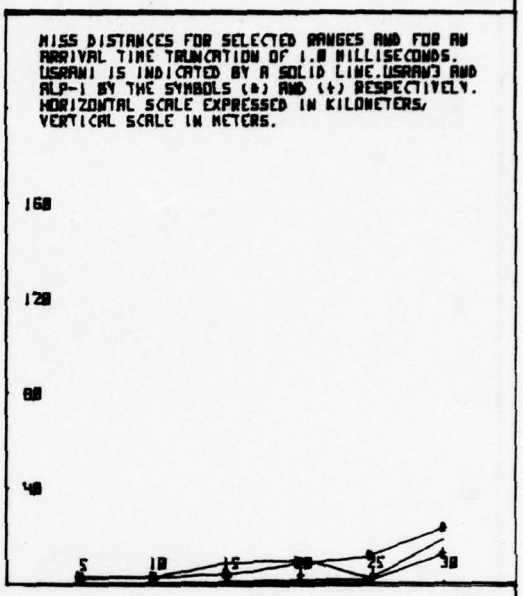

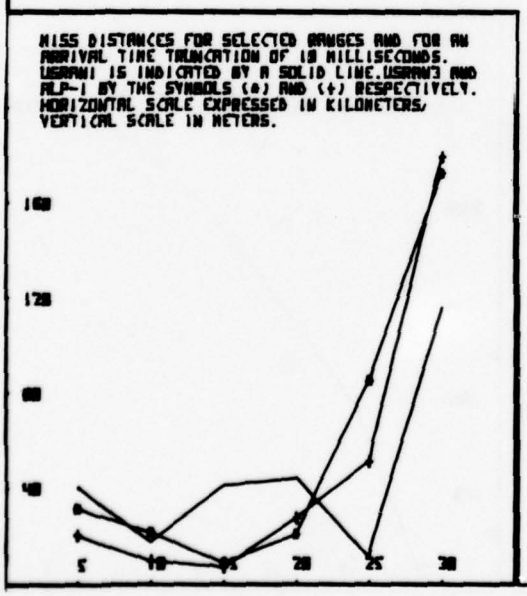

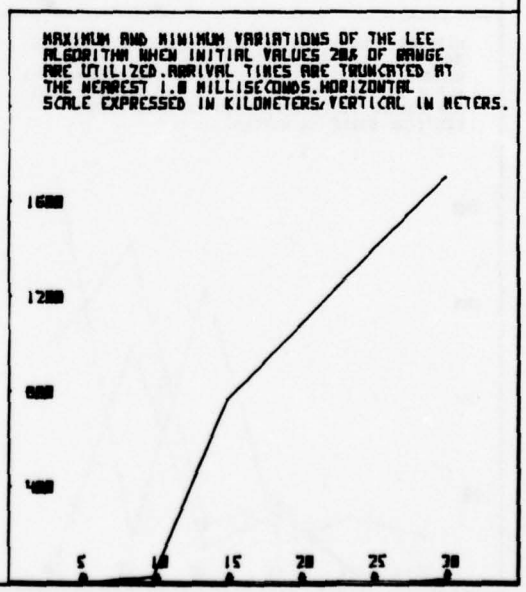

MISS DISTANCE VERSUS RANGE (METERS) FOR SOURCE POINTS LOCATED AT A 60 DEGREE FLANKING ANGLE.SELECTED TRUNCATION POINTS ARE CONSIDERED AS INDICATED BELOW.NO METEOROLOGICAL ERRORS ARE ASSUMED.

FIGURE 6

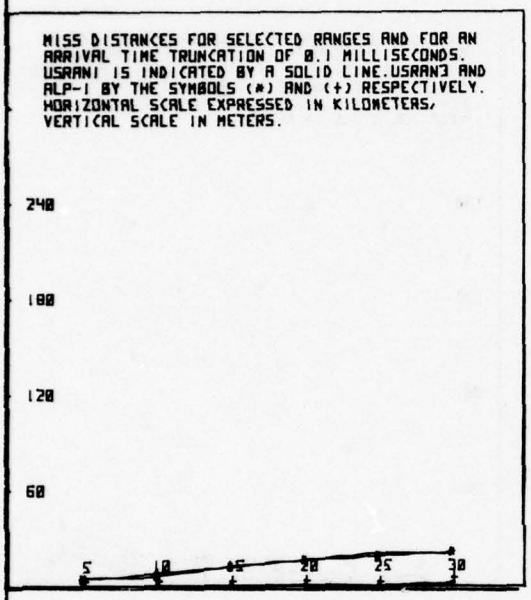

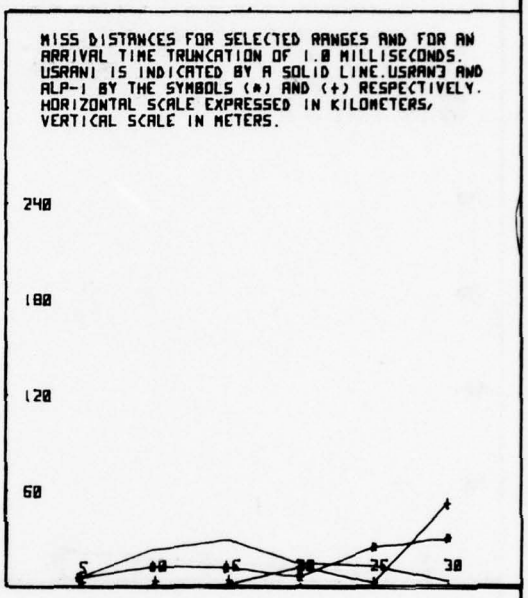

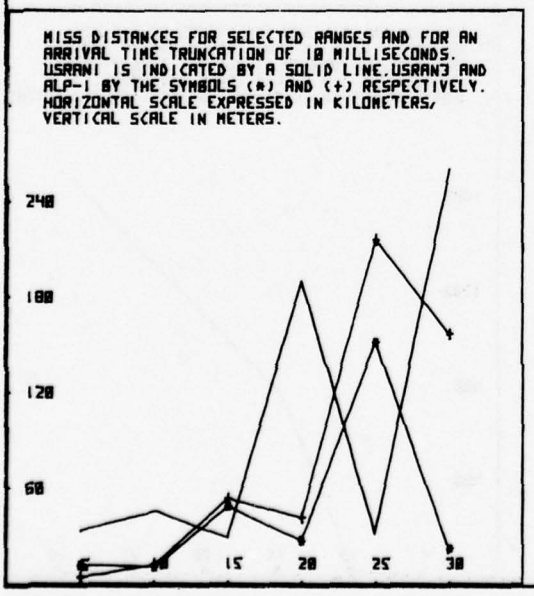

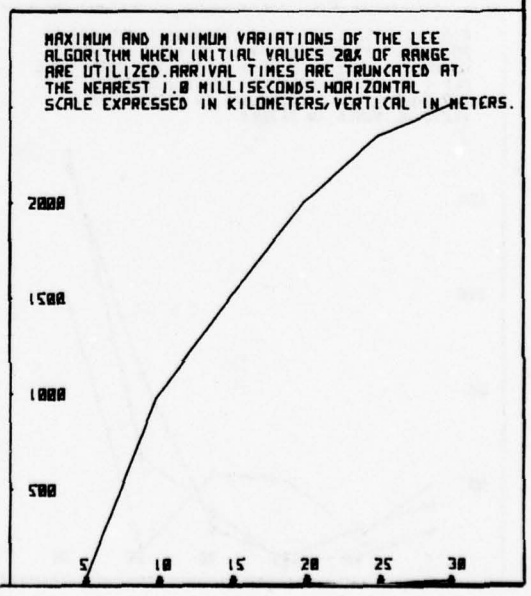

MISS DISTANCE VERSUS RANGE (METERS) FOR SOURCE POINTS LOCATED AT A 75 DEGREE FLANKING ANGLE.SELECTED TRUNCATION POINTS ARE CONSIDERED AS INDICATED BELOW.NO METEOROLOGICAL ERRORS ARE ASSUMED.

FIGURE 7

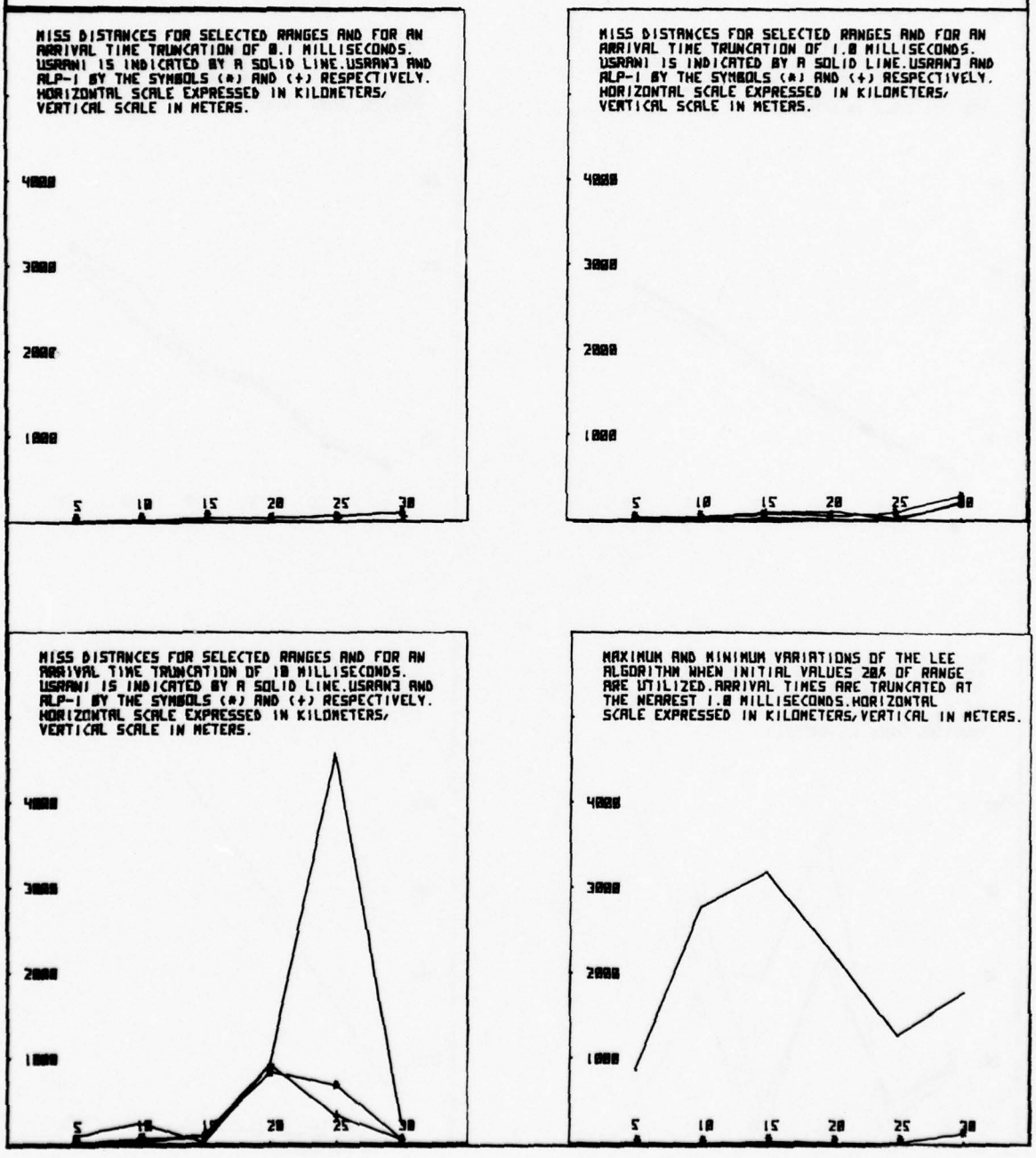

MISS DISTANCE VERSUS RANGE (METERS) FOR SOURCE POINTS LOCATED AT A 0 DEGREE FLANKING ANGLE. SELECTED TRUNCATION POINTS ARE CONSIDERED AS INDICATED BELOW. A TEMPERATURE ERROR OF +1.0 DEGREES KELVIN IS ASSUMED.

FIGURE 8

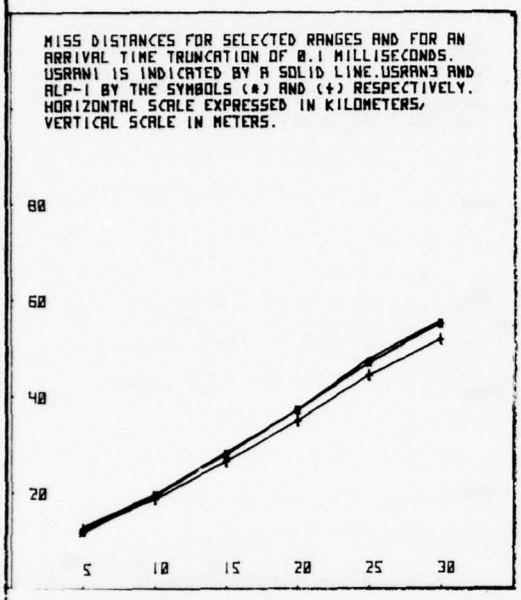

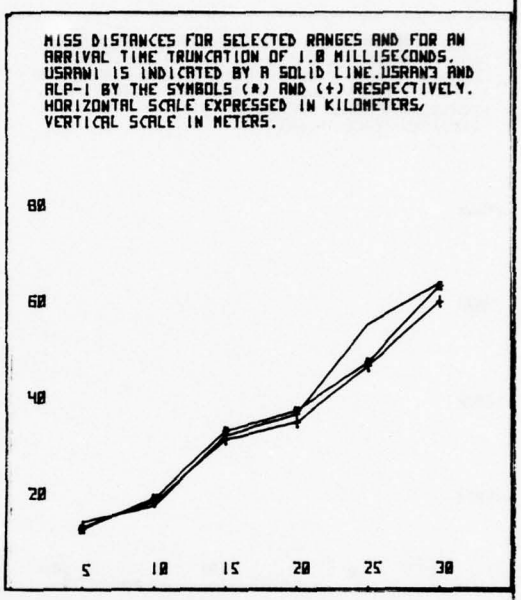

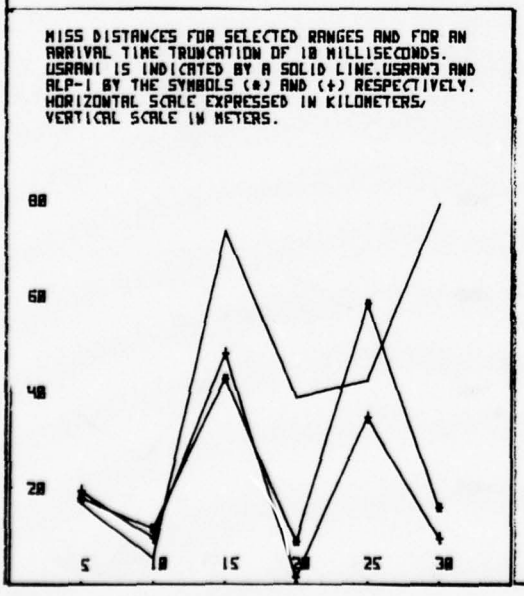

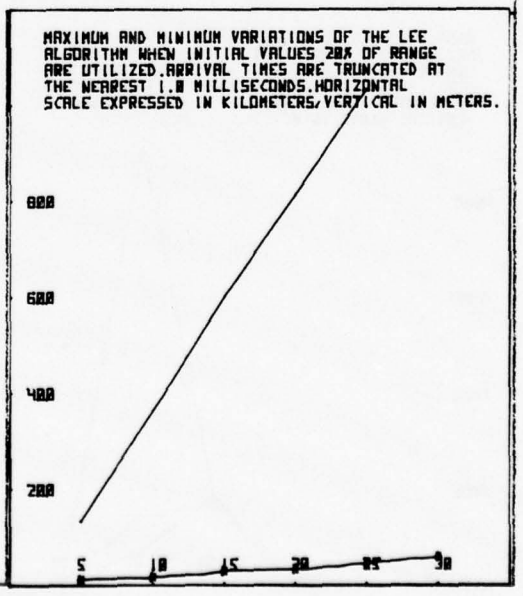

MISS DISTANCE VERSUS RANGE (METERS) FOR SOURCE POINTS LOCATED AT A 0 DEGREE FLANKING ANGLE. SELECTED TRUNCATION POINTS ARE CONSIDERED AS INDICATED BELOW. A TEMPERATURE ERROR OF -1.0 DEGREES KELVIN IS ASSUMED.

FIGURE 9

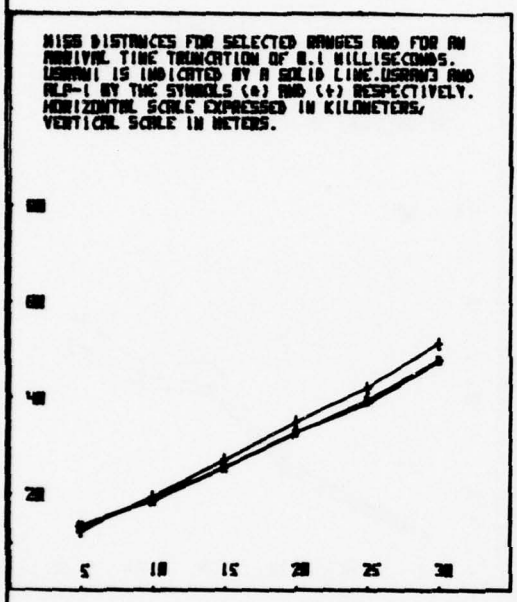

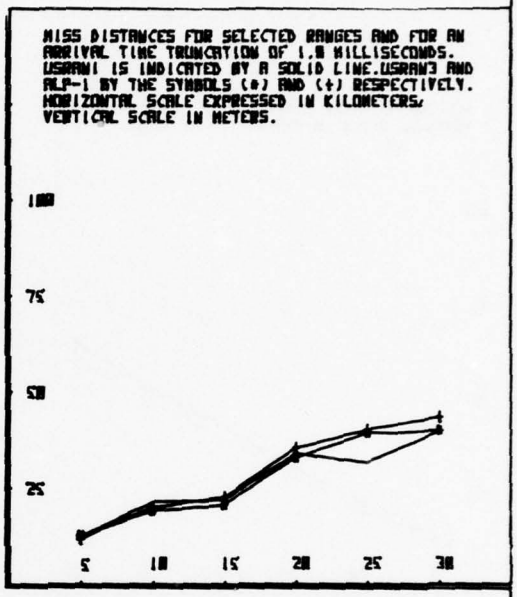

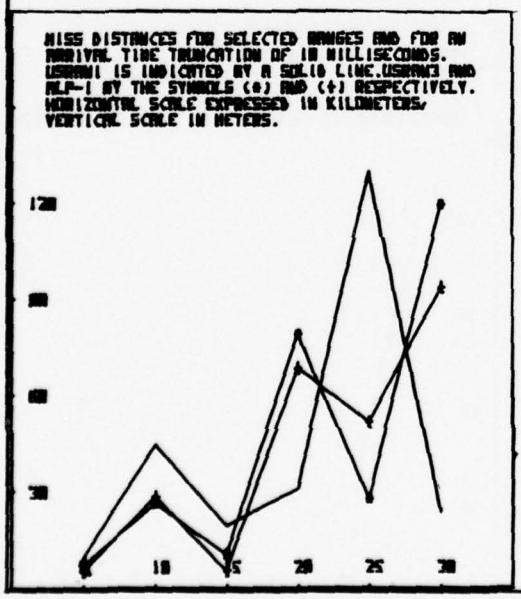

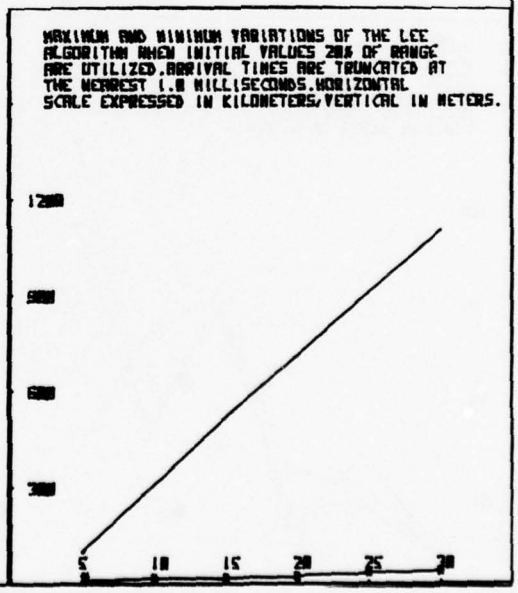

MISS DISTANCE VERSUS RANGE (METERS) FOR SOURCE POINTS LOCATED AT A 15 DEGREE FLANKING ANGLE. SELECTED TRUNCATION POINTS ARE CONSIDERED AS INDICATED BELOW. A TEMPERATURE ERROR OF +1.0 DEGREES KELVIN IS ASSUMED.

FIGURE 10

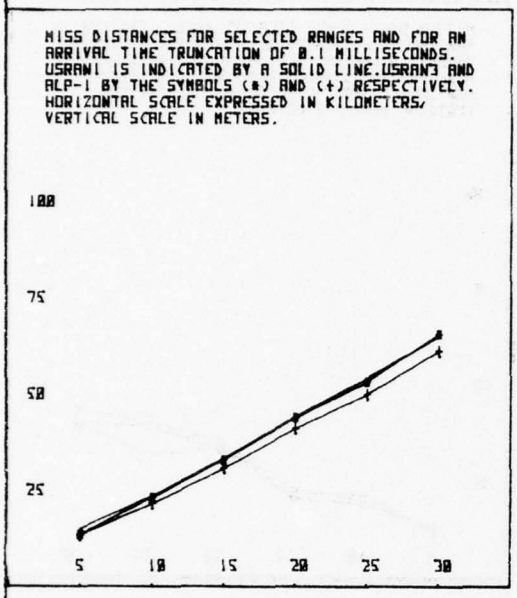

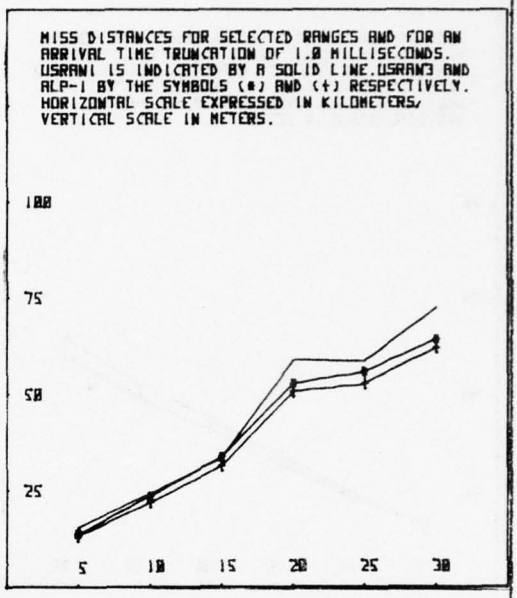

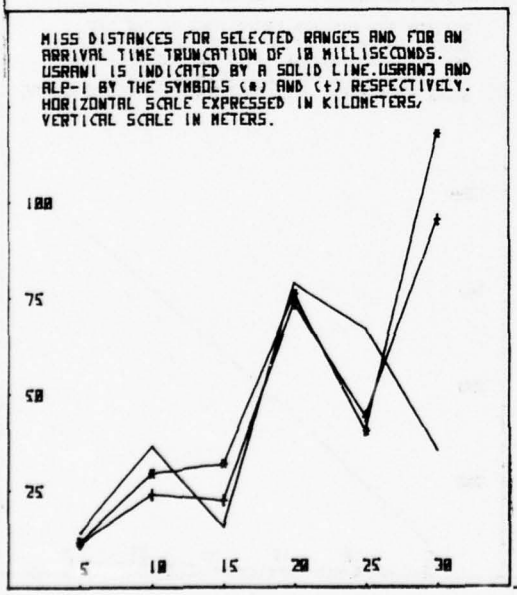

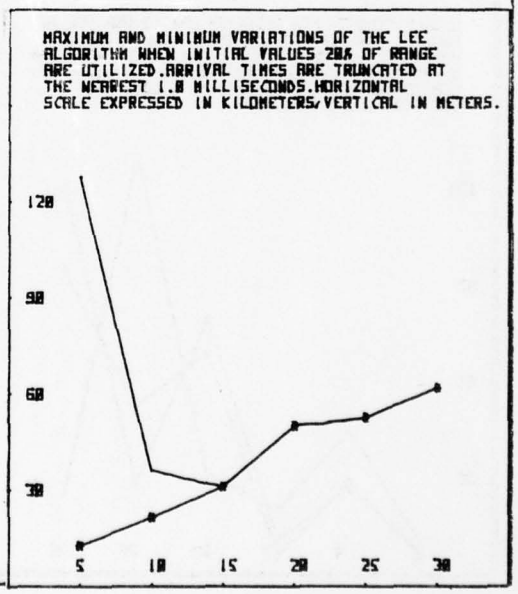

MISS DISTANCE VERSUS RANGE (METERS) FOR SOURCE POINTS LOCATED AT A 15 DEGREE FLANKING ANGLE. SELECTED TRUNCATION POINTS ARE CONSIDERED AS INDICATED BELOW. A TEMPERATURE ERROR OF -1.0 DEGREES KELVIN IS ASSUMED.

FIGURE11

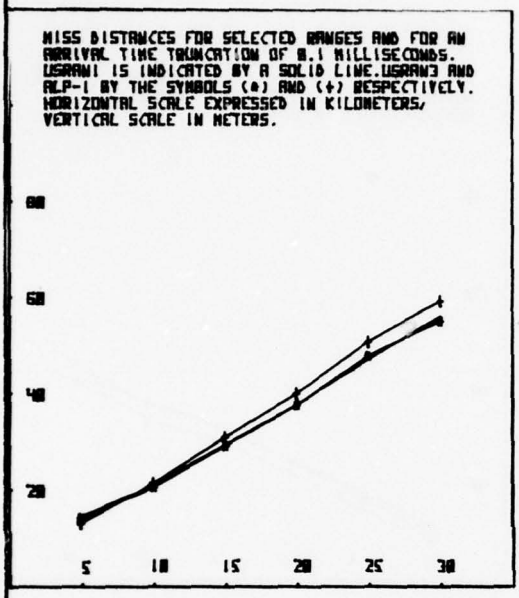

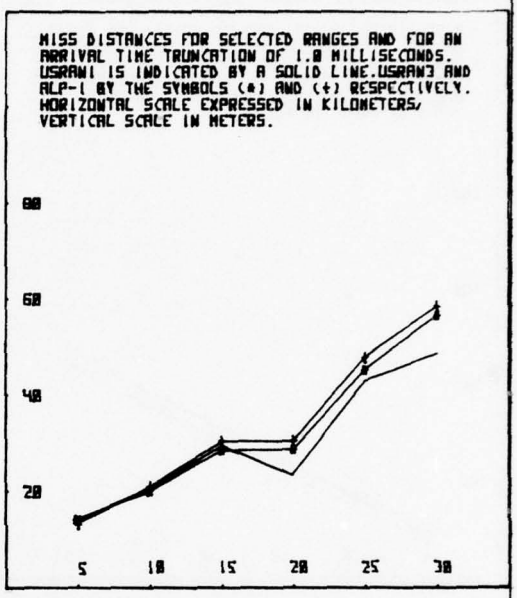

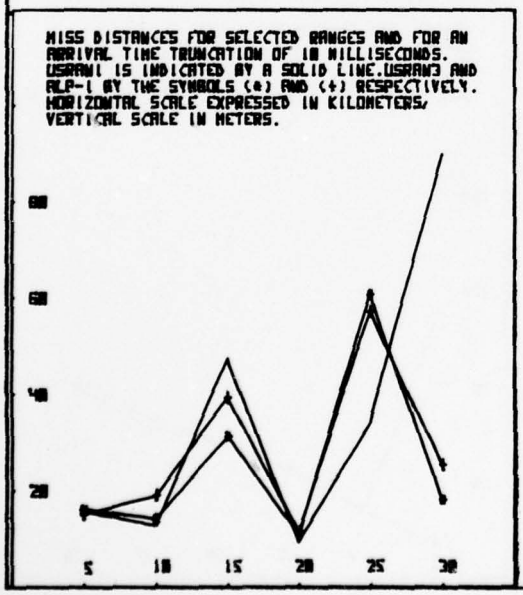

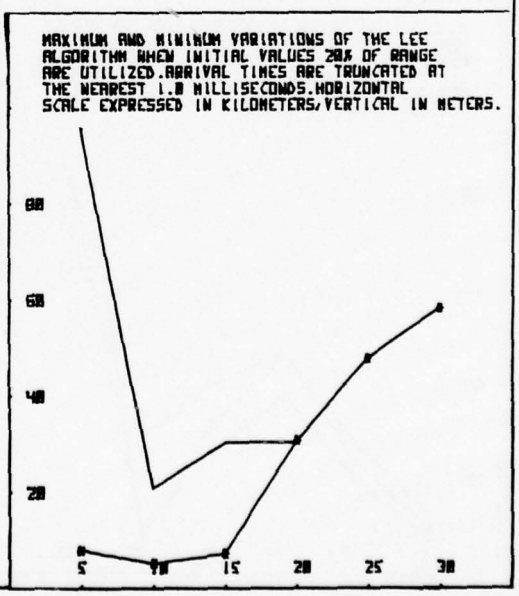

MISS DISTANCE VERSUS RANGE (METERS) FOR SOURCE POINTS LOCATED AT A 30 DEGREE FLANKING ANGLE. SELECTED TRUNCATION POINTS ARE CONSIDERED AS INDICATED BELOW. A TEMPERATURE ERROR OF +1.0 DEGREES KELVIN IS ASSUMED.

FIGURE 12

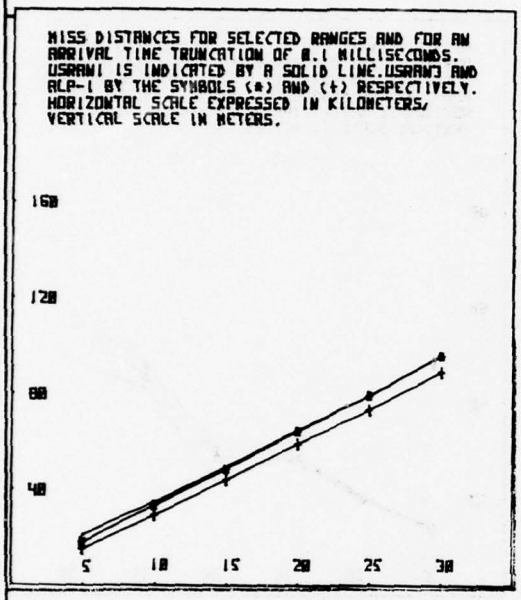

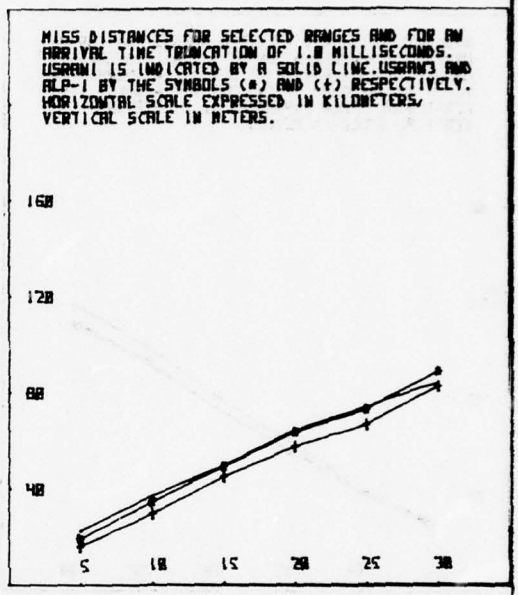

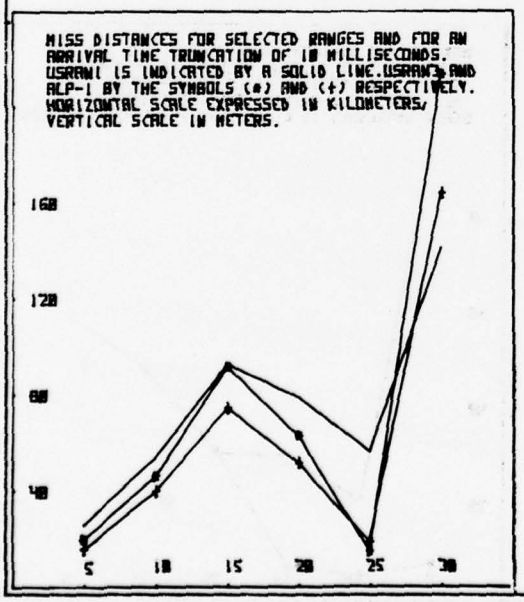

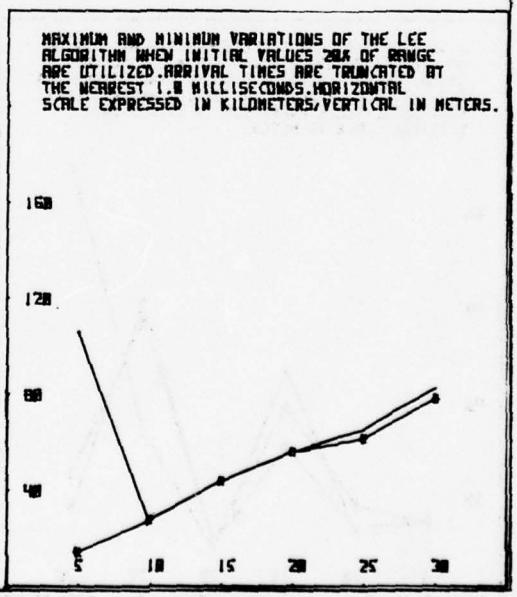

MISS DISTANCE VERSUS RANGE (METERS) FOR SOURCE POINTS LOCATED AT A 30 DEGREE FLANKING ANGLE.SELECTED TRUNCATION POINTS ARE CONSIDERED AS INDICATED BELOW.A TEMPERATURE ERROR OF -1.0 DEGREES KELVIN IS ASSUMED.

FIGURE 13

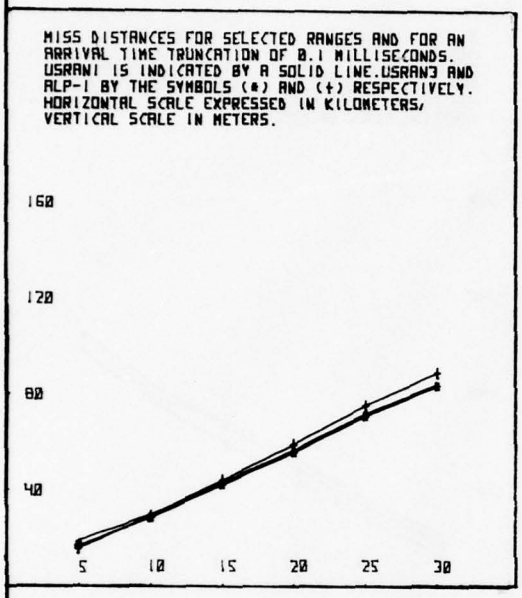

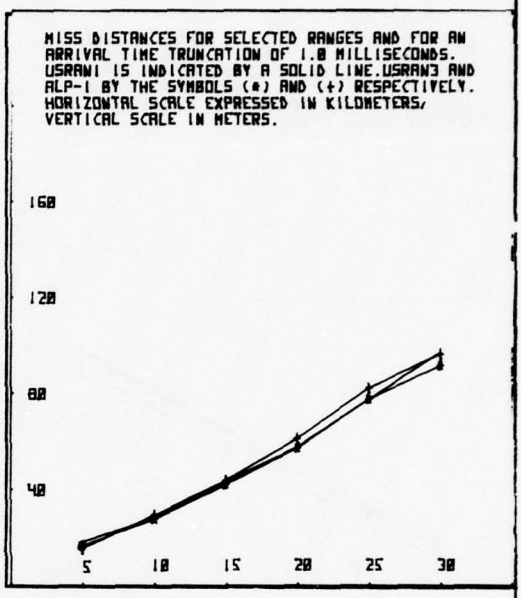

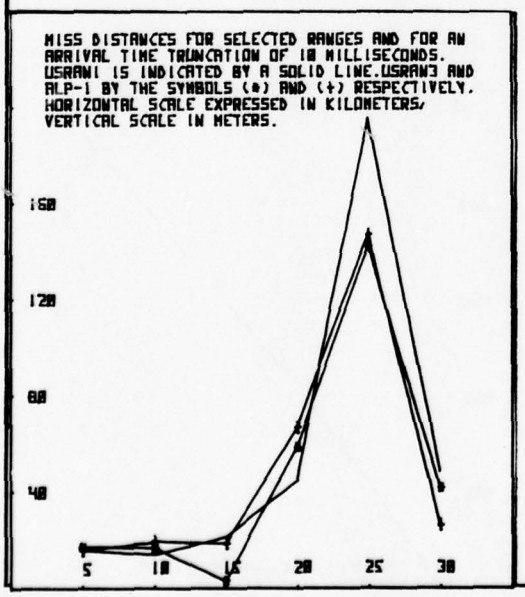

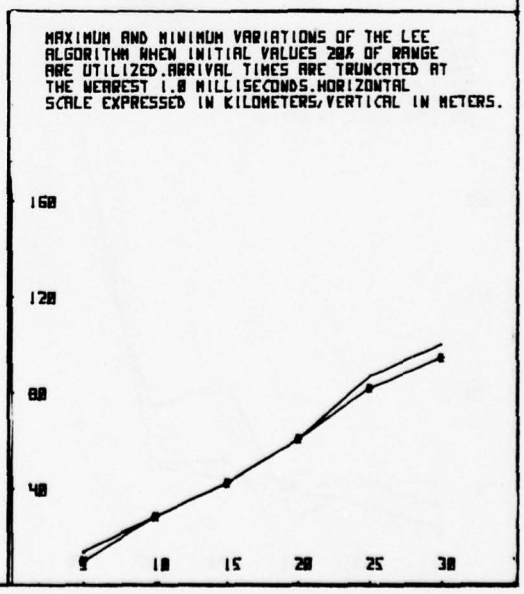

MISS DISTANCE VERSUS RANGE (METERS) FOR SOURCE POINTS LOCATED AT A 45 DEGREE FLANKING ANGLE. SELECTED TRUNCATION POINTS ARE CONSIDERED AS INDICATED BELOW. A TEMPERATURE ERROR OF +1.0 DEGREES KELVIN IS ASSUMED.

FIGURE 14

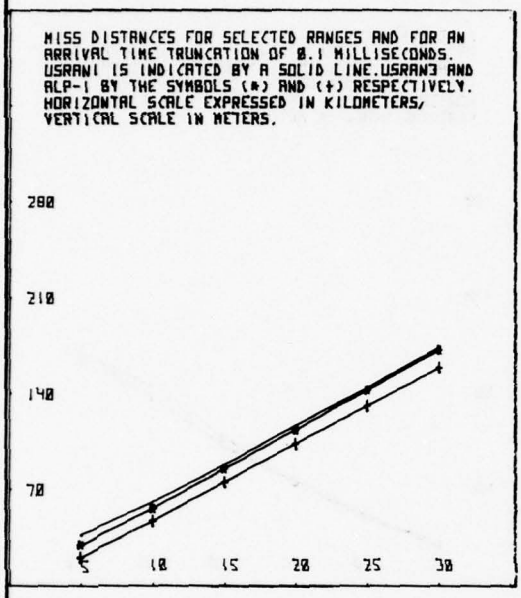

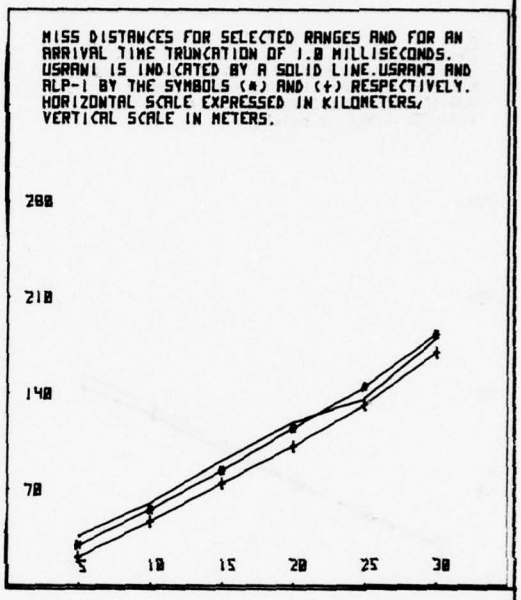

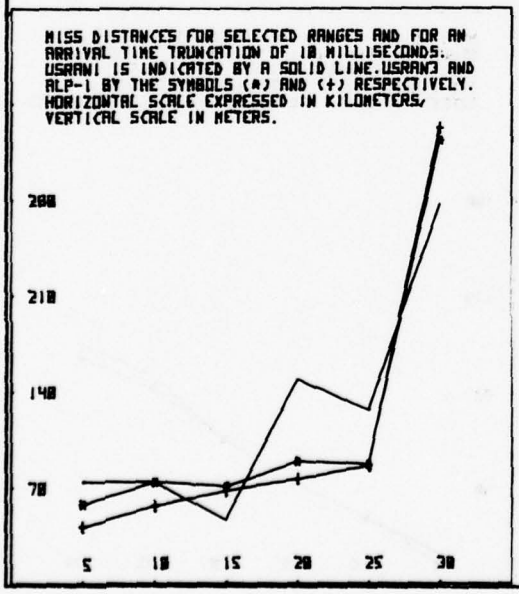

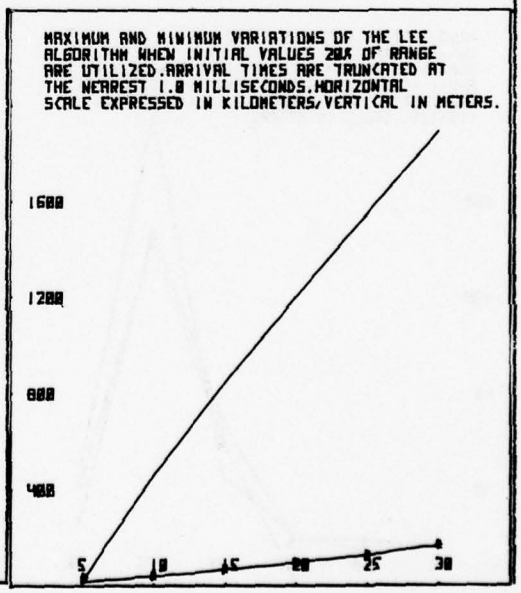

MISS DISTANCE VERSUS RANGE (METERS) FOR SOURCE POINTS LOCATED AT A 45 DEGREE FLANKING ANGLE. SELECTED TRUNCATION POINTS ARE CONSIDERED AS INDICATED BELOW. A TEMPERATURE ERROR OF -1.0 DEGREES KELVIN IS ASSUMED.

FIGURE 15

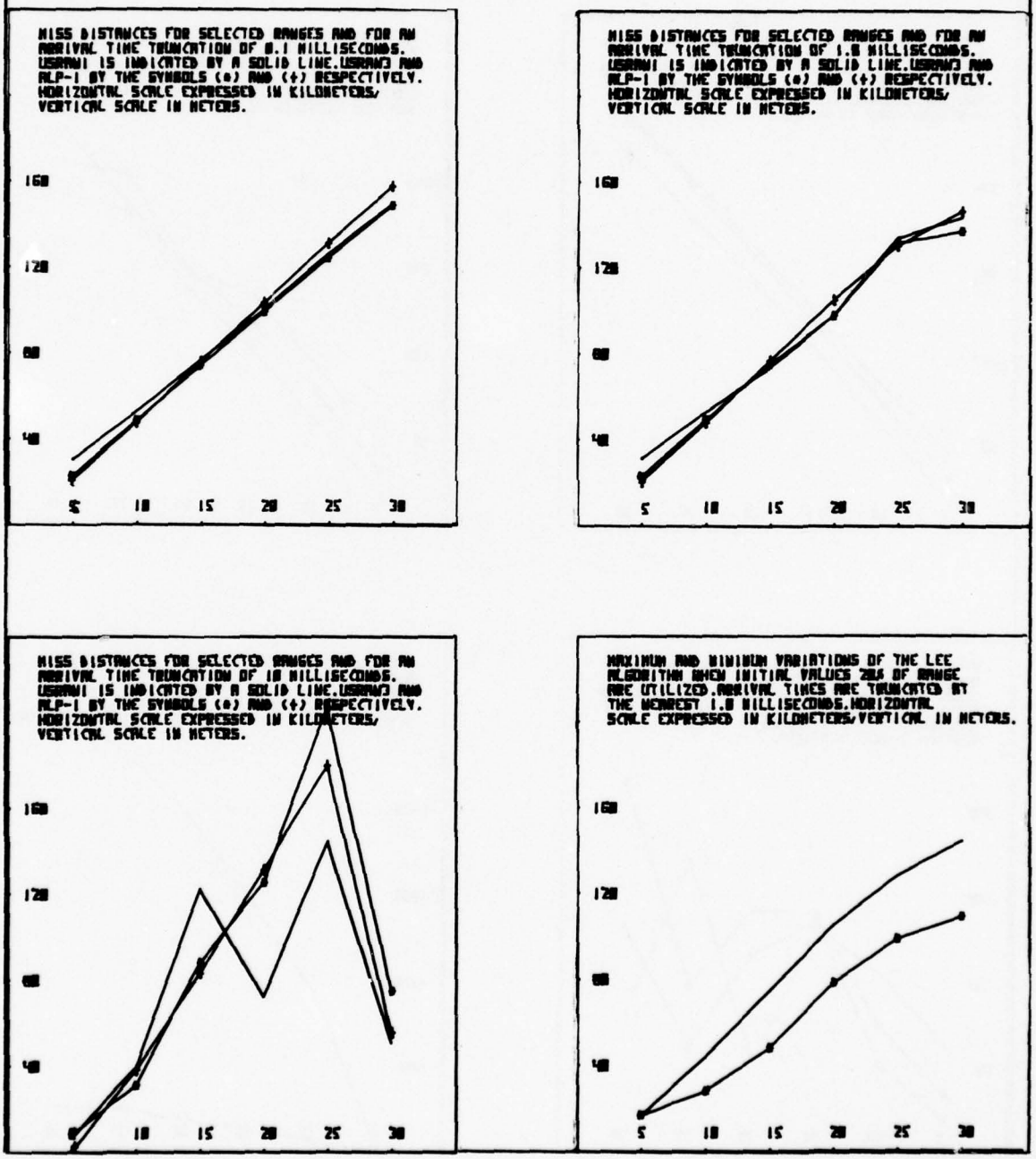

MISS DISTANCE VERSUS RANGE (METERS) FOR SOURCE POINTS LOCATED AT A 60 DEGREE FLANKING ANGLE.SELECTED TRUNCATION POINTS ARE CONSIDERED AS INDICATED BELOW.A TEMPERATURE ERROR OF +1.0 DEGREES KELVIN IS ASSUMED.

FIGURE 16

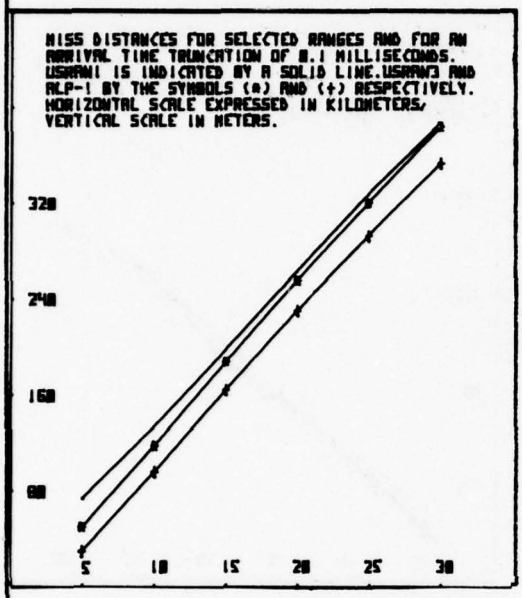

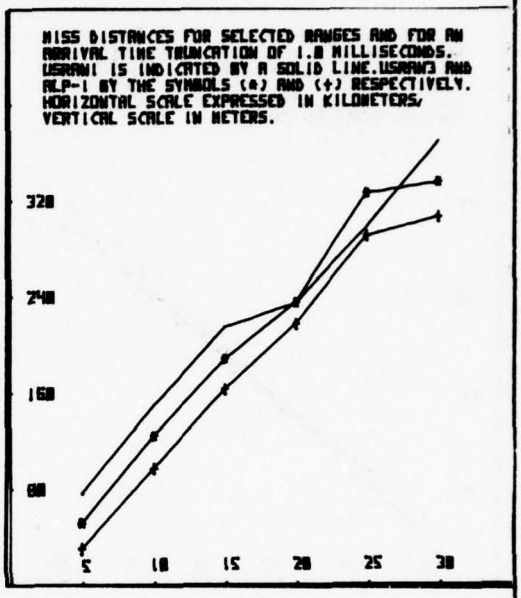

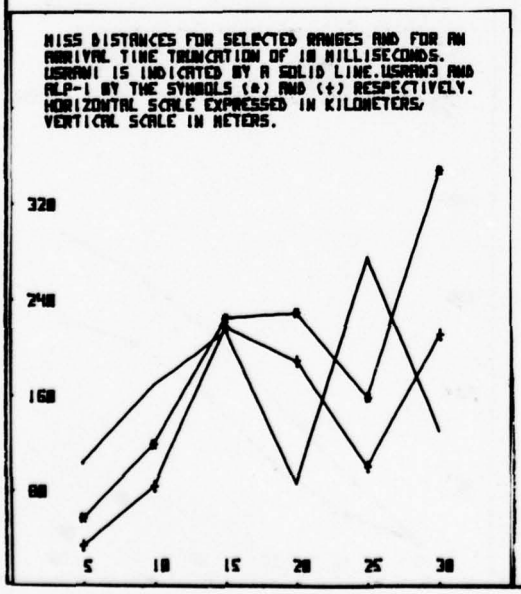

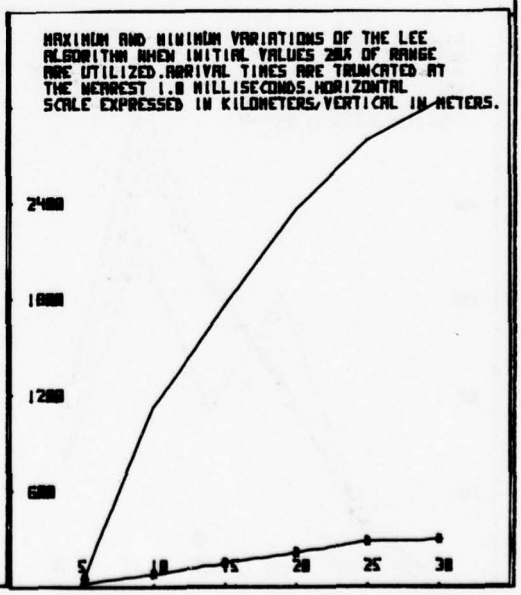

MISS DISTANCE VERSUS RANGE (METERS) FOR SOURCE POINTS LOCATED AT A 60 DEGREE FLANKING ANGLE.SELECTED TRUNCATION POINTS ARE CONSIDERED AS INDICATED BELOW.A TEMPERATURE ERROR OF -1.0 DEGREES KELVIN IS ASSUMED.

FIGURE 17

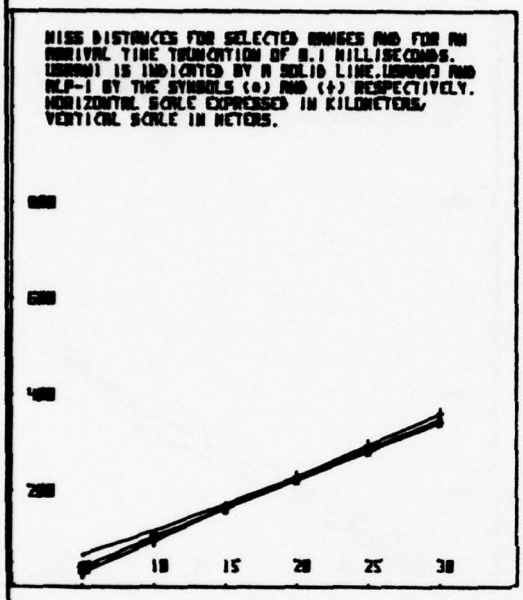

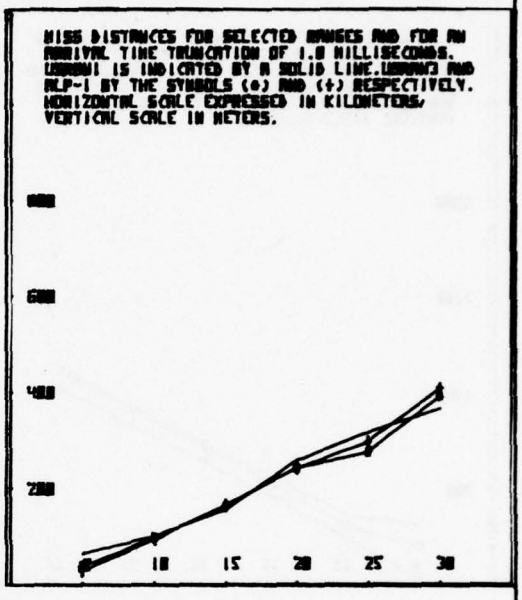

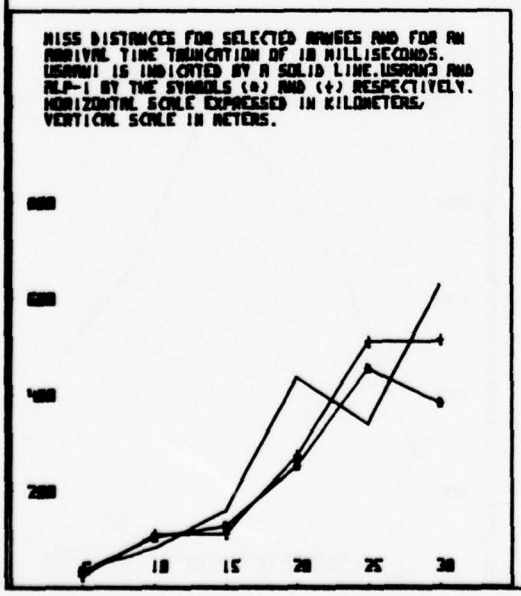

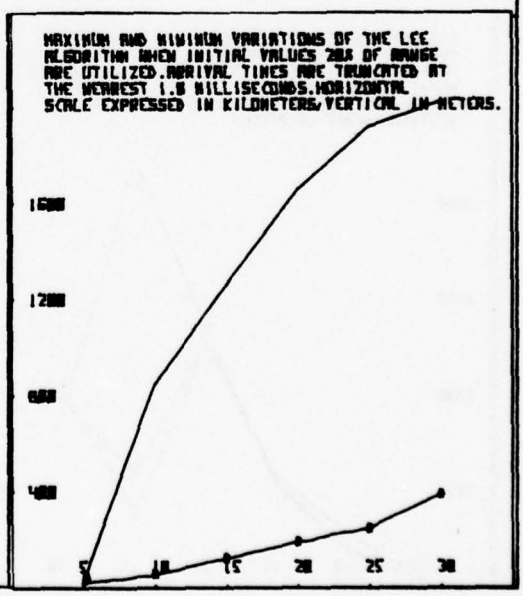

MISS DISTANCE VERSUS RANGE (METERS) FOR SOURCE POINTS LOCATED AT A 75 DEGREE FLANKING ANGLE. SELECTED TRUNCATION POINTS ARE CONSIDERED AS INDICATED BELOW. A TEMPERATURE ERROR OF +1.0 DEGREES KELVIN IS ASSUMED.

FIGURE 18

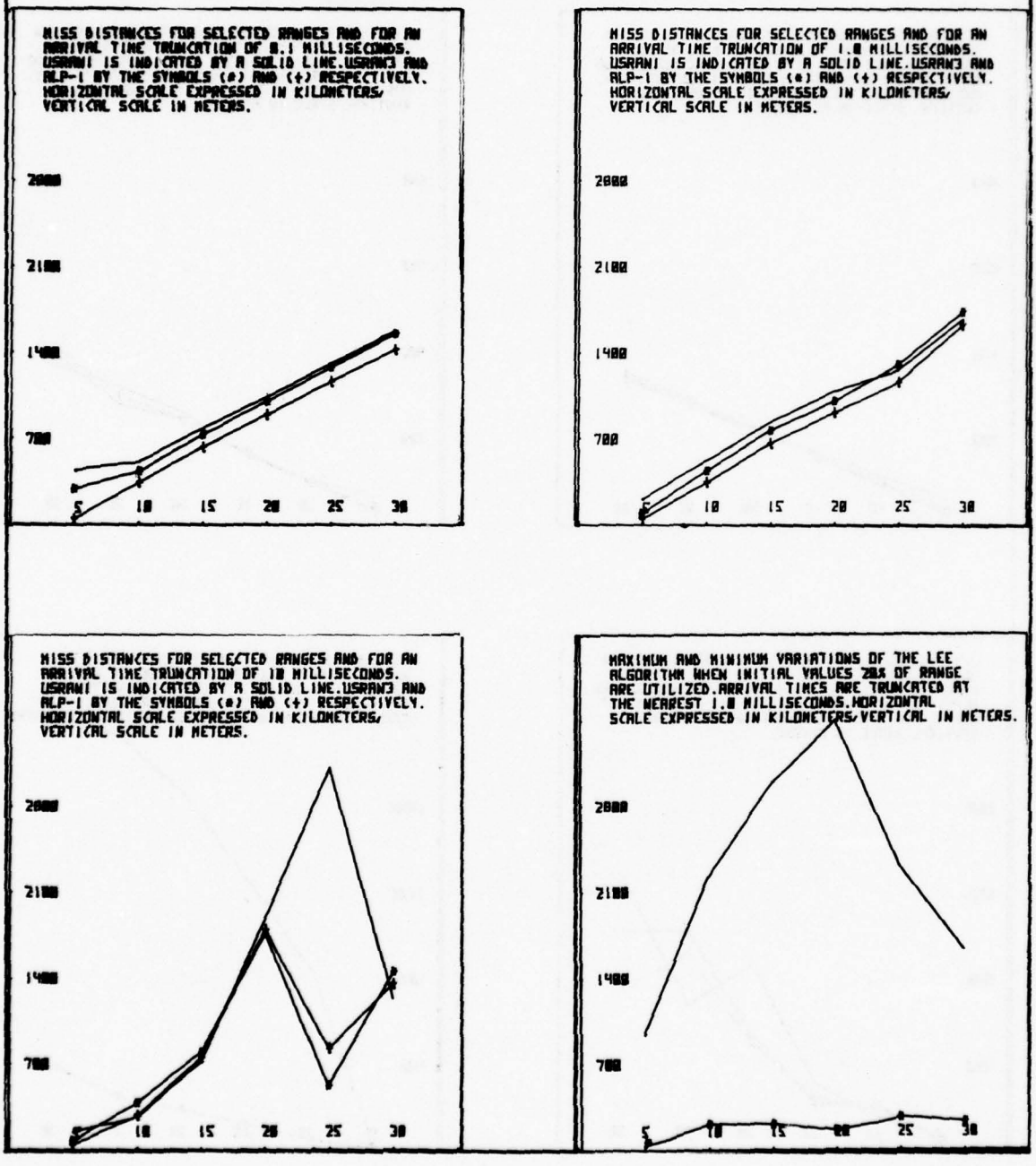

MISS DISTANCE VERSUS RANGE (METERS) FOR SOURCE POINTS LOCATED AT A 75 DEGREE FLANKING ANGLE. SELECTED TRUNCATION POINTS ARE CONSIDERED AS INDICATED BELOW. A TEMPERATURE ERROR OF -1.0 DEGREES KELVIN IS ASSUMED.

FIGURE 19

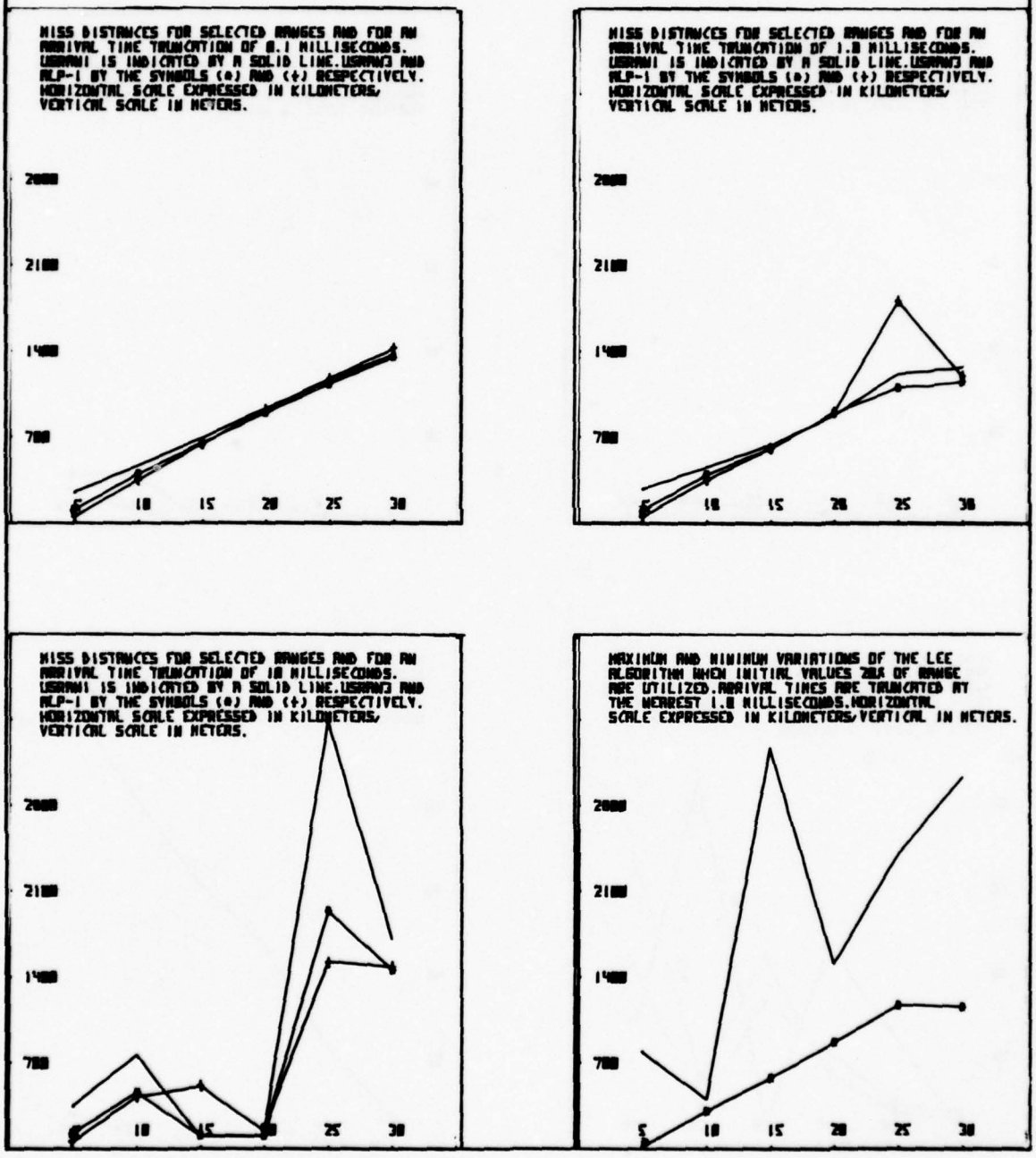

MISS DISTANCE VERSUS RANGE (METERS) FOR SOURCE POINTS LOCATED AT A 0 DEGREE FLANKING ANGLE. SELECTED TRUNCATION POINTS ARE CONSIDERED AS INDICATED BELOW. IN ADDITION, AN ERROR OF ONE METER PER SECOND IS ASSUMED IN THE SOUTH WIND COMPONENT.

FIGURE 20

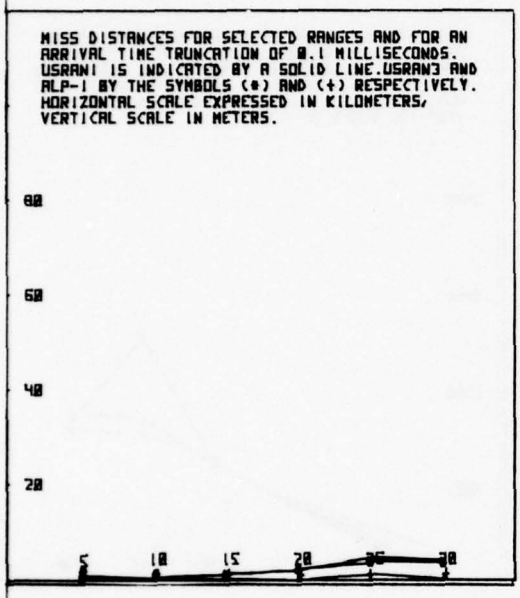

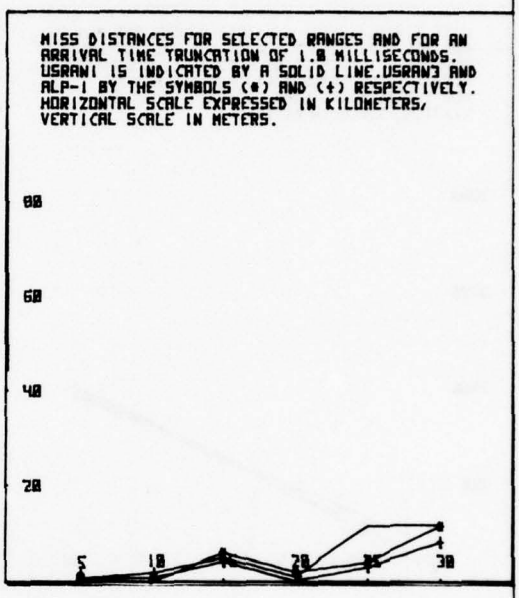

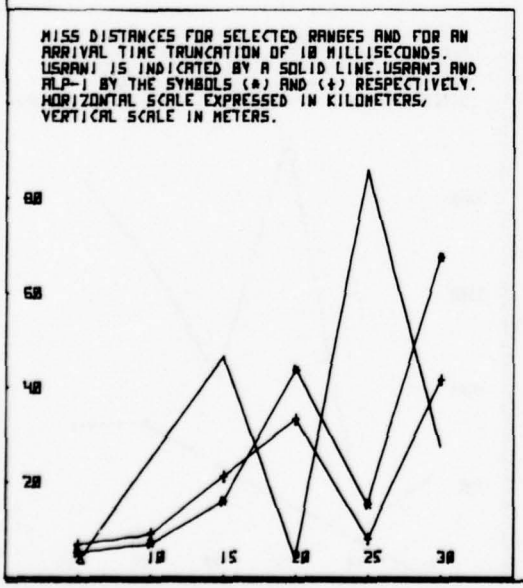

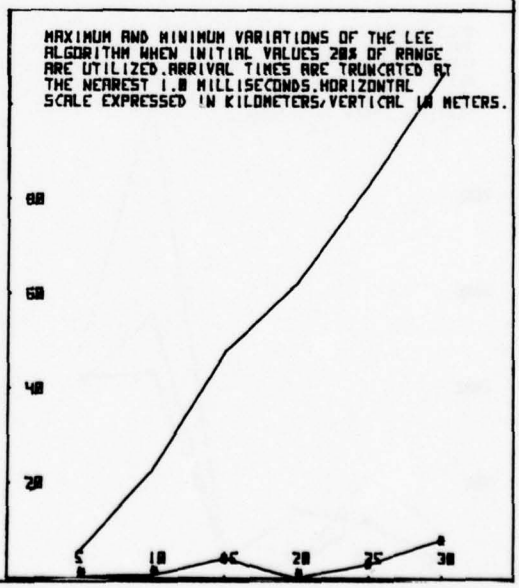

MISS DISTANCE VERSUS RANGE (METERS) FOR SOURCE POINTS LOCATED AT A 15 DEGREE FLANKING ANGLE. SELECTED TRUNCATION POINTS ARE CONSIDERED AS INDICATED BELOW. IN ADDITION, AN ERROR OF ONE METER PER SECOND IS ASSUMED IN THE SOUTH WIND COMPONENT.

FIGURE 21

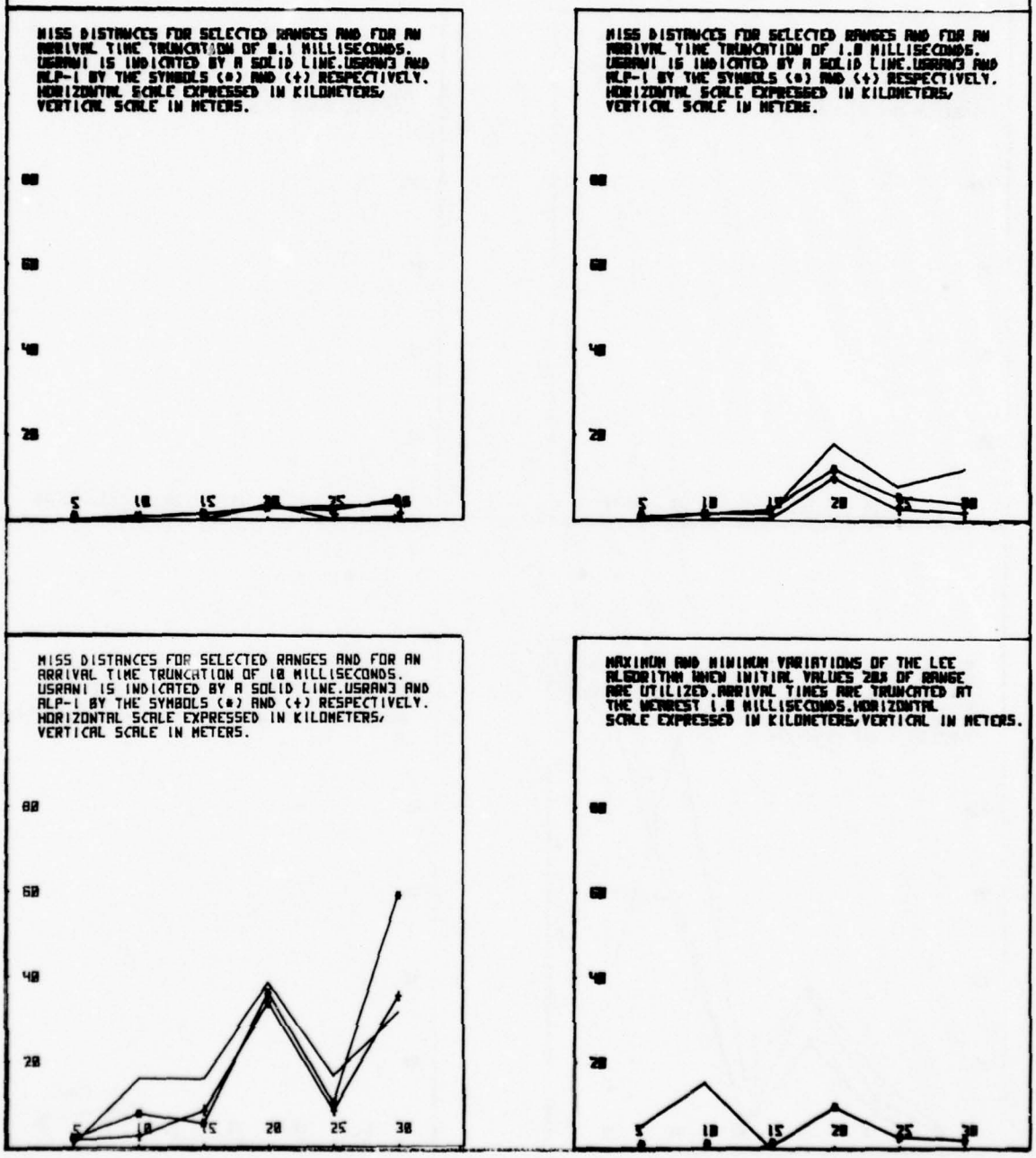

MISS DISTANCE VERSUS RANGE (METERS) FOR SOURCE POINTS LOCATED AT A 30 DEGREE FLANKING ANGLE. SELECTED TRUNCATION POINTS ARE CONSIDERED AS INDICATED BELOW. IN ADDITION, AN ERROR OF ONE METER PER SECOND IS ASSUMED IN THE SOUTH WIND COMPONENT.

FIGURE 22

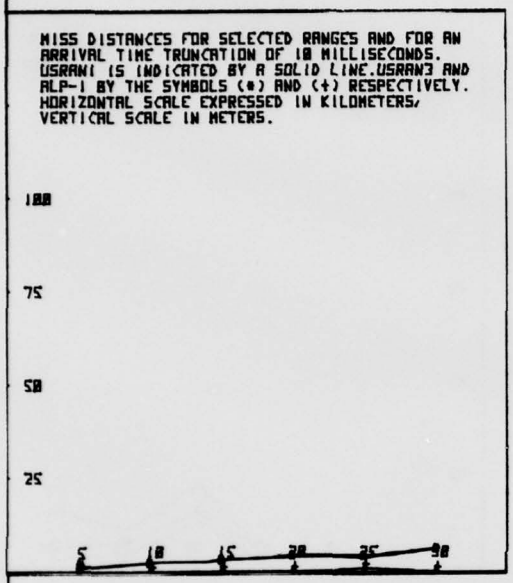

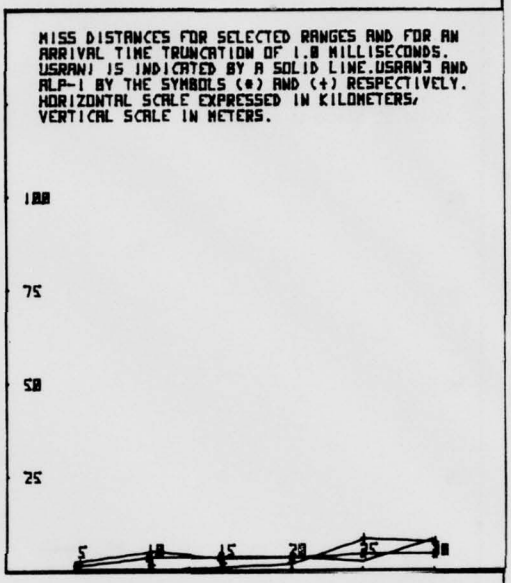

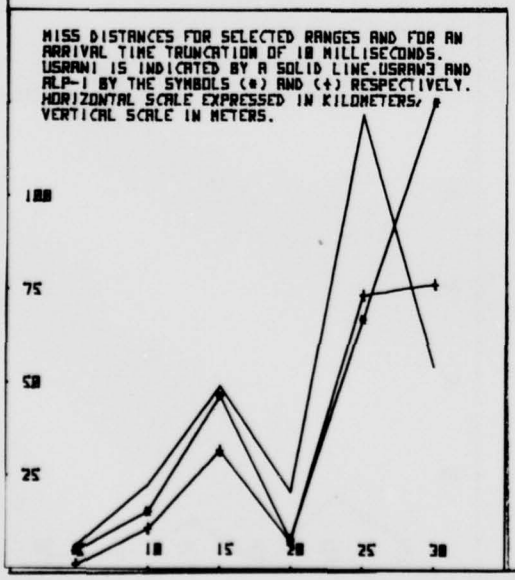

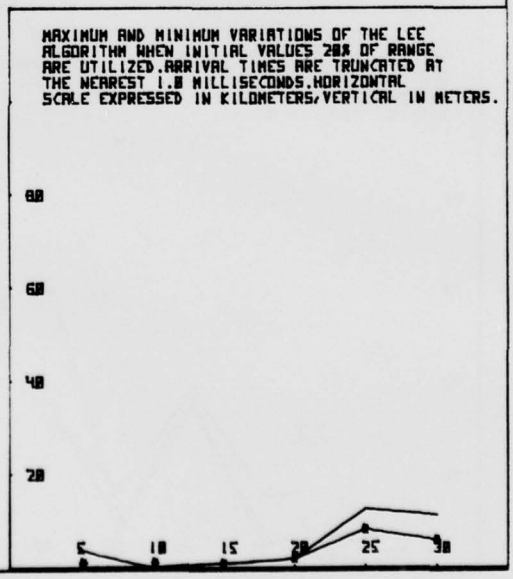

MISS DISTANCE VERSUS RANGE (METERS) FOR SOURCE POINTS LOCATED AT A 45 DEGREE FLANKING ANGLE. SELECTED TRUNCATION POINTS ARE CONSIDERED AS INDICATED BELOW. IN ADDITION, AN ERROR OF ONE METER PER SECOND IS ASSUMED IN THE SOUTH WIND COMPONENT.

FIGURE 23

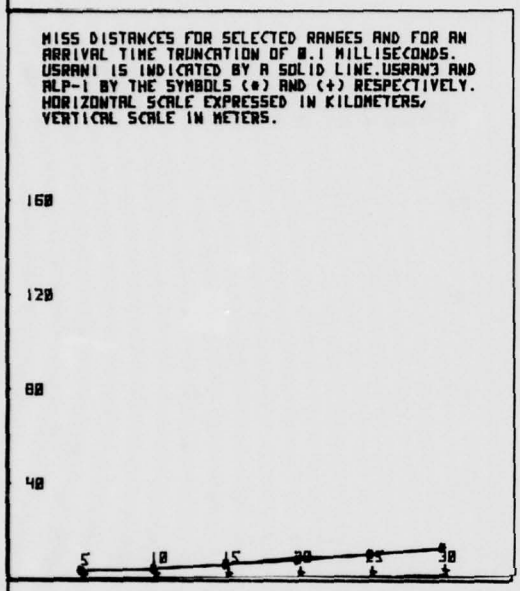

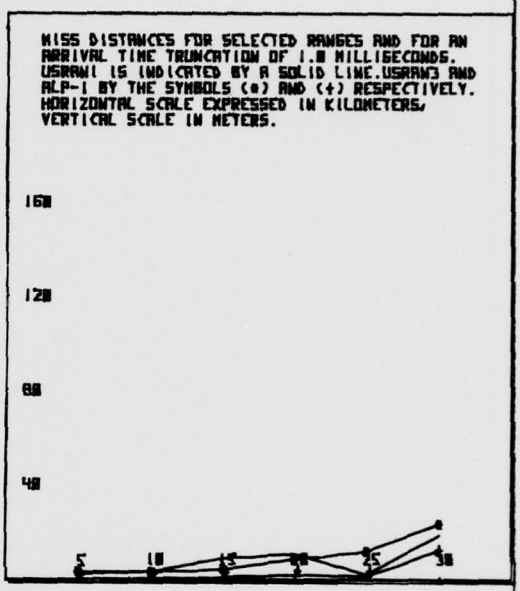

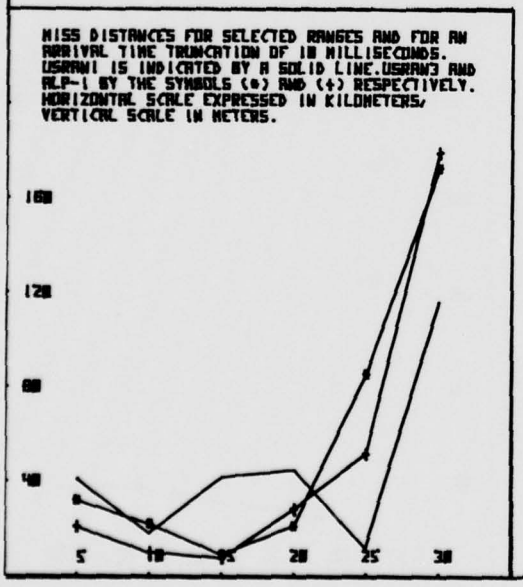

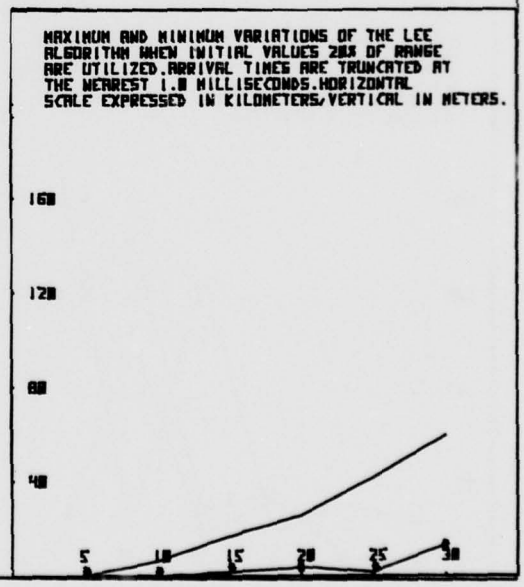

MISS DISTANCE VERSUS RANGE (METERS) FOR SOURCE POINTS LOCATED AT A 60 DEGREE FLANKING ANGLE. SELECTED TRUNCATION POINTS ARE CONSIDERED AS INDICATED BELOW. IN ADDITION, AN ERROR OF ONE METER PER SECOND IS ASSUMED IN THE SOUTH WIND COMPONENT.

FIGURE 24

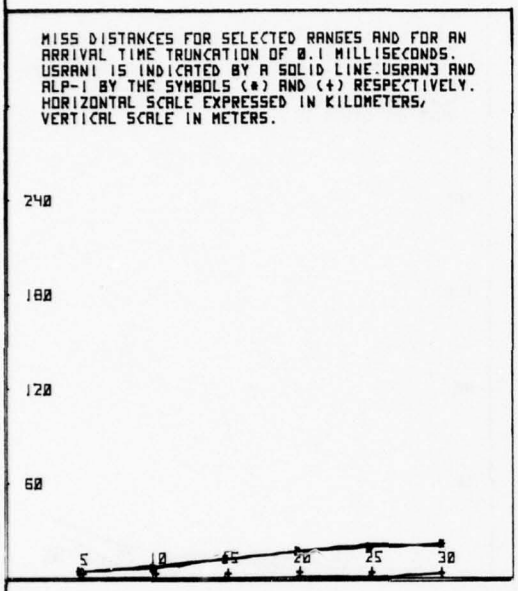

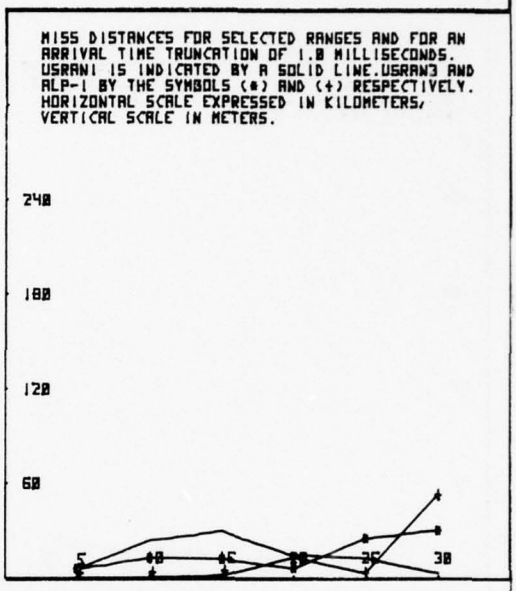

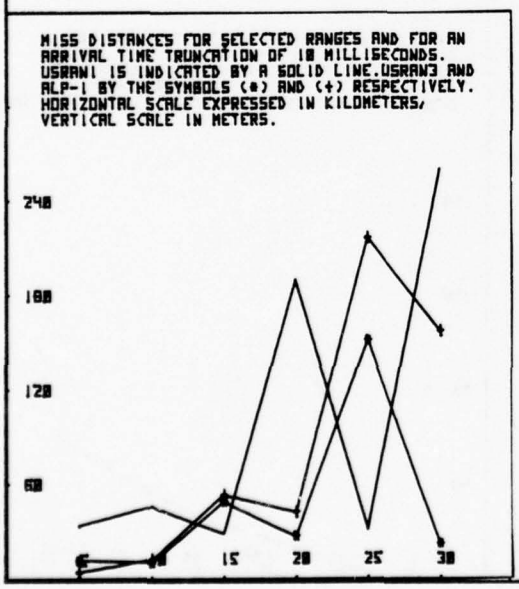

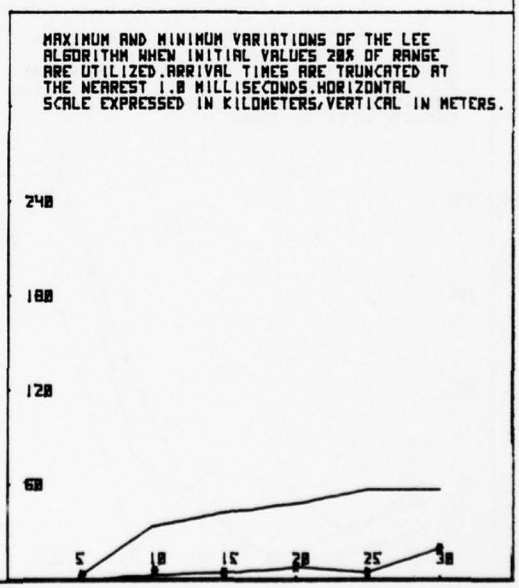

MISS DISTANCE VERSUS RANGE (METERS) FOR SOURCE POINTS LOCATED AT A 75 DEGREE FLANKING ANGLE. SELECTED TRUNCATION POINTS ARE CONSIDERED AS INDICATED BELOW. IN ADDITION, AN ERROR OF ONE METER PER SECOND IS ASSUMED IN THE SOUTH WIND COMPONENT.

FIGURE 25

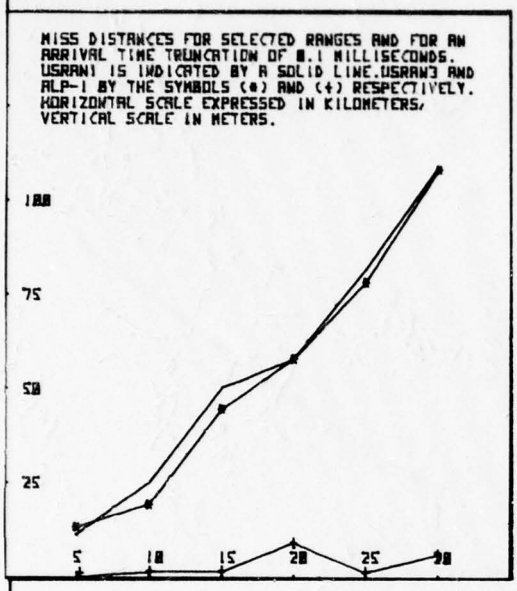

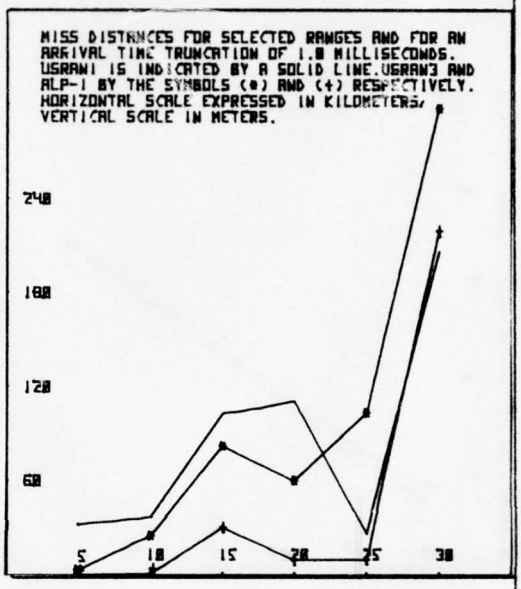

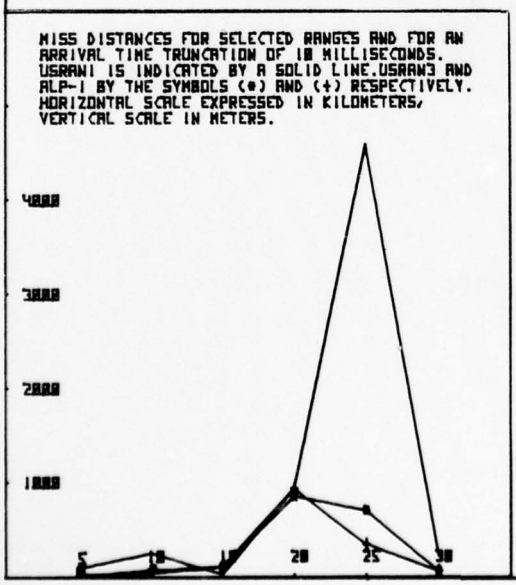

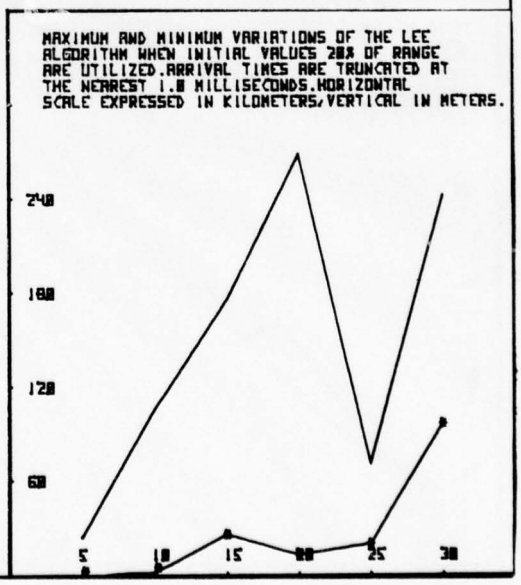

MISS DISTANCE VERSUS RANGE (METERS) FOR SOURCE POINTS LOCATED AT A 0 DEGREE FLANKING ANGLE. SELECTED TRUNCATION POINTS ARE CONSIDERED AS INDICATED BELOW. IN ADDITION, AN ERROR OF ONE METER PER SECOND IS ASSUMED IN THE WEST WIND COMPONENT.

FIGURE 26

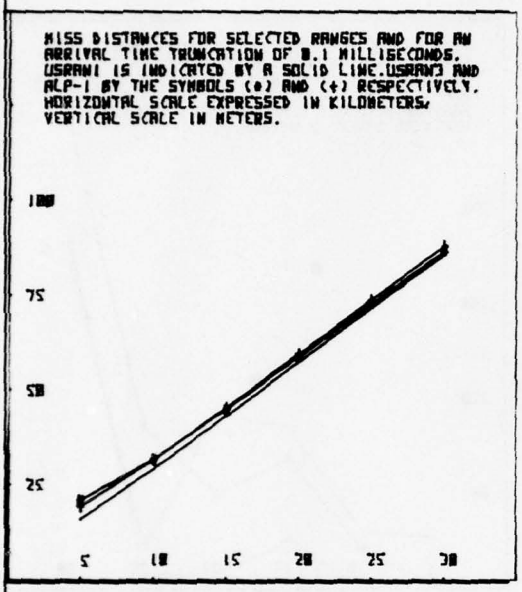

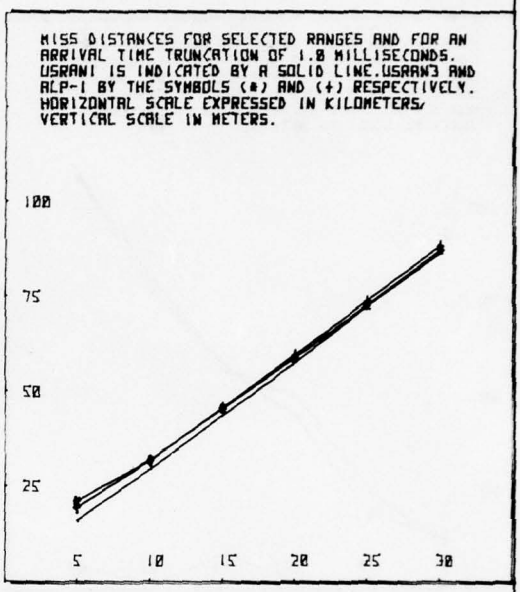

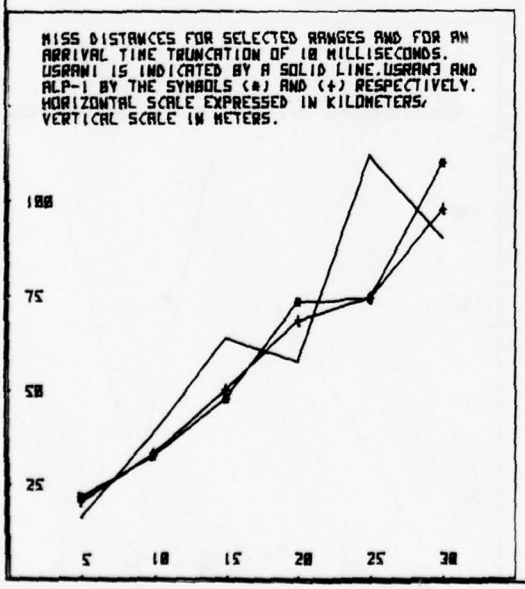

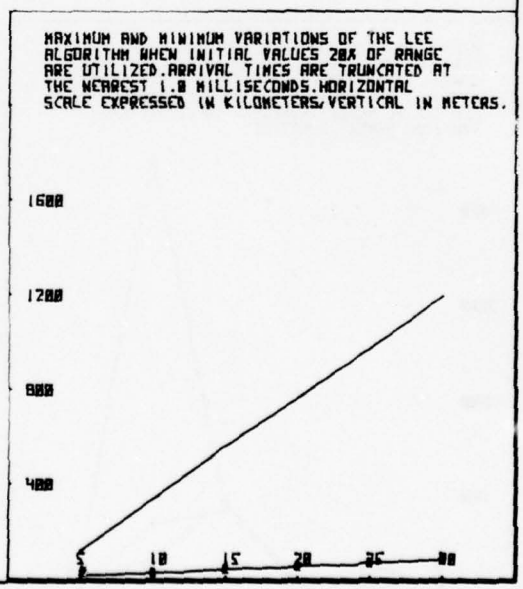

MISS DISTANCE VERSUS RANGE (METERS) FOR SOURCE POINTS LOCATED AT A 0 DEGREE FLANKING ANGLE. SELECTED TRUNCATION POINTS ARE CONSIDERED AS INDICATED BELOW. IN ADDITION, AN ERROR OF ONE METER PER SECOND IS ASSUMED IN THE EAST WIND COMPONENT.

FIGURE 27

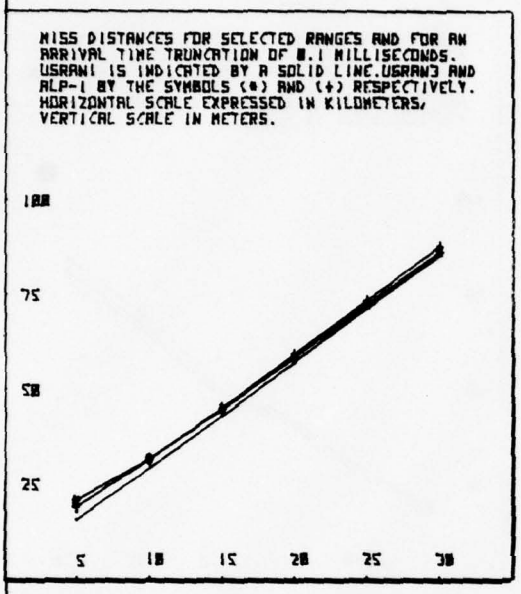

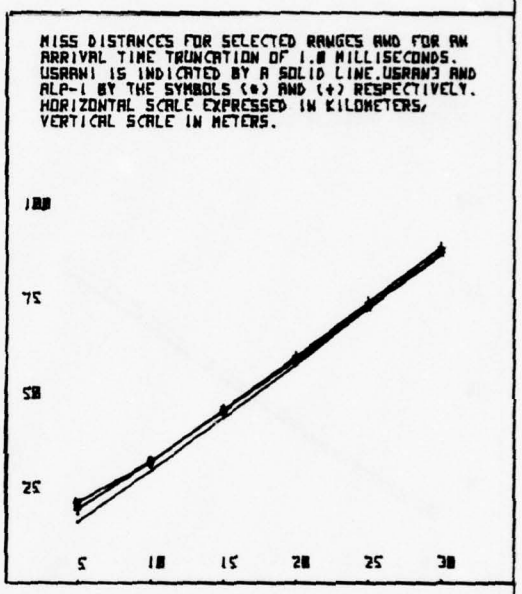

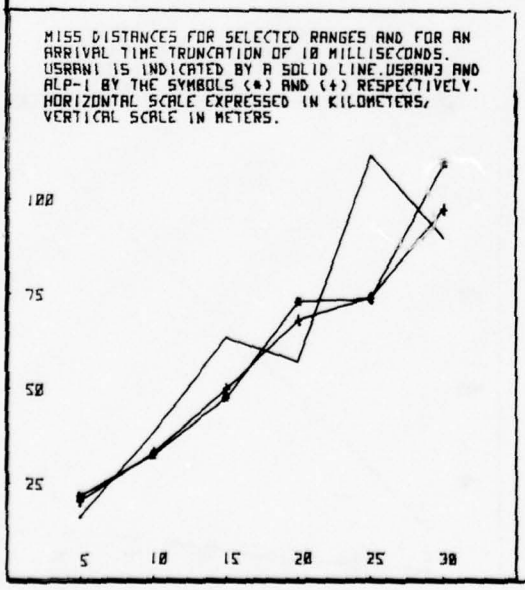

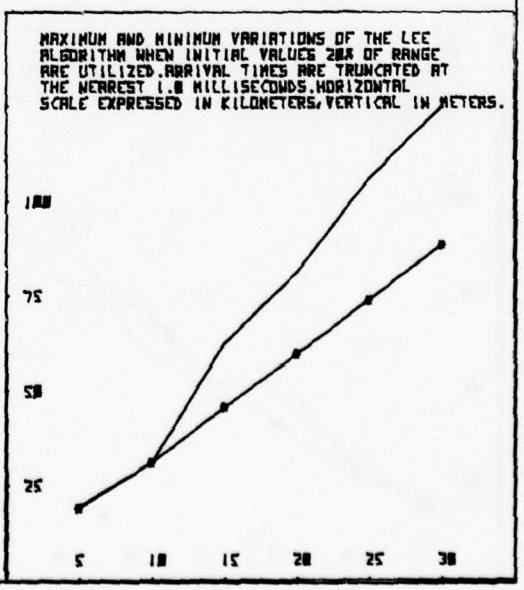

MISS DISTANCE VERSUS RANGE (METERS) FOR SOURCE POINTS LOCATED AT A 15 DEGREE FLANKING ANGLE. SELECTED TRUNCATION POINTS ARE CONSIDERED AS INDICATED BELOW. IN ADDITION, AN ERROR OF ONE METER PER SECOND IS ASSUMED IN THE WEST WIND COMPONENT.

FIGURE 28

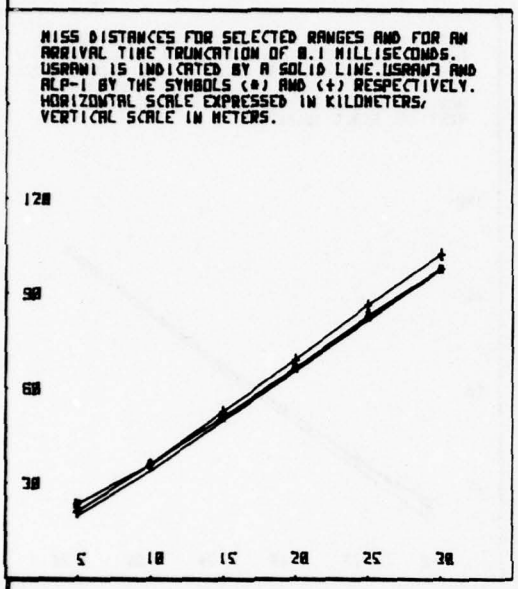

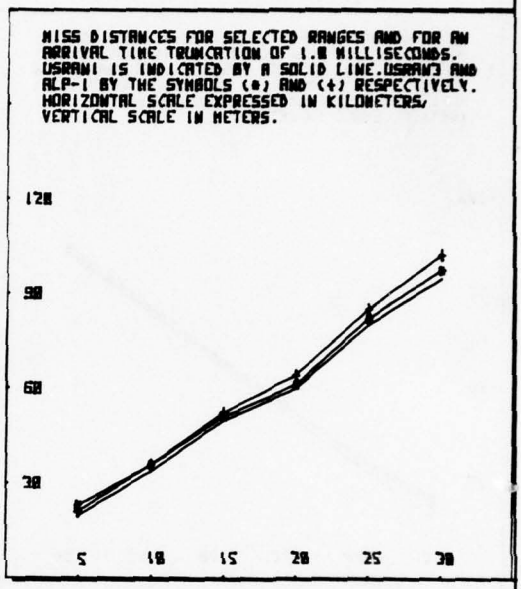

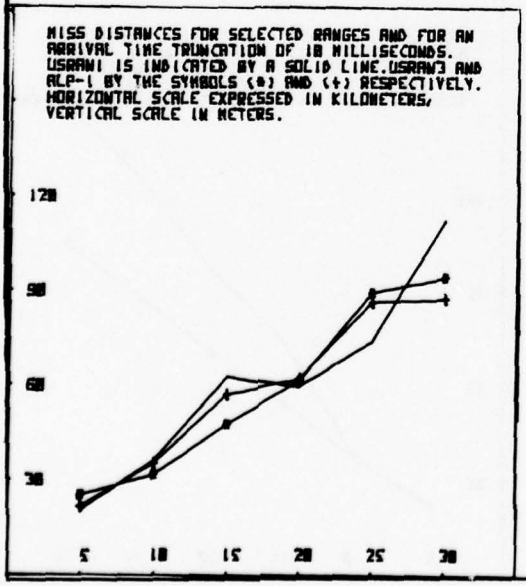

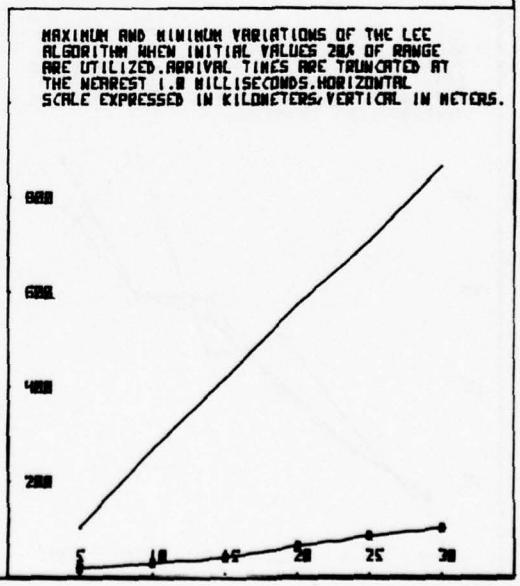

MISS DISTANCE VERSUS RANGE (METERS) FOR SOURCE POINTS LOCATED AT A 15 DEGREE FLANKING ANGLE. SELECTED TRUNCATION POINTS ARE CONSIDERED AS INDICATED BELOW. IN ADDITION, AN ERROR OF ONE METER PER SECOND IS ASSUMED IN THE EAST WIND COMPONENT.

FIGURE 29

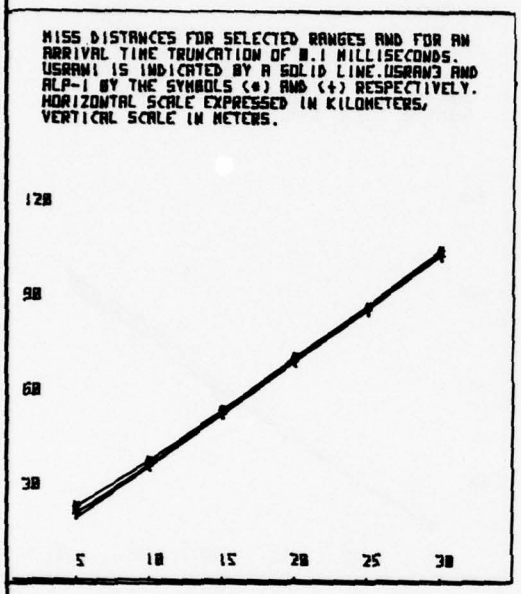

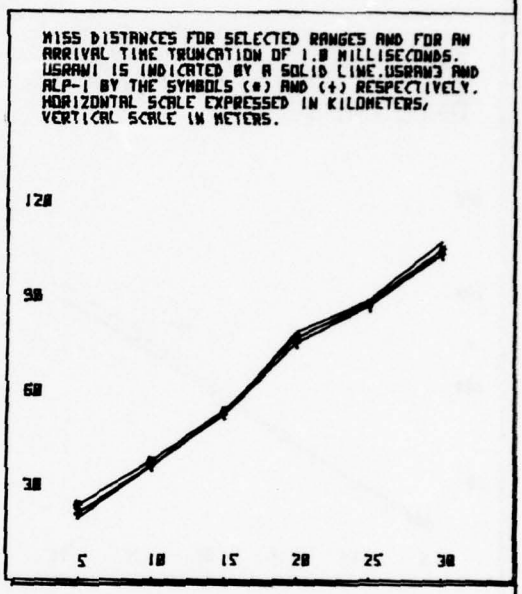

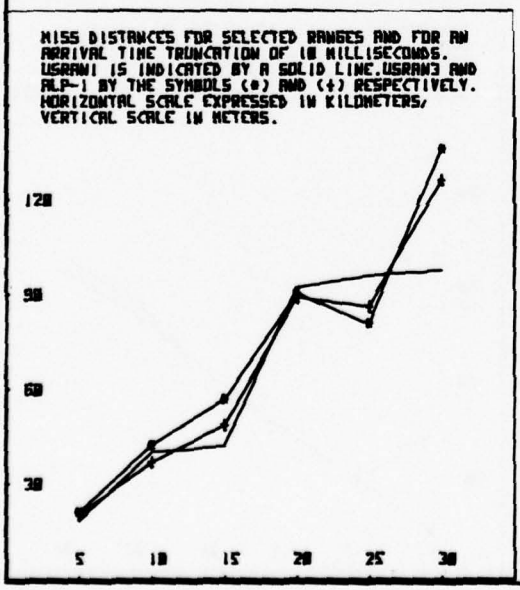

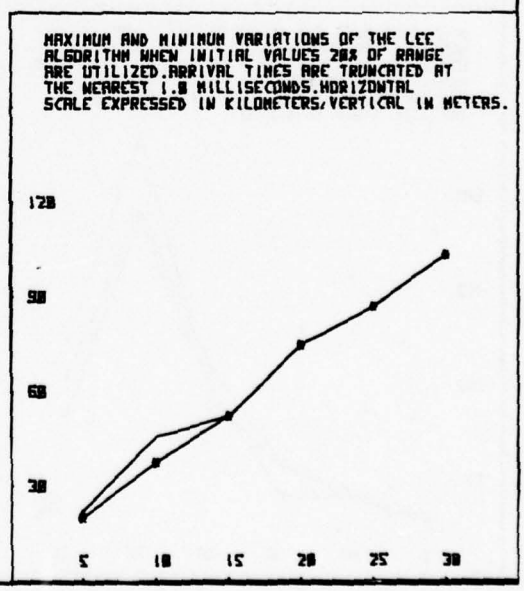

MISS DISTANCE VERSUS RANGE (METERS) FOR SOURCE POINTS LOCATED AT A 30 DEGREE FLANKING ANGLE. SELECTED TRUNCATION POINTS ARE CONSIDERED AS INDICATED BELOW. IN ADDITION, AN ERROR OF ONE METER PER SECOND IS ASSUMED IN THE WEST WIND COMPONENT.

FIGURE 30

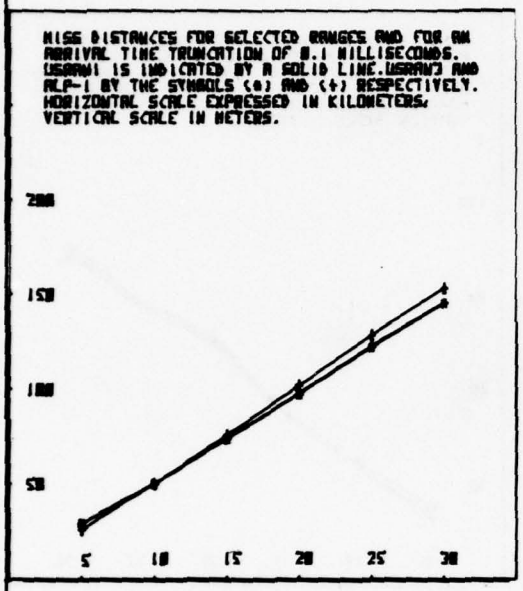

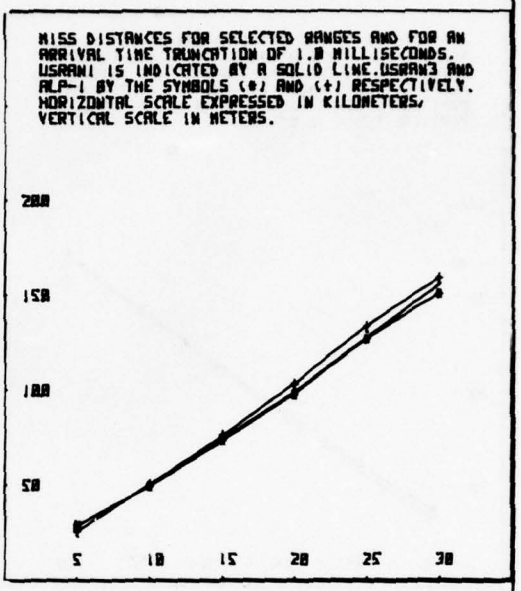

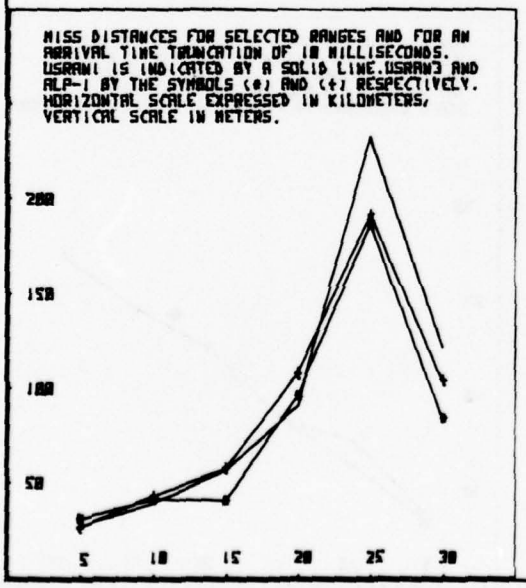

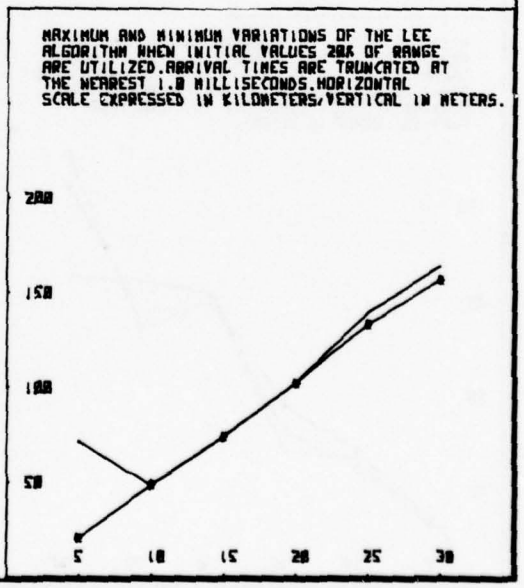

MISS DISTANCE VERSUS RANGE (METERS) FOR SOURCE POINTS LOCATED AT A 30 DEGREE FLANKING ANGLE. SELECTED TRUNCATION POINTS ARE CONSIDERED AS INDICATED BELOW. IN ADDITION, AN ERROR OF ONE METER PER SECOND IS ASSUMED IN THE EAST WIND COMPONENT.

FIGURE 31

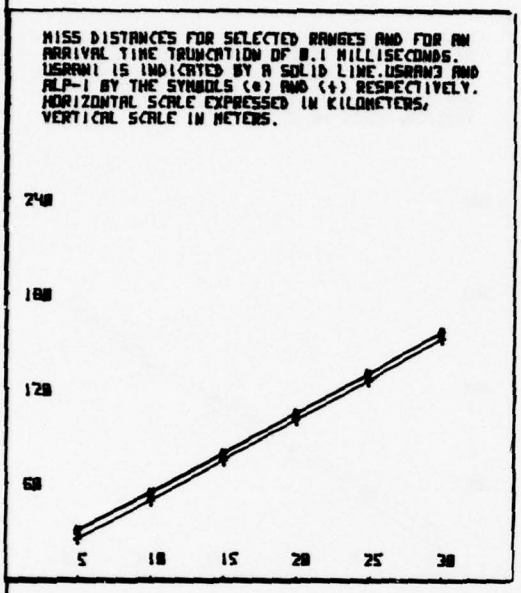

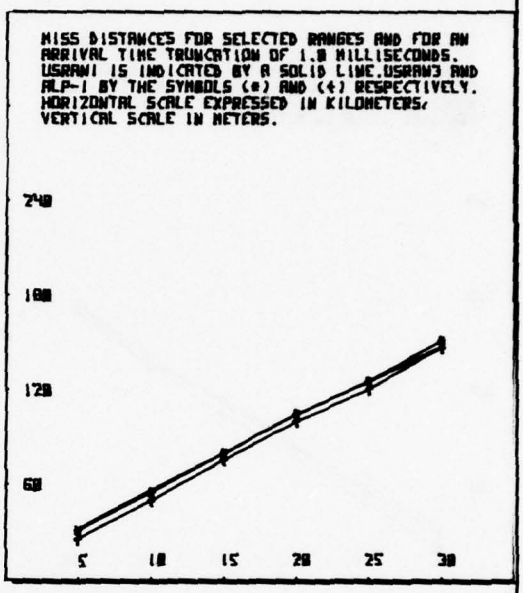

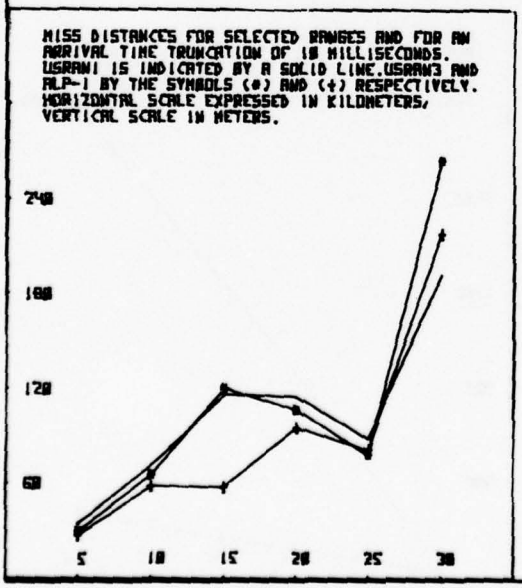

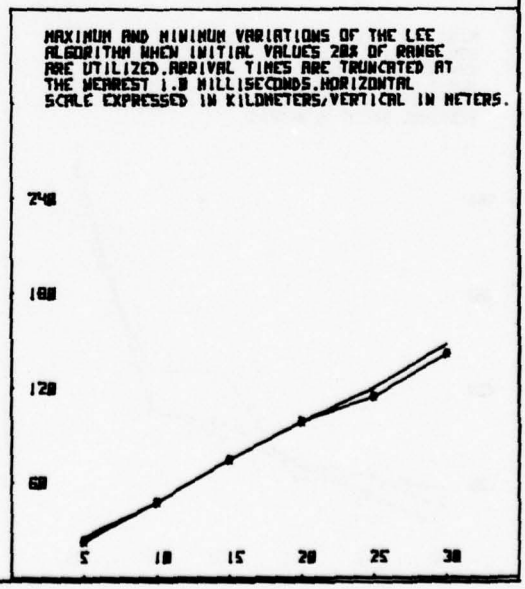

MISS DISTANCE VERSUS RANGE (METERS) FOR SOURCE POINTS LOCATED AT A 45 DEGREE FLANKING ANGLE. SELECTED TRUNCATION POINTS ARE CONSIDERED AS INDICATED BELOW. IN ADDITION, AN ERROR OF ONE METER PER SECOND IS ASSUMED IN THE EAST WIND COMPONENT.

FIGURE 32

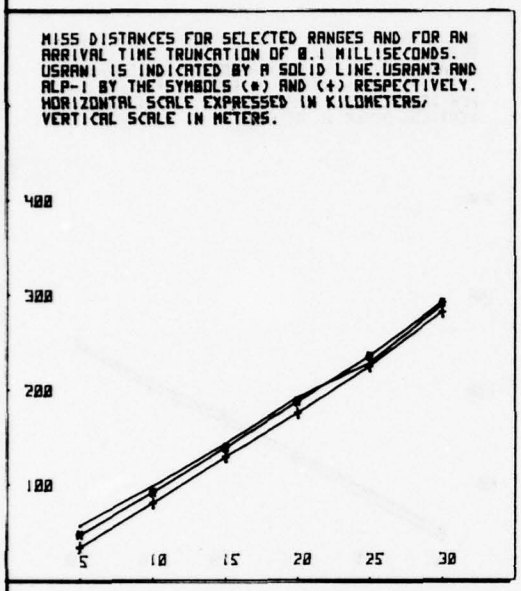

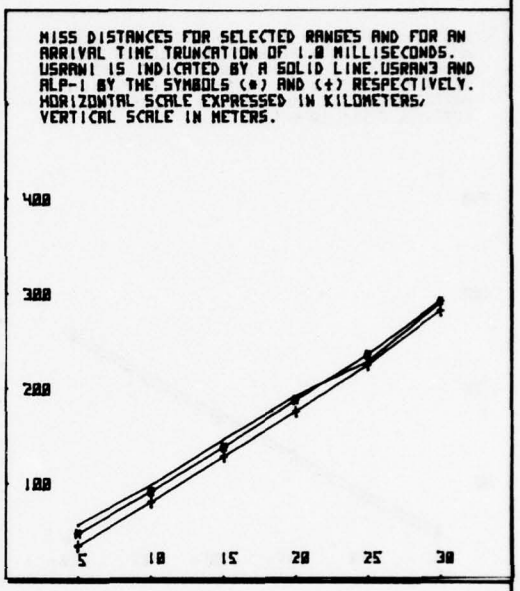

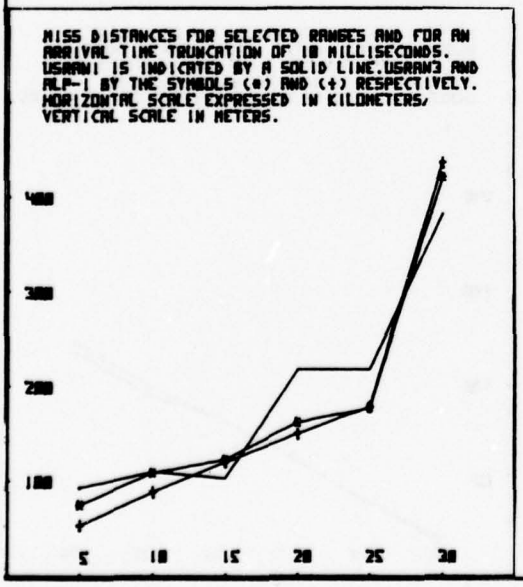

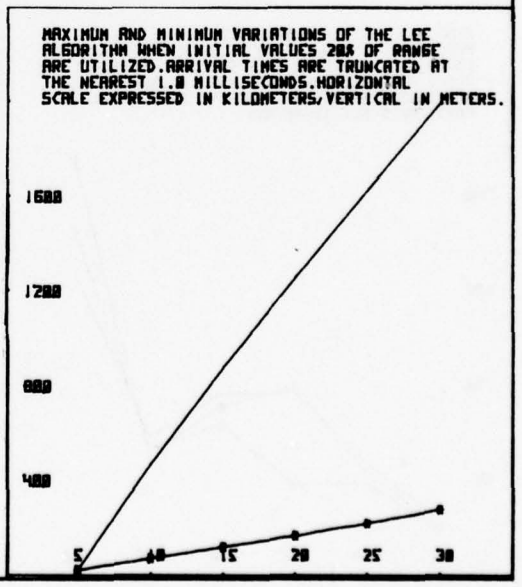

MISS DISTANCE VERSUS RANGE (METERS) FOR SOURCE POINTS LOCATED AT A 45 DEGREE FLANKING ANGLE. SELECTED TRUNCATION POINTS ARE CONSIDERED AS INDICATED BELOW. IN ADDITION, AN ERROR OF ONE METER PER SECOND IS ASSUMED IN THE WEST WIND COMPONENT.

FIGURE 33

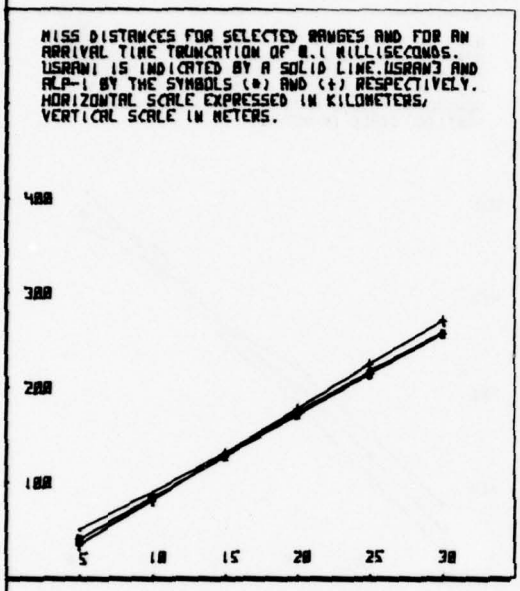

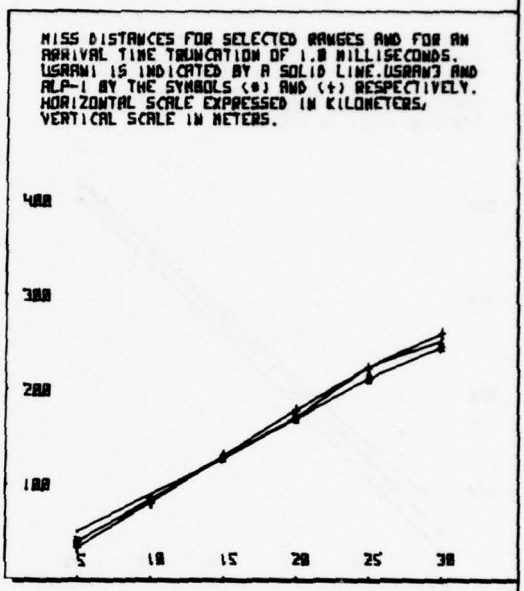

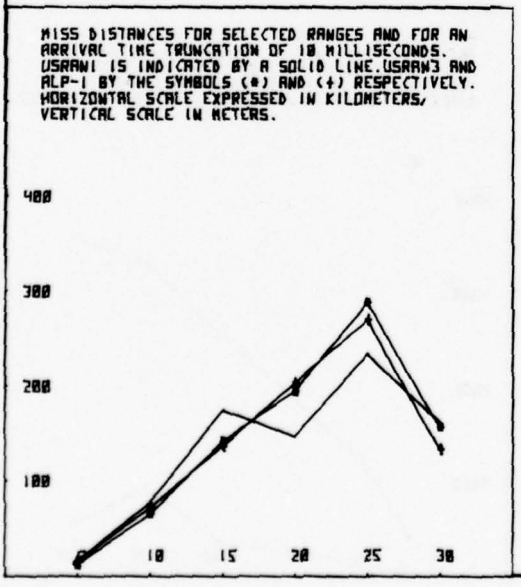

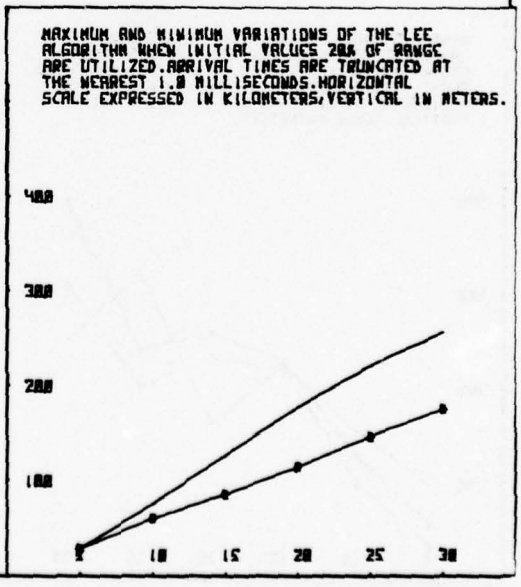

MISS DISTANCE VERSUS RANGE (METERS) FOR SOURCE POINTS LOCATED AT A 60 DEGREE FLANKING ANGLE. SELECTED TRUNCATION POINTS ARE CONSIDERED AS INDICATED BELOW. IN ADDITION, AN ERROR OF ONE METER PER SECOND IS ASSUMED IN THE EAST WIND COMPONENT.

FIGURE 34

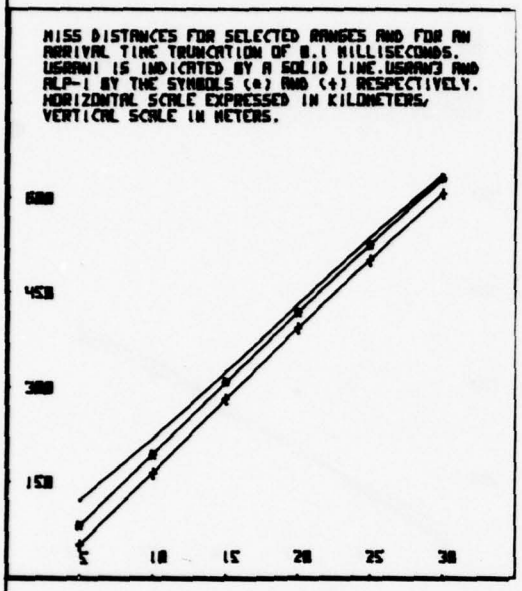

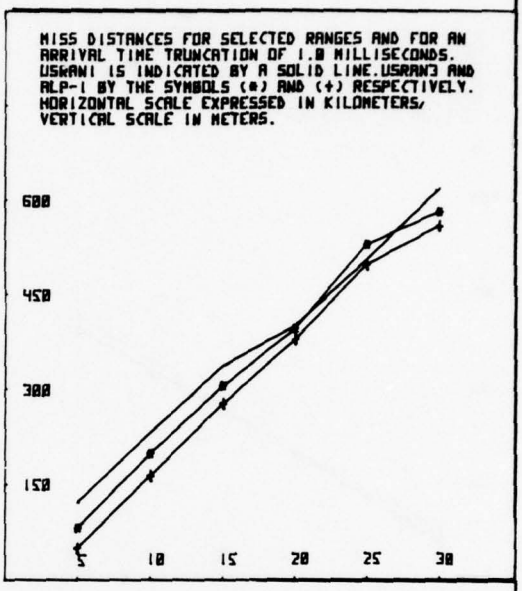

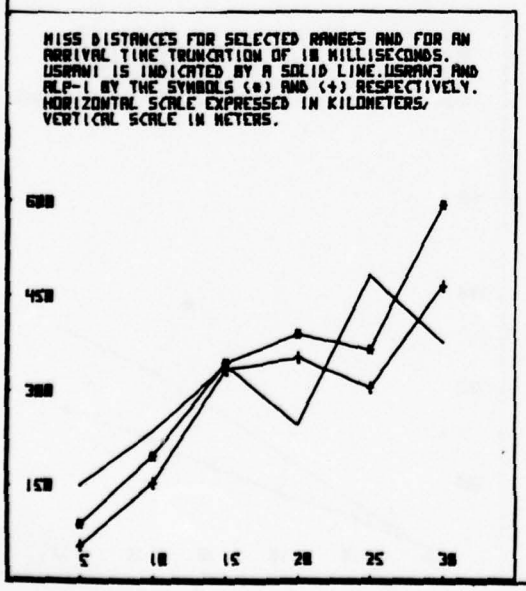

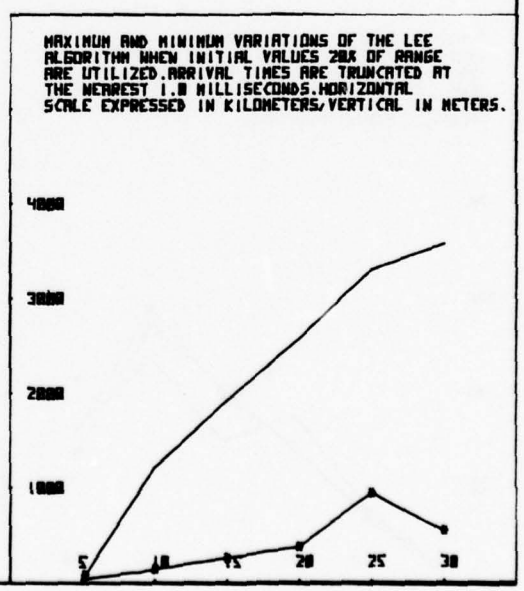

MISS DISTANCE VERSUS RANGE (METERS) FOR SOURCE POINTS LOCATED AT A 60 DEGREE FLANKING ANGLE. SELECTED TRUNCATION POINTS ARE CONSIDERED AS INDICATED BELOW. IN ADDITION, AN ERROR OF ONE METER PER SECOND IS ASSUMED IN THE WEST WIND COMPONENT.

FIGURE 35

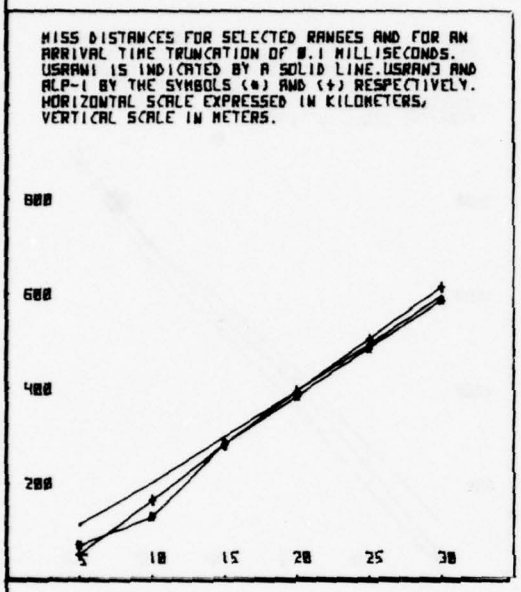

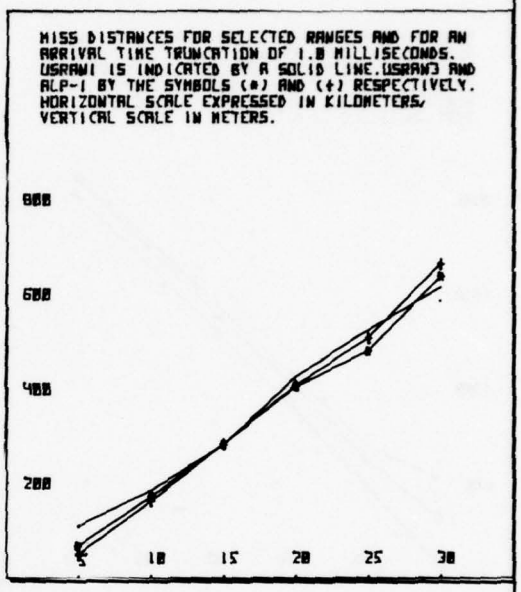

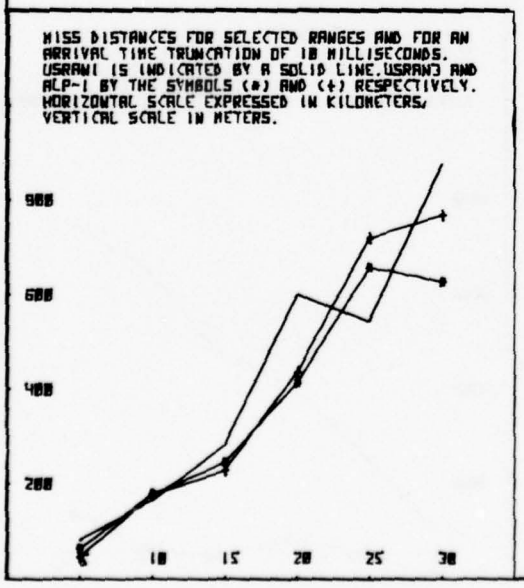

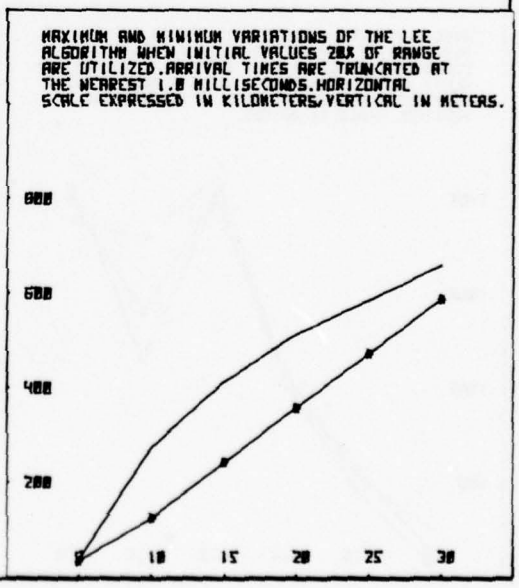

MISS DISTANCE VERSUS RANGE (METERS) FOR SOURCE POINTS LOCATED AT A 75 DEGREE FLANKING ANGLE. SELECTED TRUNCATION POINTS ARE CONSIDERED AS INDICATED BELOW. IN ADDITION, AN ERROR OF ONE METER PER SECOND IS ASSUMED IN THE EAST WIND COMPONENT.

FIGURE 36

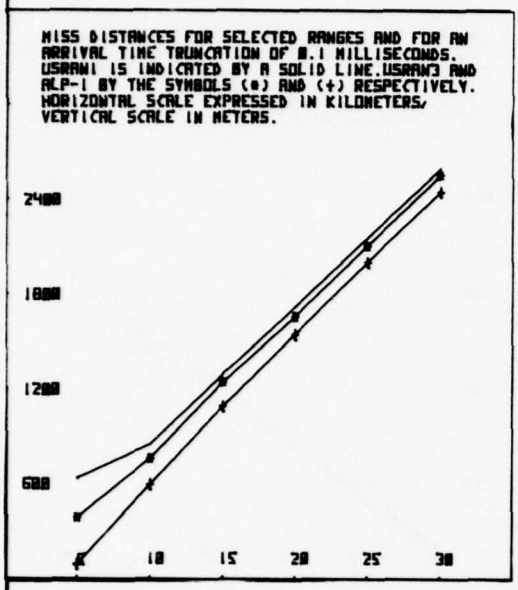

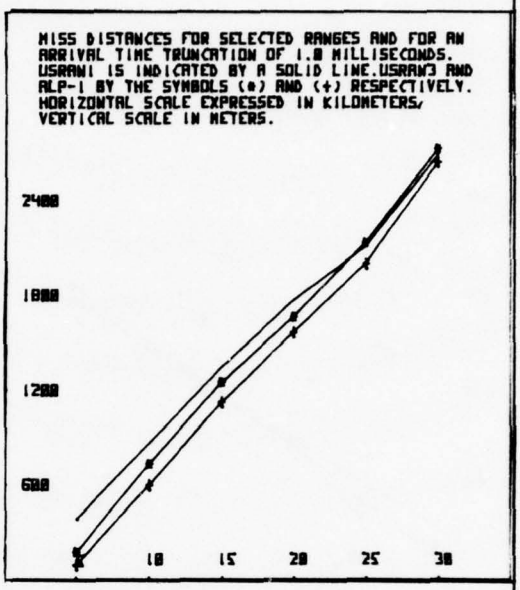

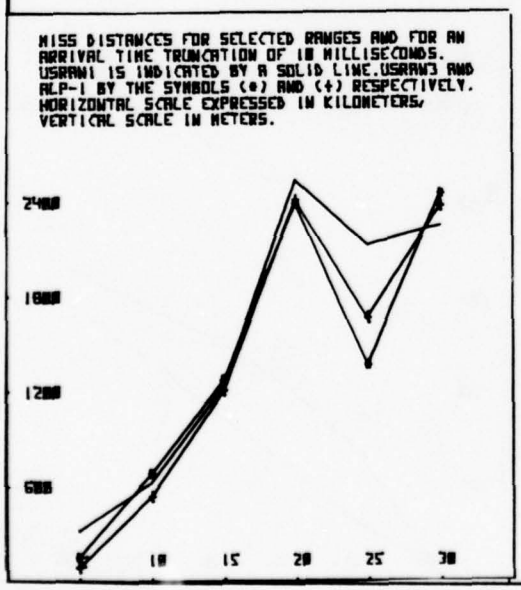

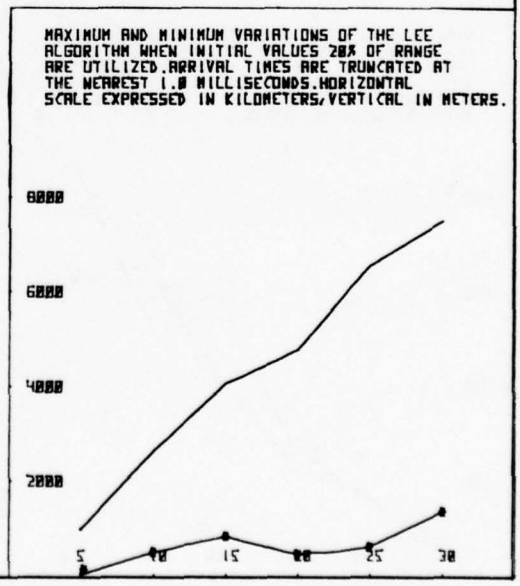

MISS DISTANCE VERSUS RANGE (METERS) FOR SOURCE POINTS LOCATED AT A 75 DEGREE FLANKING ANGLE. SELECTED TRUNCATION POINTS ARE CONSIDERED AS INDICATED BELOW. IN ADDITION, AN ERROR OF ONE METER PER SECOND IS ASSUMED IN THE WEST WIND COMPONENT.

FIGURE 37

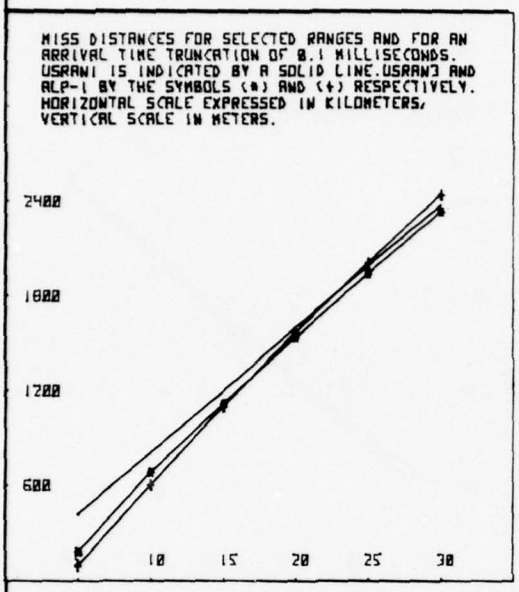

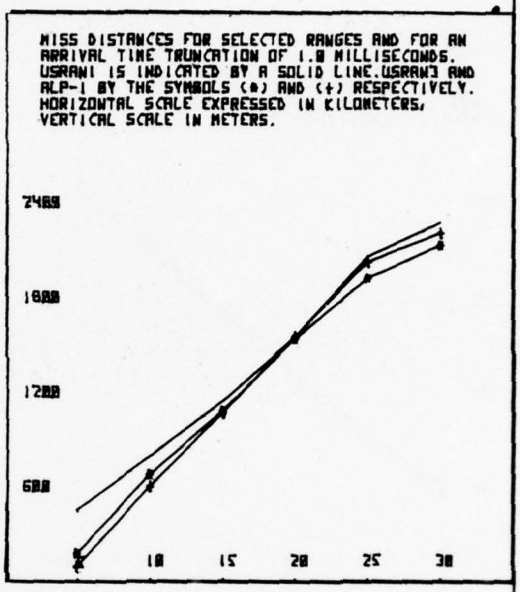

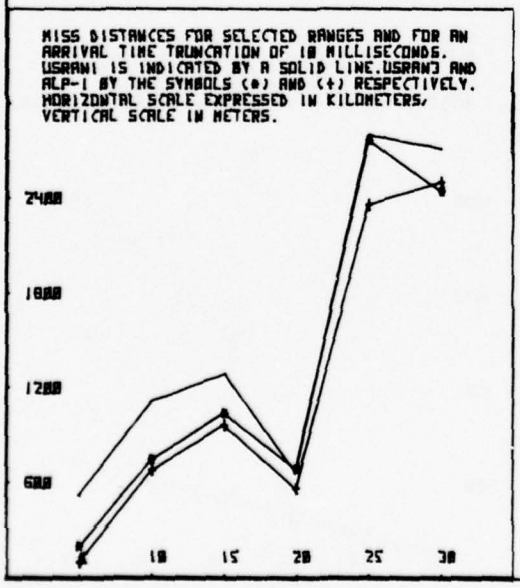

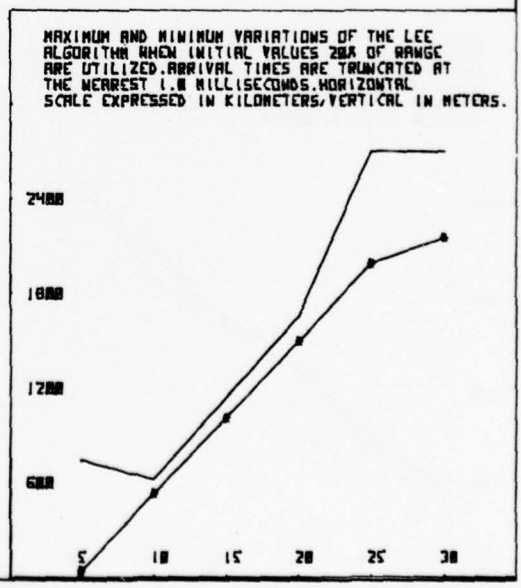

MISS DISTANCE VERSUS RANGE (METERS) FOR SOURCE POINTS LOCATED AT A 0 DEGREE FLANKING ANGLE. SELECTED TRUNCATION POINTS ARE CONSIDERED AS INDICATED BELOW. IN ADDITION, A TEMPERATURE ERROR OF 5.0 DEGREES KELVIN IS ASSUMED TOGETHER WITH SOUTH AND WEST COMPONENT ERRORS OF 5.0 METERS/SECOND.

FIGURE 38

MISS DISTANCES FOR SELECTED RANGES AND FOR AN ARRIVAL TIME TRUNCATION OF 0.1 MILLISECONDS. USRAN1 IS INDICATED BY A SOLID LINE. USRAN3 AND ALP-1 BY THE SYMBOLS (*) AND (+) RESPECTIVELY. HORIZONTAL SCALE EXPRESSED IN KILOMETERS, VERTICAL SCALE IN METERS.

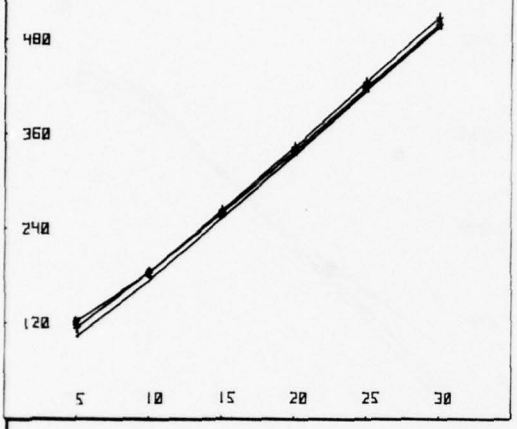

MISS DISTANCES FOR SELECTED RANGES AND FOR AN ARRIVAL TIME TRUNCATION OF 1.0 MILLISECONDS. USRAN1 IS INDICATED BY A SOLID LINE. USRAN3 AND ALP-1 BY THE SYMBOLS (*) AND (+) RESPECTIVELY. HORIZONTAL SCALE EXPRESSED IN KILOMETERS, VERTICAL SCALE IN METERS.

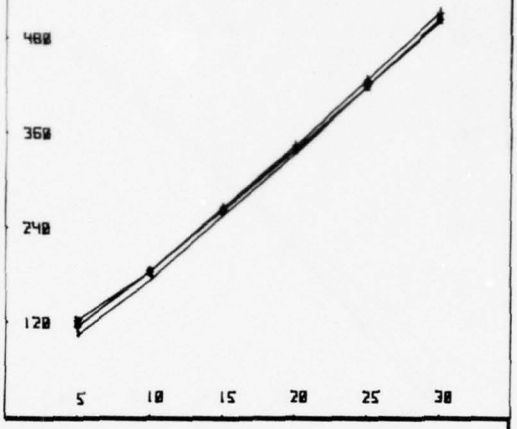

MISS DISTANCES FOR SELECTED RANGES AND FOR AN ARRIVAL TIME TRUNCATION OF 10 MILLISECONDS. USRAN1 IS INDICATED BY A SOLID LINE. USRAN3 AND ALP-1 BY THE SYMBOLS (*) AND (+) RESPECTIVELY. HORIZONTAL SCALE EXPRESSED IN KILOMETERS, VERTICAL SCALE IN METERS.

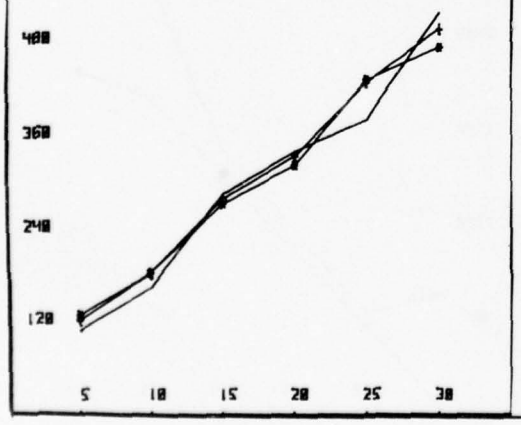

MAXIMUM AND MINIMUM VARIATIONS OF THE LEE ALGORITHM WHEN INITIAL VALUES 20% OF RANGE ARE UTILIZED. ARRIVAL TIMES ARE TRUNCATED AT THE NEAREST 1.0 MILLISECONDS. HORIZONTAL SCALE EXPRESSED IN KILOMETERS, VERTICAL IN METERS.

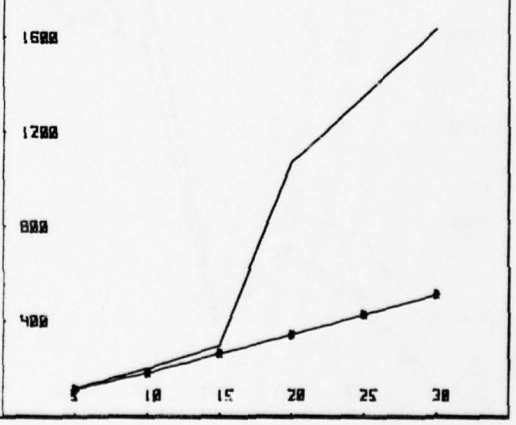

MISS DISTANCE VERSUS RANGE (METERS) FOR SOURCE POINTS LOCATED AT A 15 DEGREE FLANKING ANGLE. SELECTED TRUNCATION POINTS ARE CONSIDERED AS INDICATED BELOW. IN ADDITION, A TEMPERATURE ERROR OF 5.0 DEGREES KELVIN IS ASSUMED TOGETHER WITH SOUTH AND WEST COMPONENT ERRORS OF 5.0 METERS/SECOND.

FIGURE 39

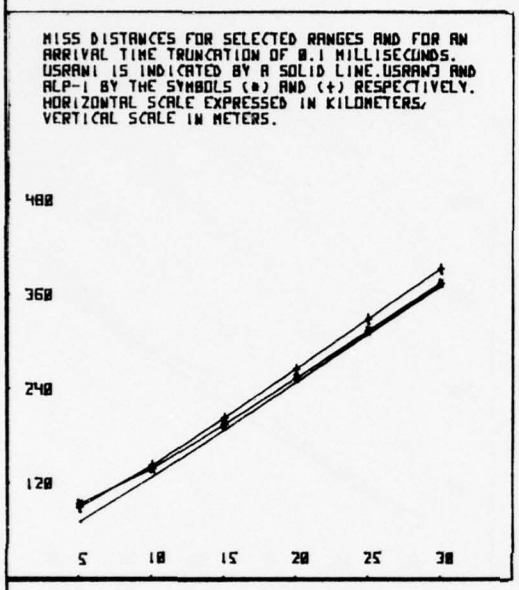

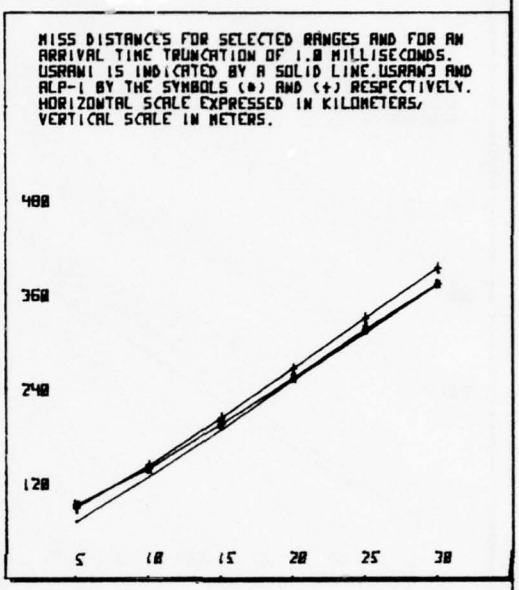

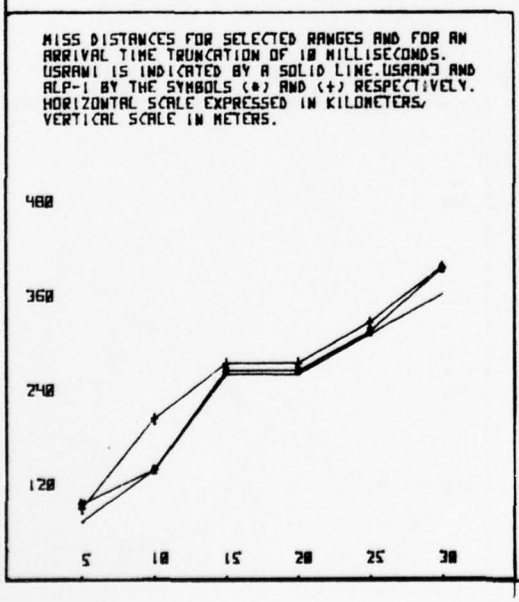

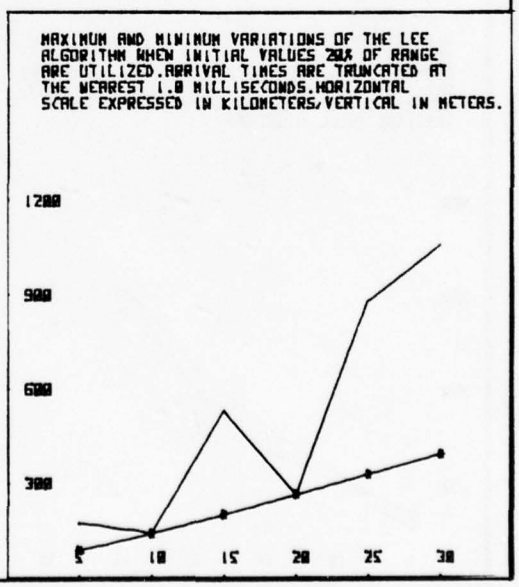

MISS DISTANCE VERSUS RANGE (METERS) FOR SOURCE POINTS LOCATED AT A 30 DEGREE FLANKING ANGLE.SELECTED TRUNCATION POINTS ARE CONSIDERED AS INDICATED BELOW.IN ADDITION,A TEMPERATURE ERROR OF 5.0 DEGREES KELVIN IS ASSUMED TOGETHER WITH SOUTH AND WEST COMPONENT ERRORS OF 5.0 METERS/SECOND..

FIGURE 40

MISS DISTANCES FOR SELECTED RANGES AND FOR AN ARRIVAL TIME TRUNCATION OF 0.1 MILLISECONDS. USRAN1 IS INDICATED BY A SOLID LINE.USRAN3 AND ALP-1 BY THE SYMBOLS (*) AND (+) RESPECTIVELY. HORIZONTAL SCALE EXPRESSED IN KILOMETERS, VERTICAL SCALE IN METERS.

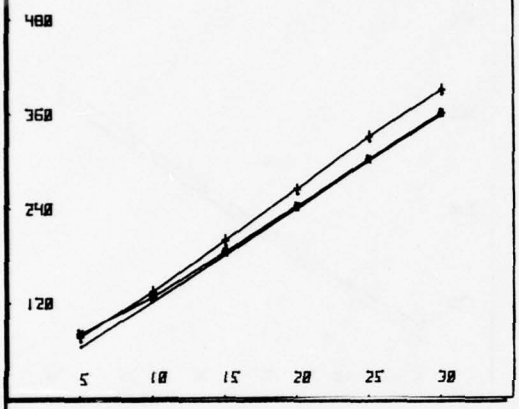

MISS DISTANCES FOR SELECTED RANGES AND FOR AN ARRIVAL TIME TRUNCATION OF 1.0 MILLISECONDS. USRAN1 IS INDICATED BY A SOLID LINE.USRAN3 AND ALP-1 BY THE SYMBOLS (*) AND (+) RESPECTIVELY. HORIZONTAL SCALE EXPRESSED IN KILOMETERS, VERTICAL SCALE IN METERS.

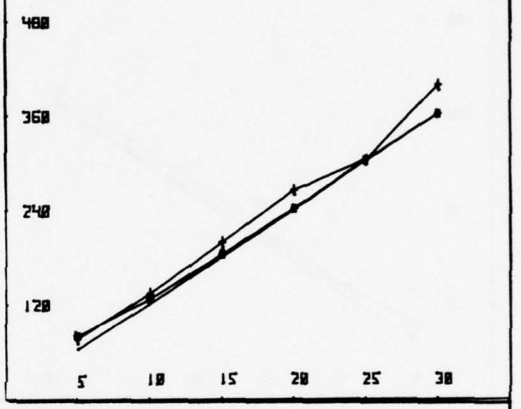

MISS DISTANCES FOR SELECTED RANGES AND FOR AN ARRIVAL TIME TRUNCATION OF 10 MILLISECONDS. USRAN1 IS INDICATED BY A SOLID LINE.USRAN3 AND ALP-1 BY THE SYMBOLS (*) AND (+) RESPECTIVELY. HORIZONTAL SCALE EXPRESSED IN KILOMETERS, VERTICAL SCALE IN METERS.

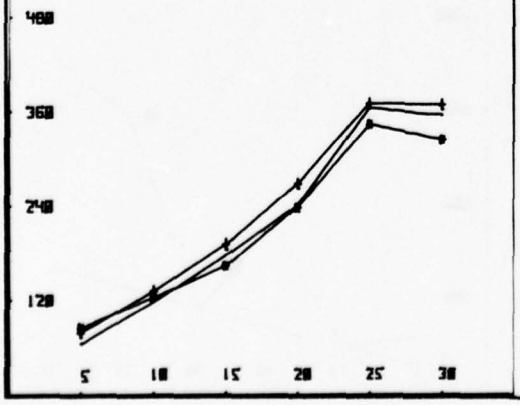

MAXIMUM AND MINIMUM VARIATIONS OF THE LEE ALGORITHM WHEN INITIAL VALUES 20% OF RANGE ARE UTILIZED.ARRIVAL TIMES ARE TRUNCATED AT THE NEAREST 1.0 MILLISECONDS.HORIZONTAL SCALE EXPRESSED IN KILOMETERS,VERTICAL IN METERS.

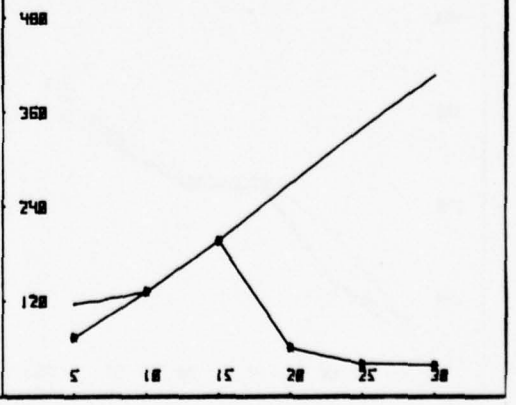

MISS DISTANCE VERSUS RANGE (METERS) FOR SOURCE POINTS LOCATED AT A 45 DEGREE FLANKING ANGLE. SELECTED TRUNCATION POINTS ARE CONSIDERED AS INDICATED BELOW. IN ADDITION, A TEMPERATURE ERROR OF 5.0 DEGREES KELVIN IS ASSUMED TOGETHER WITH SOUTH AND WEST COMPONENT ERRORS OF 5.0 METERS/SECOND.

FIGURE 41

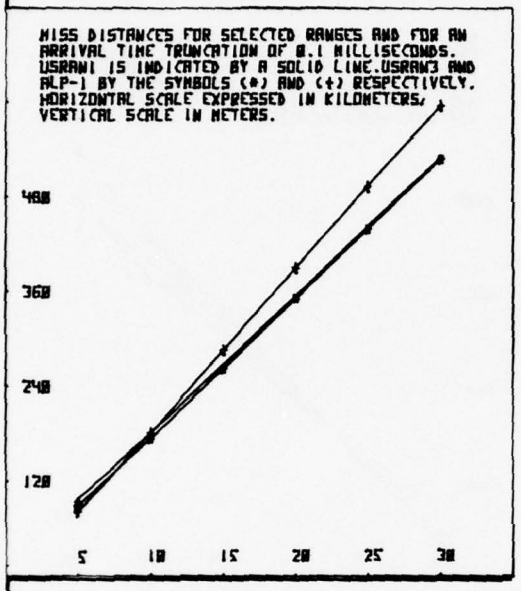

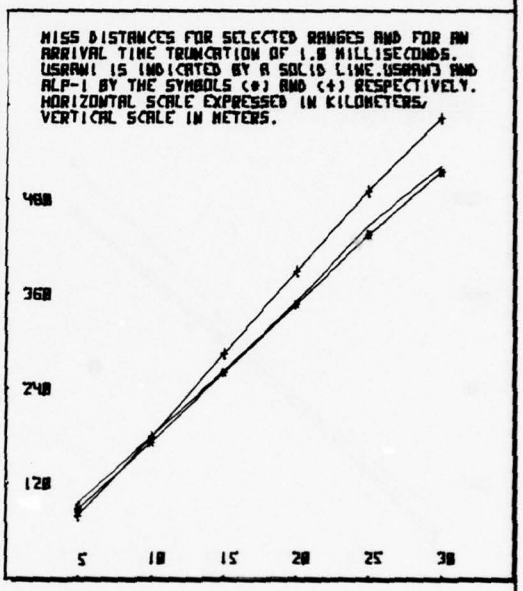

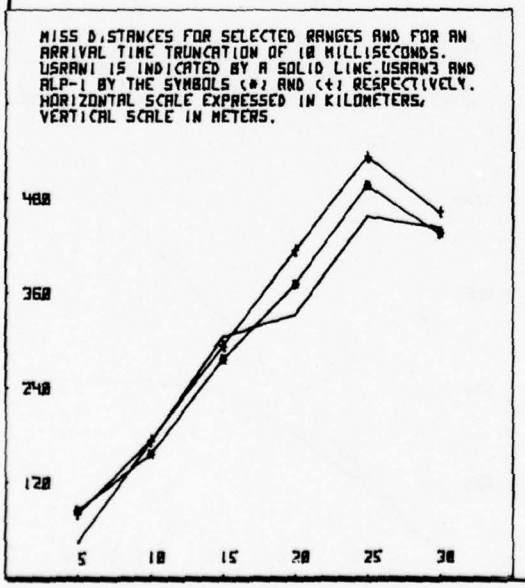

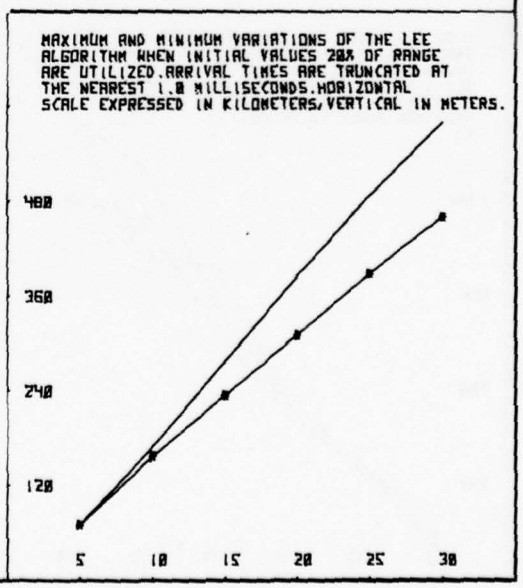

MISS DISTANCE VERSUS RANGE (METERS) FOR SOURCE POINTS LOCATED AT A 60 DEGREE FLANKING ANGLE. SELECTED TRUNCATION POINTS ARE CONSIDERED AS INDICATED BELOW. IN ADDITION, A TEMPERATURE ERROR OF 5.0 DEGREES KELVIN IS ASSUMED TOGETHER WITH SOUTH AND WEST COMPONENT ERRORS OF 5.0 METERS/SECOND.

FIGURE 42

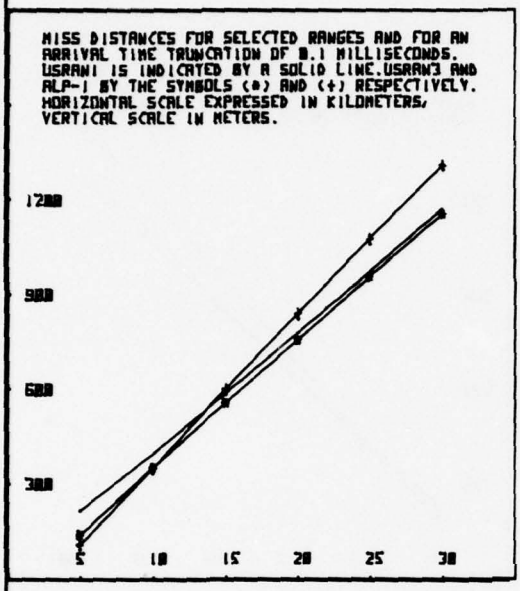

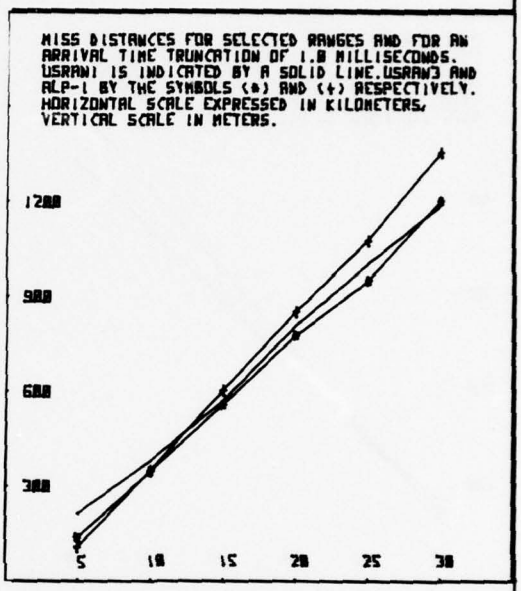

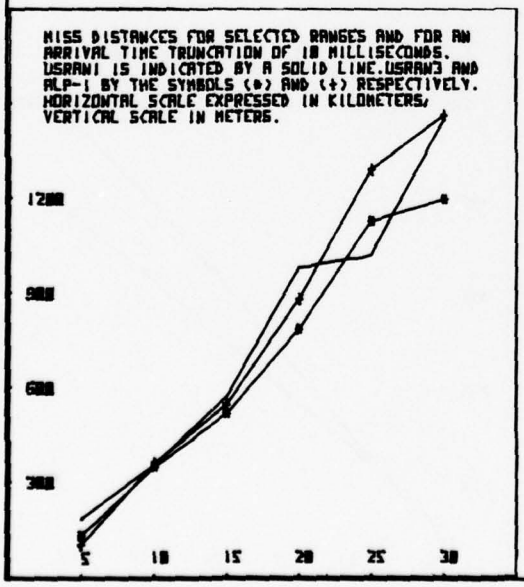

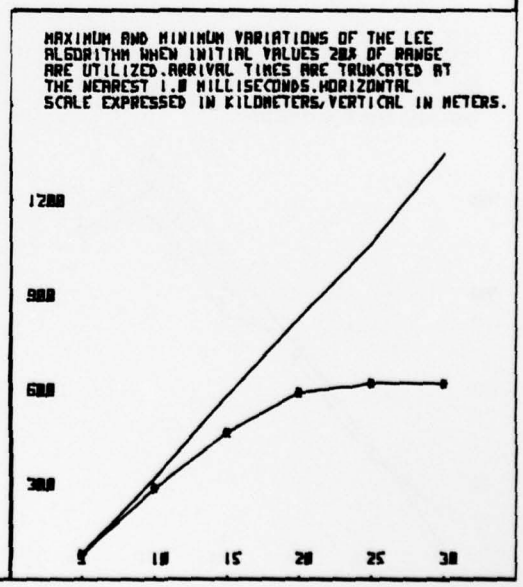

MISS DISTANCE VERSUS RANGE (METERS) FOR SOURCE POINTS LOCATED AT A 75 DEGREE FLANKING ANGLE. SELECTED TRUNCATION POINTS ARE CONSIDERED AS INDICATED BELOW. IN ADDITION, A TEMPERATURE ERROR OF 5.0 DEGREES KELVIN IS ASSUMED TOGETHER WITH SOUTH AND WEST COMPONENT ERRORS OF 5.0 METERS/SECOND.

FIGURE 43

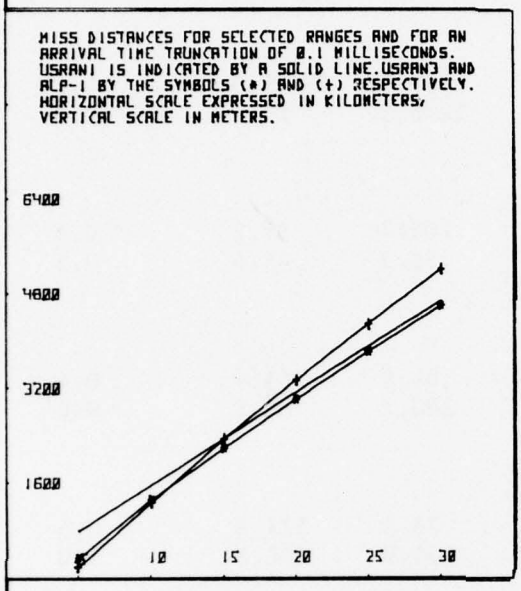

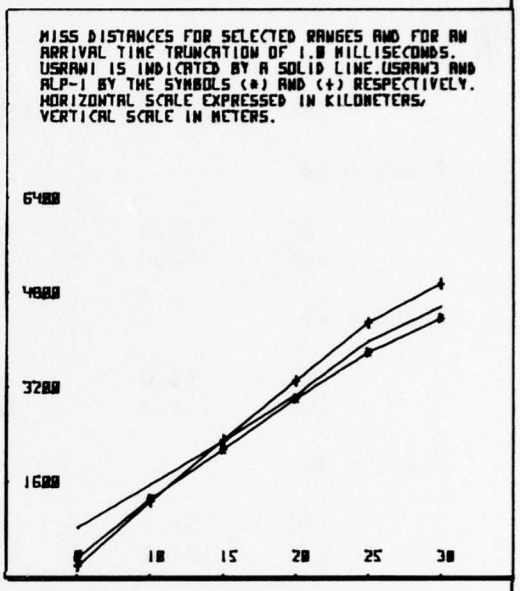

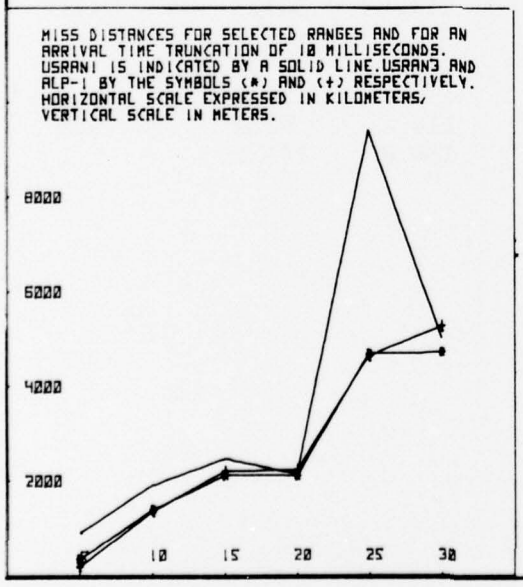

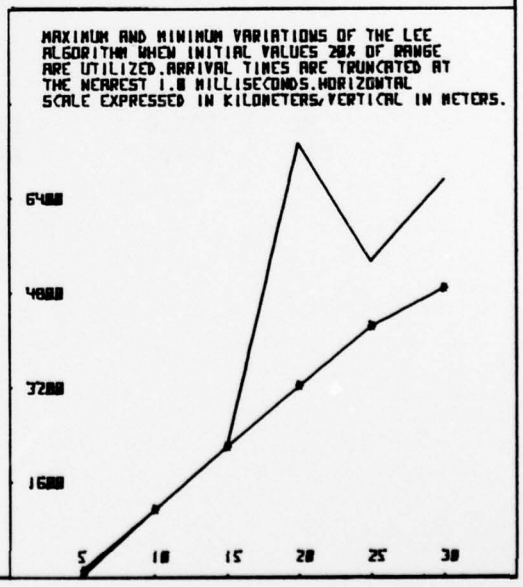

TABLE 1. MISS-DISTANCES (METERS) FOR SELECTED RANGES AND VARIOUS FLANKING ANGLES AS INDICATED. MAXIMUM TIMING ACCURACY IS EMPLOYED, AND METEOROLOGICAL ERRORS ARE ASSUMED OF 5.0 DEGREES KELVIN IN TEMPERATURE AND 5 METERS/SECOND IN SOUTH AND WEST WIND COMPONENTS.

Range	USRAN 1	USRAN 3	ALP-1	ALP-2T	ALP-2
Flank = 75					
5K	813.1	346.0	199.7	15.0	0.1
10K	1572.4	1324.6	1276.5	19.9	0.3
Flank = 60					
5K	218.6	141.9	109.7	35.2	0.3
10K	398.0	353.6	351.3	45.4	0.5
Flank = 45					
5K	98.0	90.1	81.9	64.4	0.4
10K	181.2	173.6	180.2	82.6	0.0
Flank = 30					
5K	61.6	81.6	78.2	111.8	0.5
10K	122.2	128.3	134.9	146.8	1.0
Flank = 15					
5K	72.8	94.5	90.5	204.1	0.5
10K	128.5	138.9	143.1	305.7	1.1
Flank = 0					
5K	103.8	122.3	114.7	98.2	0.5
10K	174.7	184.4	184.6	161.1	1.1

TABLE 2. MISS-DISTANCES (METERS) FOR SELECTED RANGES AND VARIOUS FLANKING ANGLES AS INDICATED. MILLISECOND TIMING ACCURACY IS EMPLOYED, AND METEOROLOGICAL ERRORS ARE ASSUMED OF 5.0 DEGREES KELVIN IN TEMPERATURE AND 5 METERS/SECOND IN SOUTH AND WEST WIND COMPONENTS.

Range	USRAN 1	USRAN 3	ALP-1	ALP-2T	ALP-2
Flank = 75					
5K	847.5	342.1	199.7	15.3	21.3
10K	1559.4	1321.2	1275.8	24.1	*
Flank = 60					
5K	216.7	140.6	109.4	34.8	7.7
10K	381.4	347.1	350.4	49.4	250.4
Flank = 45					
5K	98.4	90.6	81.8	65.0	3.4
10K	181.8	174.1	180.7	85.4	19.0
Flank = 30					
5K	65.5	81.7	78.3	111.3	1.4
10K	121.9	127.9	134.9	137.3	36.1
Flank = 15					
5K	73.3	44.2	90.6	200.9	2.2
10K	128.8	139.2	143.2	296.8	5.7
Flank = 0					
5K	104.5	122.7	115.0	98.6	7.2
10K	173.2	184.1	184.1	196.6	115.9

*Unstable

TABLE 3. MISS-DISTANCES (METERS) FOR SELECTED RANGES AND VARIOUS FLANKING ANGLES AS INDICATED. TEN-MILLISECOND TIMING ACCURACY IS EMPLOYED, AND METEOROLOGICAL ERRORS ARE ASSUMED OF 5.0 DEGREES KELVIN IN TEMPERATURE AND 5 METERS/SECOND IN SOUTH AND WEST WIND COMPONENTS.

Range	USRAN 1	USRAN 3	ALP-1	ALP-2T	ALP-2
Flank = 75					
5K	927.6	367.2	206.8	18.5	78.6
10K	1914.8	1398.1	1362.9	18.8	*
Flank = 60					
5K	188.3	135.2	106.1	36.7	85.8
10K	360.8	352.0	363.4	108.5	*
Flank = 45					
5K	95.6	85.5	81.4	68.3	22.3
10K	171.0	155.7	172.9	76.4	*
Flank = 30					
5K	66.2	85.8	79.4	99.7	20.8
10K	118.5	124.4	132.1	127.4	*
Flank = 15					
5K	73.0	95.5	89.8	187.9	10.3
10K	137.9	138.3	143.9	148.9	*
Flank = 0					
5K	106.3	125.6	118.5	110.7	52.5
10K	161.7	180.3	180.1	901.6	*

*Unstable

DISTRIBUTION LIST

Dr. Frank D. Eaton
Geophysical Institute
University of Alaska
Fairbanks, AK 99701

Commander
US Army Aviation Center
ATTN: ATZQ-D-MA
Fort Rucker, AL 36362

Chief, Atmospheric Sciences Div
Code ES-81
NASA
Marshall Space Flight Center,
AL 35812

Commander
US Army Missile R&D Command
ATTN: DRDMI-CGA (B. W. Fowler)
Redstone Arsenal, AL 35809

Redstone Scientific Information Center
ATTN: DRDMI-TBD
US Army Missile R&D Command
Redstone Arsenal, AL 35809

Commander
US Army Missile R&D Command
ATTN: DRDMI-TEM (R. Haraway)
Redstone Arsenal, AL 35809

Commander
US Army Missile R&D Command
ATTN: DRDMI-TRA (Dr. Essenwanger)
Redstone Arsenal, AL 35809

Commander
HQ, Fort Huachuca
ATTN: Tech Ref Div
Fort Huachuca, AZ 85613

Commander
US Army Intelligence Center & School
ATTN: ATSI-CD-MD
Fort Huachuca, AZ 85613

Commander
US Army Yuma Proving Ground
ATTN: Technical Library
Bldg 2100
Yuma, AZ 85364

Naval Weapons Center (Code 3173)
ATTN: Dr. A. Shlanta
China Lake, CA 93555

Sylvania Elec Sys Western Div
ATTN: Technical Reports Library
PO Box 205
Mountain View, CA 94040

Geophysics Officer
PMTC Code 3250
Pacific Missile Test Center
Point Mugu, CA 93042

Commander
Naval Ocean Systems Center (Code 4473)
ATTN: Technical Library
San Diego, CA 92152

Meteorologist in Charge
Kwajalein Missile Range
PO Box 67
APO San Francisco, 96555

Director
NOAA/ERL/APCL R31
RB3-Room 567
Boulder, CO 80302

Library-R-51-Tech Reports
NOAA/ERL
320 S. Broadway
Boulder, CO 80302

National Center for Atmos Research
NCAR Library
PO Box 3000
Boulder, CO 80307

B. Girardo
Bureau of Reclamation
E&R Center, Code 1220
Denver Federal Center, Bldg 67
Denver, CO 80225

National Weather Service
National Meteorological Center
W321, WWB, Room 201
ATTN: Mr. Quiroz
Washington, DC 20233

Mil Assistant for Atmos Sciences
Ofc of the Undersecretary of Defense
for Rsch & Engr/E&LS - Room 3D129
The Pentagon
Washington, DC 20301

Defense Communications Agency
Technical Library Center
Code 205
Washington, DC 20305

Director
Defense Nuclear Agency
ATTN: Technical Library
Washington, DC 20305

HQDA (DAEN-RDM/Dr. de Percin)
Washington, DC 20314

Director
Naval Research Laboratory
Code 5530
Washington, DC 20375

Commanding Officer
Naval Research Laboratory
Code 2627
Washington, DC 20375

Dr. J. M. MacCallum
Naval Research Laboratory
Code 1409
Washington, DC 20375

The Library of Congress
ATTN: Exchange & Gift Div
Washington, DC 20540
2

Head, Atmos Rsch Section
Div Atmospheric Science
National Science Foundation
1800 G. Street, NW
Washington, DC 20550

CPT Hugh Albers, Exec Sec
Interdept Committee on Atmos Science
National Science Foundation
Washington, DC 20550

Director, Systems R&D Service
Federal Aviation Administration
ATTN: ARD-54
2100 Second Street, SW
Washington, DC 20590

ADTC/DLODL
Eglin AFB, FL 32542

Naval Training Equipment Center
ATTN: Technical Library
Orlando, FL 32813

Det 11, 2WS/OI
ATTN: Maj Orondorff
Patrick AFB, FL 32925

USAFETAC/CB
Scott AFB, IL 62225

HQ, ESD/TOSI/S-22
Hanscom AFB, MA 01731

Air Force Geophysics Laboratory
ATTN: LCB (A. S. Carten, Jr.)
Hanscom AFB, MA 01731

Air Force Geophysics Laboratory
ATTN: LYD
Hanscom AFB, MA 01731

Meteorology Division
AFGL/LY
Hanscom AFB, MA 01731

US Army Liaison Office
MIT-Lincoln Lab, Library A-082
PO Box 73
Lexington, MA 02173

Director
US Army Ballistic Rsch Lab
ATTN: DRDAR-BLB (Dr. G. E. Keller)
Aberdeen Proving Ground, MD 21005

Commander
US Army Ballistic Rsch Lab
ATTN: DRDAR-BLP
Aberdeen Proving Ground, MD 21005

Director
US Army Armament R&D Command
Chemical Systems Laboratory
ATTN: DRDAR-CLJ-I
Aberdeen Proving Ground, MD 21010

Chief CB Detection & Alarms Div
Chemical Systems Laboratory
ATTN: DRDAR-CLC-CR (H. Tannenbaum)
Aberdeen Proving Ground, MD 21010

Commander
Harry Diamond Laboratories
ATTN: DELHD-CO
2800 Powder Mill Road
Adelphi, MD 20783

Commander
ERADCOM
ATTN: DRDEL-AP
2800 Powder Mill Road
Adelphi, MD 20783
2

Commander
ERADCOM
ATTN: DRDEL-CG/DRDEL-DC/DRDEL-CS
2800 Powder Mill Road
Adelphi, MD 20783

Commander
ERADCOM
ATTN: DRDEL-CT
2800 Powder Mill Road
Adelphi, MD 20783

Commander
ERADCOM
ATTN: DRDEL-EA
2800 Powder Mill Road
Adelphi, MD 20783

Commander
ERADCOM
ATTN: DRDEL-PA/DRDEL-ILS/DRDEL-E
2800 Powder Mill Road
Adelphi, MD 20783

Commander
ERADCOM
ATTN: DRDEL-PAO (S. Kimmel)
2800 Powder Mill Road
Adelphi, MD 20783

Chief
Intelligence Materiel Dev & Support Ofc
ATTN: DELEW-WL-I
Bldg 4554
Fort George G. Meade, MD 20755

Acquisitions Section, IRDB-D823
Library & Info Service Div, NOAA
6009 Executive Blvd
Rockville, MD 20852

Naval Surface Weapons Center
White Oak Library
Silver Spring, MD 20910

The Environmental Research
Institute of MI
ATTN: IRIA Library
PO Box 8618
Ann Arbor, MI 48107

Mr. William A. Main
USDA Forest Service
1407 S. Harrison Road
East Lansing, MI 48823

Dr. A. D. Belmont
Research Division
PO Box 1249
Control Data Corp
Minneapolis, MN 55440

Director
Naval Oceanography & Meteorology
NSTL Station
Bay St Louis, MS 39529

Director
US Army Engr Waterways Experiment Sta
ATTN: Library
PO Box 631
Vicksburg, MS 39180

Environmental Protection Agency
Meteorology Laboratory
Research Triangle Park, NC 27711

US Army Research Office
ATTN: DRXRO-PP
PO Box 12211
Research Triangle Park, NC 27709

Commanding Officer
US Army Armament R&D Command
ATTN: DRDAR-TSS Bldg 59
Dover, NJ 07801

Commander
HQ, US Army Avionics R&D Activity
ATTN: DAVAA-O
Fort Monmouth, NJ 07703

Commander/Director
US Army Combat Surveillance & Target
Acquisition Laboratory
ATTN: DELCS-D
Fort Monmouth, NJ 07703

Commander
US Army Electronics R&D Command
ATTN: DELCS-S
Fort Monmouth, NJ 07703

US Army Materiel Systems
Analysis Activity
ATTN: DRXSY-MP
Aberdeen Proving Ground, MD 21005

Director
US Army Electronics Technology &
Devices Laboratory
ATTN: DELET-D
Fort Monmouth, NJ 07703

Commander
US Army Electronic Warfare Laboratory
ATTN: DELEW-D
Fort Monmouth, NJ 07703

Commander
US Army Night Vision &
Electro-Optics Laboratory
ATTN: DELNV-L (Dr. Rudolf Buser)
Fort Monmouth, NJ 07703

Commander
ERADCOM Technical Support Activity
ATTN: DELSD-L
Fort Monmouth, NJ 07703

Project Manager, FIREFINDER
ATTN: DRCPM-FF
Fort Monmouth, NJ 07703

Project Manager, REMBASS
ATTN: DRCPM-RBS
Fort Monmouth, NJ 07703

Commander
US Army Satellite Comm Agency
ATTN: DRCPM-SC-3
Fort Monmouth, NJ 07703

Commander
ERADCOM Scientific Advisor
ATTN: DRDEL-SA
Fort Monmouth, NJ 07703

6585 TG/WE
Holloman AFB, NM 88330

AFWL/WE
Kirtland, AFB, NM 87117

AFWL/Technical Library (SUL)
Kirtland AFB, NM 87117

Commander
US Army Test & Evaluation Command
ATTN: STEWS-AD-L
White Sands Missile Range, NM 88002

Rome Air Development Center
ATTN: Documents Library
TSLD (Bette Smith)
Griffiss AFB, NY 13441

Commander
US Army Tropic Test Center
ATTN: STETC-TD (Info Center)
APO New York 09827

Commandant
US Army Field Artillery School
ATTN: ATSF-CD-R (Mr. Farmer)
Fort Sill, OK 73503

Commandant
US Army Field Artillery School
ATTN: ATSF-CF-R
Fort Sill, OK 73503

Director CFD
US Army Field Artillery School
ATTN: Met Division
Fort Sill, OK 73503

Commandant
US Army Field Artillery School
ATTN: Morris Swett Library
Fort Sill, OK 73503

Commander
US Army Dugway Proving Ground
ATTN: MT-DA-L
Dugway, UT 84022

William Peterson
Research Associates
Utah State University, UNC 48
Logan, UT 84322

Inge Dirmhirn, Professor
Utah State University, UNC 48
Logan, UT 84322

Defense Documentation Center
ATTN: DDC-TCA
Cameron Station, Bldg 5
Alexandria, VA 22314
12

Commanding Officer
US Army Foreign Sci & Tech Center
ATTN: DRXST-ISI
220 7th Street, NE
Charlottesville, VA 22901

Naval Surface Weapons Center
Code G65
Dahlgren, VA 22448

Commander
US Army Night Vision
& Electro-Optics Lab
ATTN: DELNV-D
Fort Belvoir, VA 22060

Commander and Director
US Army Engineer Topographic Lab
ETL-TD-MB
Fort Belvoir, VA 22060

Director
Applied Technology Lab
DAVDL-EU-TSD
ATTN: Technical Library
Fort Eustis, VA 23604

Department of the Air Force
OL-C, 5WW
Fort Monroe, VA 23651

Department of the Air Force
5WW/DN
Langley AFB, VA 23665

Director
Development Center MCDEC
ATTN: Firepower Division
Quantico, VA 22134

US Army Nuclear & Chemical Agency
ATTN: MONA-WE
Springfield, VA 22150

Director
US Army Signals Warfare Laboratory
ATTN: DELSW-OS (Dr. R. Burkhardt)
Vint Hill Farms Station
Warrenton, VA 22186

Commander
US Army Cold Regions Test Center
ATTN: STECR-OP-PM
APO Seattle, 98733

Commander
US Army Dugway Proving Ground
ATTN: STEDP-MT-DA-M (Mr. Paul Carlson)
Dugway, UT 84022

Commander
TRASANA
ATTN: DELAS-ATAA-PL
(Dolores Anguiano)
White Sands Missile Range, NM 88002

ATMOSPHERIC SCIENCES RESEARCH PAPERS

1. Lindberg, J.D., "An Improvement to a Method for Measuring the Absorption Coefficient of Atmospheric Dust and other Strongly Absorbing Powders, " ECOM-5565, July 1975.
2. Avara, Elton, P., "Mesoscale Wind Shears Derived from Thermal Winds," ECOM-5566, July 1975.
3. Gomez, Richard B., and Joseph H. Pierluissi, "Incomplete Gamma Function Approximation for King's Strong-Line Transmittance Model," ECOM-5567, July 1975.
4. Blanco, A.J., and B.F. Engebos, "Ballistic Wind Weighting Functions for Tank Projectiles," ECOM-5568, August 1975.
5. Taylor, Fredrick J., Jack Smith, and Thomas H. Pries, "Crosswind Measurements through Pattern Recognition Techniques," ECOM-5569, July 1975.
6. Walters, D.L., "Crosswind Weighting Functions for Direct-Fire Projectiles," ECOM-5570, August 1975.
7. Duncan, Louis D., "An Improved Algorithm for the Iterated Minimal Information Solution for Remote Sounding of Temperature," ECOM-5571, August 1975.
8. Robbiani, Raymond L., "Tactical Field Demonstration of Mobile Weather Radar Set AN/TPS-41 at Fort Rucker, Alabama," ECOM-5572, August 1975.
9. Miers, B., G. Blackman, D. Langer, and N. Lorimier, "Analysis of SMS/GOES Film Data," ECOM-5573, September 1975.
10. Manquero, Carlos, Louis Duncan, and Rufus Bruce, "An Indication from Satellite Measurements of Atmospheric CO2 Variability," ECOM-5574, September 1975.
11. Petracca, Carmine, and James D. Lindberg, "Installation and Operation of an Atmospheric Particulate Collector," ECOM-5575, September 1975.
12. Avara, Elton P., and George Alexander, "Empirical Investigation of Three Iterative Methods for Inverting the Radiative Transfer Equation," ECOM-5576, October 1975.
13. Alexander, George D., "A Digital Data Acquisition Interface for the SMS Direct Readout Ground Station — Concept and Preliminary Design," ECOM-5577, October 1975.
14. Cantor, Israel, "Enhancement of Point Source Thermal Radiation Under Clouds in a Nonattenuating Medium," ECOM-5578, October 1975.
15. Norton, Colburn, and Glenn Hoidale, "The Diurnal Variation of Mixing Height by Month over White Sands Missile Range, N.M," ECOM-5579, November 1975.
16. Avara, Elton P., "On the Spectrum Analysis of Binary Data," ECOM-5580, November 1975.
17. Taylor, Fredrick J., Thomas H. Pries, and Chao-Huan Huang, "Optimal Wind Velocity Estimation," ECOM-5581, December 1975.
18. Avara, Elton P., "Some Effects of Autocorrelated and Cross-Correlated Noise on the Analysis of Variance, " ECOM-5582, December 1975.
19. Gillespie, Patti S., R.L. Armstrong, and Kenneth O. White, "The Spectral Characteristics and Atmospheric CO2 Absorption of the Ho^{+3}:YLF Laser at 2.05μm," ECOM-5583, December 1975.
20. Novlan, David J. "An Empirical Method of Forecasting Thunderstorms for the White Sands Missile Range," ECOM-5584, February 1976.
21. Avara, Elton P., "Randomization Effects in Hypothesis Testing with Autocorrelated Noise," ECOM-5585, February 1976.
22. Watkins, Wendell R., "Improvements in Long Path Absorption Cell Measurement," ECOM-5586, March 1976.
23. Thomas, Joe, George D. Alexander, and Marvin Dubbin, "SATTEL — An Army Dedicated Meteorological Telemetry System," ECOM-5587. March 1976.
24. Kennedy, Bruce W., and Delbert Bynum, "Army User Test Program for the RDT&E-XM-75 Meteorological Rocket," ECOM-5588, April 1976.

25. Barnett, Kenneth M., "A Description of the Artillery Meteorological Comparisons at White Sands Missle Range, October 1974 - December 1974 ('PASS' - Prototype Artillery [Meteorological] Subsystem)," ECOM-5589, April 1976.
26. Miller, Walter B., "Preliminary Analysis of Fall-of-Shot From Project 'PASS'," ECOM-5590, April 1976.
27. Avara, Elton P., "Error Analysis of Minimum Information and Smith's Direct Methods for Inverting the Radiative Transfer Equation," ECOM-5591, April 1976.
28. Yee, Young P., James D. Horn, and George Alexander, "Synoptic Thermal Wind Calculations from Radiosonde Observations Over the Southwestern United States," ECOM-5592, May 1976.
29. Duncan, Louis D., and Mary Ann Seagraves, "Applications of Empirical Corrections to NOAA-4 VTPR Observations," ECOM-5593, May 1976.
30. Miers, Bruce T., and Steve Weaver, "Applications of Meterological Satellite Data to Weather Sensitive Army Operations,"ECOM-5594, May 1976.
31. Sharenow, Moses, "Redesign and Improvement of Balloon ML-566," ECOM-5595, June, 1976.
32. Hansen, Frank V., "The Depth of the Surface Boundary Layer," ECOM-5596, June 1976.
33. Pinnick, R.G., and E.B. Stenmark, "Response Calculations for a Commercial Light-Scattering Aerosol Counter," ECOM-5597, July 1976.
34. Mason, J., and G.B. Hoidale, "Visibility as an Estimator of Infrared Transmittance," ECOM-5598, July 1976.
35. Bruce, Rufus E., Louis D. Duncan, and Joseph H. Pierluissi, "Experimental Study of the Relationship Between Radiosonde Temperatures and Radiometric-Area Temperatures," ECOM-5599, August 1976.
36. Duncan, Louis D., "Stratospheric Wind Shear Computed from Satellite Thermal Sounder Measurements," ECOM-5800, September 1976.
37. Taylor, F., P. Mohan, P. Joseph and T. Pries, "An All Digital Automated Wind Measurement System," ECOM-5801, September 1976.
38. Bruce, Charles, "Development of Spectrophones for CW and Pulsed Radiation Sources," ECOM-5802, September 1976.
39. Duncan, Louis D., and Mary Ann Seagraves,"Another Method for Estimating Clear Column Radiances," ECOM-5803, October 1976.
40. Blanco, Abel J., and Larry E. Taylor, "Artillery Meteorological Analysis of Project Pass," ECOM-5804, October 1976.
41. Miller, Walter, and Bernard Engebos," A Mathematical Structure for Refinement of Sound Ranging Estimates," ECOM-5805, November, 1976.
42. Gillespie, James B., and James D. Lindberg, "A Method to Obtain Diffuse Reflectance Measurements from 1.0 to 3.0 μm Using a Cary 17I Spectrophotometer," ECOM-5806, November 1976.
43. Rubio, Roberto, and Robert O. Olsen,"A Study of the Effects of Temperature Variations on Radio Wave Absorption,"ECOM-5807, November 1976.
44. Ballard, Harold N., "Temperature Measurements in the Stratosphere from Balloon-Borne Instrument Platforms, 1968-1975," ECOM-5808, December 1976.
45. Monahan, H.H., "An Approach to the Short-Range Prediction of Early Morning Radiation Fog," ECOM-5809, January 1977.
46. Engebos, Bernard Francis, "Introduction to Multiple State Multiple Action Decision Theory and Its Relation to Mixing Structures," ECOM-5810, January 1977.
47. Low, Richard D.H.,"Effects of Cloud Particles on Remote Sensing from Space in the 10-Micrometer Infrared Region," ECOM-5811, January 1977.
48. Bonner, Robert S., and R. Newton, "Application of the AN/GVS-5 Laser Rangefinder to Cloud Base Height Measurements," ECOM-5812, February 1977.
49. Rubio, Roberto, "Lidar Detection of Subvisible Reentry Vehicle Erosive Atmospheric Material," ECOM-5813, March 1977.
50. Low, Richard D.H., and J.D. Horn, "Mesoscale Determination of Cloud-Top Height: Problems and Solutions," ECOM-5814, March 1977.

51. Duncan, Louis D., and Mary Ann Seagraves, "Evaluation of the NOAA-4 VTPR Thermal Winds for Nuclear Fallout Predictions," ECOM-5815, March 1977.
52. Randhawa, Jagir S., M. Izquierdo, Carlos McDonald and Zvi Salpeter, "Stratospheric Ozone Density as Measured by a Chemiluminescent Sensor During the Stratcom VI-A Flight," ECOM-5816, April 1977.
53. Rubio, Roberto, and Mike Izquierdo, "Measurements of Net Atmospheric Irradiance in the 0.7- to 2.8-Micrometer Infrared Region," ECOM-5817, May 1977.
54. Ballard, Harold N., Jose M. Serna, and Frank P. Hudson Consultant for Chemical Kinetics, "Calculation of Selected Atmospheric Composition Parameters for the Mid-Latitude, September Stratosphere," ECOM-5818, May 1977.
55. Mitchell, J.D., R.S. Sagar, and R.O. Olsen, "Positive Ions in the Middle Atmosphere During Sunrise Conditions," ECOM-5819, May 1977.
56. White, Kenneth O., Wendell R. Watkins, Stuart A. Schleusener, and Ronald L. Johnson, "Solid-State Laser Wavelength Identification Using a Reference Absorber," ECOM-5820, June 1977.
57. Watkins, Wendell R., and Richard G. Dixon, "Automation of Long-Path Absorption Cell Measurements," ECOM-5821, June 1977.
58. Taylor, S.E., J.M. Davis, and J.B. Mason, "Analysis of Observed Soil Skin Moisture Effects on Reflectance," ECOM-5822, June 1977.
59. Duncan, Louis D. and Mary Ann Seagraves, "Fallout Predictions Computed from Satellite Derived Winds," ECOM-5823. June 1977.
60. Snider, D.E., D.G. Murcray, F.H. Murcray, and W.J. Williams, "Investigation of High-Altitude Enhanced Infrared Backround Emissions" (U), SECRET, ECOM-5824, June 1977.
61. Dubbin, Marvin H. and Dennis Hall, "Synchronous Meteorlogical Satellite Direct Readout Ground System Digital Video Electronics," ECOM-5825, June 1977.
62. Miller, W., and B. Engebos, "A Preliminary Analysis of Two Sound Ranging Algorithms," ECOM-5826, July 1977.
63. Kennedy, Bruce W., and James K. Luers, "Ballistic Sphere Techniques for Measuring Atomspheric Parameters," ECOM-5827, July 1977.
64. Duncan, Louis D., "Zenith Angle Variation of Satellite Thermal Sounder Measurements," ECOM-5828, August 1977.
65. Hansen, Frank V., "The Critical Richardson Number," ECOM-5829, September 1977.
66. Ballard, Harold N., and Frank P. Hudson (Compilers), "Stratospheric Composition Balloon-Borne Experiment," ECOM-5830, October 1977.
67. Barr, William C., and Arnold C. Peterson, "Wind Measuring Accuracy Test of Meteorological Systems," ECOM-5831, November 1977.
68. Ethridge, G.A. and F.V. Hansen, "Atmospheric Diffusion: Similarity Theory and Empirical Derivations for Use in Boundary Layer Diffusion Problems," ECOM-5832, November 1977.
69. Low, Richard D.H., "The Internal Cloud Radiation Field and a Technique for Determining Cloud Blackness," ECOM-5833, December 1977.
70. Watkins, Wendell R., Kenneth O. White, Charles W. Bruce, Donald L. Walters, and James D. Lindberg, "Measurements Required for Prediction of High Energy Laser Transmission," ECOM-5834, December 1977.
71. Rubio, Robert, "Investigation of Abrupt Decreases in Atmospherically Backscattered Laser Energy," ECOM-5835. December 1977.
72. Monahan, H.H. and R.M. Cionco, "An Interpretative Review of Existing Capabilities for Measuring and Forecasting Selected Weather Variables (Emphasizing Remote Means)," ASL-TR-0001, January 1978.
73. Heaps, Melvin G., "The 1979 Solar Eclipse and Validation of D-Region Models," ASL-TR-0002. March 1978.

74. Jennings, S.G., and J.B. Gillespie, "M.I.E. Theory Sensitivity Studies - The Effects of Aerosol Complex Refractive Index and Size Distribution Variations on Extinction and Absorption Coefficients Part II: Analysis of the Computational Results," ASL-TR-0003, March 1978.
75. White, Kenneth O. et al, "Water Vapor Continuum Absorption in the 3.5μm to 4.0μm Region," ASL-TR-0004, March 1978.
76. Olsen, Robert O., and Bruce W. Kennedy, "ABRES Pretest Atmospheric Measurements," ASL-TR-0005, April 1978.
77. Ballard, Harold N., Jose M. Serna, and Frank P. Hudson, "Calculation of Atmospheric Composition in the High Latitude September Stratosphere," ASL-TR-0006, May 1978.
78. Watkins, Wendell R. et al, "Water Vapor Absorption Coefficients at HF Laser Wavelengths," ASL-TR-0007, May 1978.
79. Hansen, Frank V., "The Growth and Prediction of Nocturnal Inversions," ASL-TR-0008, May 1978.
80. Samuel, Christine, Charles Bruce, and Ralph Brewer, "Spectrophone Analysis of Gas Samples Obtained at Field Site," ASL-TR-0009, June 1978.
81. Pinnick, R.G. et al., "Vertical Structure in Atmospheric Fog and Haze and its Effects on IR Extinction," ASL-TR-0010, July 1978.
82. Low, Richard D.H., Louis D. Duncan, and Richard B. Gomez, "The Microphysical Basis of Fog Optical Characterization," ASL-TR-0011, August 1978.
83. Heaps, Melvin G., "The Effect of a Solar Proton Event on the Minor Neutral Constituents of the Summer Polar Mesosphere," ASL-TR-0012, August 1978.
84. Mason, James B., "Light Attenuation in Falling Snow," ASL-TR-0013, August 1978.
85. Blanco, Abel J., "Long-Range Artillery Sound Ranging: "PASS" Meteorological Application," ASL-TR-0014, September 1978.
86. Heaps, M.G., and F.E. Niles, "Modeling the Ion Chemistry of the D-Region: A case Study Based Upon the 1966 Total Solar Eclipse," ASL-TR-0015, September 1978.
87. Jennings, S.G., and R.G. Pinnick, "Effects of Particulate Complex Refractive Index and Particle Size Distribution Variations on Atmospheric Extinction and Absorption for Visible Through Middle-Infrared Wavelengths," ASL-TR-0016, September 1978.
88. Watkins, Wendell R., Kenneth O. White, Lanny R. Bower, and Brian Z. Sojka, " Pressure Dependence of the Water Vapor Continuum Absorption in the 3.5- to 4.0-Micrometer Region," ASL-TR-0017, September 1978.
89. Miller, W.B., and B.F. Engebos, "Behavior of Four Sound Ranging Techniques in an Idealized Physical Enviroment," ASL-TR-0018, September 1978.

☆ U.S. GOVERNMENT PRINTING OFFICE: 1978 777-093/ 22